

Imperfect Influence, Preserved Rankings: A Theory of TRAK for Data Attribution

Han Tong¹ Shubhangi Ghosh¹ Haolin Zou¹ Arian Maleki¹

Abstract

Data attribution, tracing a model’s prediction back to specific training data, is an important tool for interpreting sophisticated AI models. The widely used TRAK algorithm addresses this challenge by first approximating the underlying model with a kernel machine and then leveraging techniques developed for approximating the leave-one-out (ALO) risk. Despite its strong empirical performance, the theoretical conditions under which the TRAK approximations are accurate as well as the regimes in which they break down remain largely unexplored. In this paper, we provide a theoretical analysis of the TRAK algorithm, characterizing its performance and quantifying the errors introduced by the approximations on which the method relies. We show that although the approximations incur significant errors, TRAK’s estimated influence remains highly correlated with the original influence and therefore largely preserves the relative ranking of data points. We corroborate our theoretical results through extensive simulations and empirical studies.

1. Introduction

1.1. Related work and contributions

Modern machine learning systems, including large language models, rely heavily on massive training datasets, where data quality significantly impacts model performance. This dependence has motivated growing interest in *data attribution*, the task of tracing a model’s predictions back to individual training samples, to better understand model behavior, identify harmful or redundant data, and improve data efficiency.

A popular class of data attribution methods is based on counterfactual reasoning: asking how a model’s prediction

would change if a particular training point were removed or reweighted. Popular approaches rely on quantities such as the Shapley value (Jia et al., 2019; Ghorbani & Zou, 2019; Wang et al., 2024) and influence functions (Hampel, 1974; Sagun et al., 2018; Yeh et al., 2019; Han et al., 2020; Hammoudeh & Lowd, 2022; Ilyas et al., 2022; Park et al., 2023; Guu et al., 2023; Hammoudeh & Lowd, 2024), whose computation is often prohibitively expensive or even intractable for modern AI models. Recently, the TRAK algorithm (Park et al., 2023) was proposed as a scalable data attribution method tailored to modern neural networks and has since gained popularity (Ye et al., 2023; Xia et al., 2024; Hammoudeh & Lowd, 2024). Its computational efficiency stems from three key approximations of the influence functions: linearization, random projection, and Approximate-Leave-one-Out (ALO) corrections (Rad & Maleki, 2020; Auddy et al., 2024). TRAK has demonstrated strong empirical performance on large models and datasets.

Despite its practical success, little is known about the theoretical conditions under which TRAK provides accurate attributions, or about the error introduced by its multiple approximation steps. This lack of theoretical understanding limits our ability to determine when and for what tasks TRAK can be reliably used, and what information is lost by its approximations.

This paper aims to close this gap. We provide the first systematic theoretical analysis of TRAK by evaluating the errors each approximation step of TRAK introduces. To give a high-level overview of our contributions, let $\mathcal{I}^{\text{True}}(\mathbf{z}_i, \mathbf{z}_{\text{new}})$ denote the true influence of datapoint \mathbf{z}_i on a test data point \mathbf{z}_{new} (Koh & Liang, 2017). This quantity will be defined more formally in (2). Furthermore, let $\mathcal{I}^{\text{TRAK}}(\mathbf{z}_i, \mathbf{z}_{\text{new}})$ denote the TRAK approximation of $\mathcal{I}^{\text{True}}(\mathbf{z}_i, \mathbf{z}_{\text{new}})$.

Our analysis reveals the following facts about TRAK:

1. **Negative result:** While the error introduced by the ALO approximation is typically small and benign, both the linearization step and the projection step, especially when the number of projections is much smaller than the number of parameters, can introduce substantial errors. As a result, the exact ranking of training data points induced by $\mathcal{I}^{\text{TRAK}}(\mathbf{z}_i, \mathbf{z}_{\text{new}})$ can differ signifi-

¹Department of Statistics, Columbia University, New York, NY, USA. Correspondence to: Han Tong <ht2672@columbia.edu>, Arian Maleki <mm4338@columbia.edu>.

cantly from that induced by $\mathcal{I}^{\text{True}}(\mathbf{z}_i, \mathbf{z}_{\text{new}})$.

2. Positive result: Despite the large errors TRAK introduces, it can detect datapoints that have large influences from the ones that have small influences. Informally speaking, if the influence of datapoint \mathbf{z}_i , i.e. $\mathcal{I}^{\text{True}}(\mathbf{z}_i, \mathbf{z}_{\text{new}})$ is much larger than the $\mathcal{I}^{\text{True}}(\mathbf{z}_j, \mathbf{z}_{\text{new}})$, then the $\mathcal{I}^{\text{TRAK}}(\mathbf{z}_i, \mathbf{z}_{\text{new}})$ remains much larger than $\mathcal{I}^{\text{True}}(\mathbf{z}_j, \mathbf{z}_{\text{new}})$ as well. Hence, when the objective is to identify the most influential data points, TRAK provides accurate and reliable information.

1.2. TRAK Influence function

In this section, we formally present the three approximations employed by the TRAK algorithm. In the next section, we study the errors introduced by each approximation step to shed light on the performance of TRAK. Consider the standard supervised learning setting, in which we are given a dataset

$$\mathcal{D} = \{(y_1, \mathbf{x}_1), (y_2, \mathbf{x}_2), \dots, (y_n, \mathbf{x}_n)\},$$

where $y_i \in \mathbb{R}$ represents the response, and $\mathbf{x}_i \in \mathbb{R}^p$ denotes the corresponding feature vector. The goal is to learn a predictor that, given a new feature vector \mathbf{x}_{new} , can accurately predict its associated response. Many successful approaches in AI and machine learning, including generalized linear models and neural networks, use predictors of the form $f(\mathbf{x}; \beta)$, where $\beta \in \mathbb{R}^d$ are parameters (to be learned from data), and $f(\cdot; \beta)$ is a linear or nonlinear function that produces the predictions. In most applications, the model parameters are estimated using empirical risk minimization:

$$\hat{\beta} \triangleq \arg \min_{\beta \in \mathbb{R}^d} \left\{ \sum_{i=1}^n \ell(y_i, f(\mathbf{x}_i; \beta)) \right\}, \quad (1)$$

where $\ell(y, f(\mathbf{x}; \beta))$ denotes the loss function, such as the squared loss or cross-entropy loss, depending on the application and the nature of the response variable.

To interpret model predictions, many data attribution techniques seek to quantify the influence of individual training samples on a model's output. Specifically, the influence of a training datapoint $\mathbf{z}_i = (y_i, \mathbf{x}_i)$ on the model's prediction at a new datapoint $\mathbf{z}_{\text{new}} = (y_{\text{new}}, \mathbf{x}_{\text{new}})$ is defined as

$$\mathcal{I}^{\text{True}}(\mathbf{z}_i, \mathbf{z}_{\text{new}}) \triangleq f(\mathbf{x}_{\text{new}}; \hat{\beta}_{/i}) - f(\mathbf{x}_{\text{new}}; \hat{\beta}). \quad (2)$$

where

$$\hat{\beta}_{/i} \triangleq \arg \min_{\beta \in \mathbb{R}^d} \left\{ \sum_{j \neq i} \ell(y_j, f(\mathbf{x}_j; \beta)) \right\}. \quad (3)$$

A fundamental challenge in applying (2) for data valuation is its prohibitive computational cost. Computing the influence of a single training sample requires solving the leave-one-out optimization problem in (3). In modern machine learning and AI applications, where both the sample size n and the model dimension d are large, the exact computation of $\hat{\beta}_{/i}$ becomes computationally prohibitive, especially when it must be performed repeatedly for many training data points. The TRAK algorithm mitigates this issue by approximating $\hat{\beta}_{/i}$ using the following sequence of steps:

Step 1: Linearization. The first step in TRAK is to linearly approximate $f(\mathbf{x}, \beta)$ around $\hat{\beta}$. Define

$$\begin{aligned} \mathbf{g}_j &= \nabla f(\mathbf{x}_j, \hat{\beta}), \\ \mathbf{b}_j &= f(\mathbf{x}_j, \hat{\beta}) - \nabla f(\mathbf{x}_j, \hat{\beta})^\top \hat{\beta}. \end{aligned}$$

Instead of solving the nonlinear optimization problem (3), TRAK solves the following linearized version:

$$\check{\beta}_{/i} \triangleq \arg \min_{\beta \in \mathbb{R}^d} \left\{ \sum_{j \neq i} \ell(y_j, \mathbf{g}_j^\top \beta + \mathbf{b}_j) \right\}. \quad (4)$$

The intuition is that the linear approximation of $f(\mathbf{x}, \beta)$ around $\hat{\beta}$ provides a sufficiently accurate surrogate, and the corresponding optimization problem changes only slightly. As a result, we can use the linear function of $\{\mathbf{g}_i\}_{i \in [n]}$ as an approximation of $f(\mathbf{x}_i, \beta)$ when β is close to $\hat{\beta}$.

Step 2: Random projection. To further reduce computational cost, TRAK applies random projection to the gradients \mathbf{g}_i . The idea is to reduce dimensionality while approximately preserving inner products. More specifically, we define the gradient matrix used in the TRAK algorithm as:

$$\mathbf{G}(\beta) := (\nabla f(\mathbf{x}_1, \beta), \dots, \nabla f(\mathbf{x}_n, \beta))^\top, \quad (5)$$

and for notational simplicity, we write $\mathbf{G} := \mathbf{G}(\hat{\beta})$. Using a random projection matrix $\mathbf{S} \in \mathbb{R}^{p \times k}$ with $k \ll p$, TRAK defines the feature map $\phi(\mathbf{x}) = \mathbf{S}^\top \mathbf{g}(\mathbf{x})$, where $\mathbf{g}(\mathbf{x}) = \nabla f(\mathbf{x}, \hat{\beta})$. Accordingly, we define $\Phi = (\phi_1, \dots, \phi_n)^\top \in \mathbb{R}^{n \times k}$, where $\phi_i = \mathbf{S}^\top \mathbf{g}_i$ and $\phi_{\text{new}} = \mathbf{S}^\top \mathbf{g}_{\text{new}}$.

Step 3: Approximate Leave-One-Out (ALO). Building on the ideas of approximate leave-one-out Rad & Maleki (2020); Beirami et al. (2017), TRAK estimates the influence via the ALO formula¹, which provides the following

¹In the TRAK paper, the authors note that replacing $\text{diag}[\check{\ell}(\check{\beta})]$ with the identity matrix and ignoring the denominator in (6) does not significantly affect empirical performance. As a result, they use the simplified expression

$$\dot{\ell}_i(\check{\beta}) \phi_{\text{new}}^\top (\Phi^\top \Phi)^{-1} \phi_i.$$

However, for theoretical analysis, we will consider the complete form in (6).

approximation for $\mathcal{I}^{\text{True}}(\mathbf{z}_i, \mathbf{z}_{\text{new}})$:

$$\begin{aligned} \mathcal{I}^{\text{TRAK}}(\mathbf{z}_i, \mathbf{z}_{\text{new}}; k) \\ \triangleq \frac{\dot{\ell}_i(\check{\beta}) \phi_{\text{new}}^\top (\Phi^\top \text{diag}[\ddot{\ell}(\check{\beta})] \Phi)^{-1} \phi_i}{1 - \ddot{\ell}_i(\check{\beta}) \phi_i^\top (\Phi^\top \text{diag}[\ddot{\ell}(\check{\beta})] \Phi)^{-1} \phi_i}, \end{aligned} \quad (6)$$

where k is the projection dimension, $\dot{\ell}(y, z)$ and $\ddot{\ell}(y, z)$ denote the first and second order derivative of the loss function with respect to z respectively, $\dot{\ell}_i(\check{\beta}) = \dot{\ell}(y_i, \mathbf{x}_i^\top \check{\beta})$, and $\dot{\ell}(\check{\beta}) = [\dot{\ell}_1(\check{\beta}), \dot{\ell}_2(\check{\beta}), \dots, \dot{\ell}_n(\check{\beta})]^\top$. Finally, $\check{\beta}$ is defined by

$$\check{\beta} = \arg \min_{\beta \in \mathbb{R}^d} \left\{ \sum_{i=1}^n \ell(y_i, \mathbf{g}_i^\top \beta + \mathbf{b}_i) \right\}. \quad (7)$$

We should also note that TRAK includes two additional steps: (i) Ensemble averaging, which mitigates variability arising from random initialization and the inherent randomness of optimization algorithms used to find minima of the training loss, and (ii) the application of soft thresholding to the influence estimates, introducing shrinkage under the assumption that only a small subset of training points meaningfully affects the prediction for a given test example. However, since we only study the accuracy of approximations involved in TRAK, we skip these two steps.

1.3. Notations

Inspired by recent advances in AI models with billions of parameters trained on massive datasets, we study regimes in which n , p , and d are all large. Hence, throughout the paper we will use the following standard notations. For deterministic sequences $\{a_n\}$ and $\{b_n\}$, we write $a_n = O(b_n)$ if there exists a constant $C > 0$ such that $|a_n| \leq C|b_n|$ for all sufficiently large n , and $a_n = o(b_n)$ if $a_n/b_n \rightarrow 0$ as $n \rightarrow \infty$. We write $a_n = \Theta(b_n)$ if $a_n = O(b_n)$ and $b_n = O(a_n)$. For random sequences $\{X_n\}$, we write $X_n = O_p(b_n)$ if for every $\varepsilon > 0$ there exist constants $C > 0$ and N such that $\mathbb{P}(|X_n| > Cb_n) < \varepsilon$ for all $n \geq N$, and $X_n = o_p(b_n)$ if X_n/b_n goes to zero in probability.

2. Main theoretical contributions

2.1. Our theoretical framework

Throughout the theoretical part of the paper we assume that the elements of \mathcal{D} are independent draws from the joint distribution

$$(y_i, \mathbf{x}_i) \sim q(y_i \mid f(\mathbf{x}_i; \beta^*)) p(\mathbf{x}_i). \quad (8)$$

Here, $\beta^* \in \mathbb{R}^d$ denotes the true parameter vector. Unlike classical linear models, the parameter dimension d may differ from the feature dimension p ; for example, in neural networks, d corresponds to the total number of weights.

We define the loss function as the negative log-likelihood

$$\ell(y, f(\mathbf{x}; \beta)) = -\log q(y \mid f(\mathbf{x}; \beta)).$$

Motivated by modern machine learning and AI applications, where the models have billions or even trillions of parameters and are trained on gigabytes of data, in our theoretical studies we focus on the regime that the sample size n , the number of features p , and number of parameters d are all large. In other words, in our analysis we will ignore the errors that are negligible for large values of n, p and d .

In addition to this assumption, to characterize the scaling behavior of the approximation errors introduced by TRAK, we impose the following structural assumptions. Their precise formal statements are deferred to Appendix B.1.2.

Assumption 2.1 (Data and Model Regularity). We make the following structural assumptions throughout the paper.

(A1) Sub-Gaussian design. Let \mathbf{X}_n denote the matrix with rows \mathbf{x}_i^\top . The rows of $\mathbf{X}_n \in \mathbb{R}^{n \times p}$ are mean-zero sub-Gaussian random vectors with covariance matrix Σ_p . Moreover, there exist constants $c, C > 0$ such that $\frac{c}{\|\beta^*\|^2} \leq \lambda_{\min}(\Sigma_p) \leq \lambda_{\max}(\Sigma_p) \leq \frac{C}{\|\beta^*\|^2}$.

(A2) Model and loss regularity. In addition to assumptions about feature vectors we require some regularity conditions on the loss function and $f(\cdot, \cdot)$. Since the precise technical statements of these assumptions require additional space, we provide a brief and informal description here and defer the exact definitions to the supplementary material.

- The norm of $\nabla f(\mathbf{x}, \beta^*)$ is sub-Gaussian with a bounded second-moment. See Assumptions B.2 and B.7 for formal statement.
- The Hessian of the empirical risk in (1) and (7) are well-conditioned in a small vicinity of $\check{\beta}$. See Assumptions B.3 and B.4 for formal statement.
- The loss ℓ is strongly convex, and both ℓ and its gradient are Lipschitz continuous. See Assumption B.5 for the formal definition.

In the online supplement, we provide additional intuition for the chosen scalings and discuss why the underlying assumptions are satisfied. For instance, we verify in Appendix B.4 that our regularity assumptions on the loss function ℓ (Assumption B.5) hold for commonly used objectives, including the squared loss, cross-entropy loss, and the Poisson loss with a softplus link.

Below, we present two canonical models and demonstrate that all of our assumptions hold for both.

Example 2.2 (Linear model). Consider the class of generalized linear model that are popular in Statistics and machine

learning. In these models we have

$$f(\mathbf{x}, \boldsymbol{\beta}) = \mathbf{x}^\top \boldsymbol{\beta}.$$

For these models all the assumptions Assumptions B.2, B.3, B.4, B.5 and B.7 hold.

The proof can be found in Section B.5 of the Appendix.

Example 2.3 (Neural network). Consider a neural network with one hidden layer. For such models,

$$f(\mathbf{x}, \mathbf{W}, \mathbf{v}) = \mathbf{v}^\top \sigma(\mathbf{W}\mathbf{x}),$$

where $\mathbf{W} \in \mathbb{R}^{h \times p}$, $\mathbf{v} \in \mathbb{R}^h$, and $\sigma(\cdot)$ is an elementwise activation function with bounded derivative. For this model Assumptions B.2, B.3, B.4, B.5 and B.7 hold. The proof can be found in Section B.5.

Based on these assumptions, we now present our main theoretical results.

2.2. Theoretical Results

2.2.1. OVERVIEW OF THE RESULTS

Our contributions here are presented in four sections:

- Section 2.2.2 characterizes the size of $\mathcal{I}^{\text{True}}(\mathbf{z}_i, \mathbf{z}_{\text{new}})$ in two settings: (1) when \mathbf{z}_i is related to \mathbf{z}_{new} , in which case the influence of \mathbf{z}_i on \mathbf{z}_{new} is expected to be large; and (2) when \mathbf{z}_i and \mathbf{z}_{new} are unrelated, in which case the influence of \mathbf{z}_i on \mathbf{z}_{new} is expected to be small. These order-of-magnitude characterizations will be used in the next sections to interpret and explain the properties of $\mathcal{I}^{\text{True}}(\mathbf{z}_i, \mathbf{z}_{\text{new}})$.
- Section 2.2.3 studies the error introduced by the linearization step in TRAK and highlights the key limitations of this approximation, and also its interesting features.
- Section 2.2.4 studies the error that is introduced by the ALO approximation in TRAK, and shows that the error that is introduced in this step is benign and substantially smaller than the errors that are introduced in the linearization and projection steps of TRAK.
- Section 2.2.5 studies the error that is introduced by the projection step in TRAK and shows the important limitations of the projection step, specially when the dimension of the projection is much smaller than the number of parameters.

2.2.2. SIZE OF INFLUENCE

In this section, we study the magnitude of $\mathcal{I}^{\text{True}}(\mathbf{z}_i, \mathbf{z}_{\text{new}})$. Our first result obtains an upper bound on the influence function and shows its sharpness.

Proposition 2.4. *Under Assumption 2.1 (formally, Assumptions B.1–B.7 in the Appendix), for any $\epsilon > 0$ such that $\|\boldsymbol{\beta}^*\|^2 \leq n^{1-\epsilon}$, there exists an absolute constant C^{True}*

such that, with probability tending to 1,

$$\sup_{i \in [n]} |\mathcal{I}^{\text{True}}(\mathbf{z}_i, \mathbf{z}_{\text{new}})| \leq C^{\text{True}} \frac{\|\boldsymbol{\beta}^*\|^2 \text{poly}(\log n)}{n},$$

where $\text{poly}(\log n)$ denotes a polynomial function of $\log(n)$. Furthermore, if Assumption B.8 holds, then there exists an absolute constant \tilde{C}^{True} such that, with probability tending to 1,

$$|\mathcal{I}^{\text{True}}(\mathbf{z}_i, \mathbf{z}_i)| \geq \tilde{C}^{\text{True}} \frac{\|\boldsymbol{\beta}^*\|^2}{n}. \quad (9)$$

The proof of this proposition is presented in Section B.2.1 of the Appendix. This theorem shows how large an influence of a datapoint on \mathbf{z}_{new} can be. But to understand this result better, we have to discuss how large $|\mathcal{I}^{\text{True}}(\mathbf{z}_i, \mathbf{z}_{\text{new}})|$ can get when \mathbf{z}_{new} is independent of the training set. In such cases, we expect the influence to be small. Our next theorem addresses this question.

Proposition 2.5. *Suppose that \mathbf{z}_{new} is independent of the training set \mathcal{D} . Under Assumption 2.1 (formally, Assumptions B.1–B.7 in the Appendix), for any $\epsilon > 0$ such that $\|\boldsymbol{\beta}^*\|^2 \leq n^{1-\epsilon}$, there exists an absolute constant C^{True} such that, with probability tending to 1,*

$$\sup_{i \in [n]} |\mathcal{I}^{\text{True}}(\mathbf{z}_i, \mathbf{z}_{\text{new}})| \leq C^{\text{True}} \frac{\|\boldsymbol{\beta}^*\|}{n^{1-\epsilon}}.$$

The proof of Proposition 2.5 is shown in Appendix B.2.2.

Note that since n , p , and d are all assumed to be large, we expect $\|\boldsymbol{\beta}^*\|$ to be much larger than 1. Comparing the results of the two theorems, we observe a substantial gap between the influence of data points \mathbf{z}_i that are strongly correlated with \mathbf{z}_{new} and those that are largely independent of \mathbf{z}_{new} . The key takeaway is that, even when the approximations to $\mathcal{I}^{\text{True}}(\mathbf{z}_i, \mathbf{z}_{\text{new}})$ are not quantitatively accurate, they can still reliably identify the most influential data points due to the pronounced separation in influence magnitudes.

As we clarify in the next sections, this large separation is in fact one of the reasons behind the empirical success of the TRAK method.

2.2.3. LINEARIZATION STEP

In this section, we aim to understand the error that is introduced in the influence function because of the linearization step of TRAK. If the projection and ALO are removed from the TRAK, then the approximate influence function is given by

$$\mathcal{I}^{\text{Linear}}(\mathbf{z}_i, \mathbf{z}_{\text{new}}) \triangleq \mathbf{g}_{\text{new}}^\top (\check{\boldsymbol{\beta}}_{/i} - \check{\boldsymbol{\beta}}), \quad (10)$$

where $\mathbf{g}_{\text{new}} = \nabla f(\mathbf{x}_{\text{new}}, \hat{\boldsymbol{\beta}})$, $\check{\boldsymbol{\beta}}_{/i}$ is defined in (4) and

$$\check{\boldsymbol{\beta}} = \arg \min_{\boldsymbol{\beta} \in \mathbb{R}^d} \left\{ \sum_{j=1}^n \ell(y_j, \mathbf{g}_j^\top \boldsymbol{\beta} + \mathbf{b}_j) \right\}. \quad (11)$$

Following our approach from the last section we aim to study $|\mathcal{I}^{\text{Linear}}(\mathbf{z}_i, \mathbf{z}_{\text{new}}) - \mathcal{I}^{\text{True}}(\mathbf{z}_i, \mathbf{z}_{\text{new}})|$ for two cases: (i) \mathbf{z}_i and \mathbf{z}_{new} are strongly correlated and (ii) \mathbf{z}_i and \mathbf{z}_{new} are independent. We start with the strongly correlated case.

Theorem 2.6. *Under Assumptions 2.1 (formally, Assumptions B.1–B.7 in the Appendix), for any $\epsilon > 0$ such that $\|\beta^*\|^2 \leq n^{1-\epsilon}$, there exists an absolute constant C^{Linear} such that, with probability tending to 1, the linearization error satisfies:*

$$\sup_{i \in [n]} |\mathcal{I}^{\text{True}}(\mathbf{z}_i, \mathbf{z}_i) - \mathcal{I}^{\text{Linear}}(\mathbf{z}_i, \mathbf{z}_i)| \leq C^{\text{Linear}} \frac{\|\beta^*\|^2}{n}.$$

Furthermore, if Assumption B.8 holds, then there exists an absolute constant c^{Linear} such that, with probability tending to 1,

$$|\mathcal{I}^{\text{Linear}}(\mathbf{z}_i, \mathbf{z}_i)| \geq c^{\text{Linear}} \frac{\|\beta^*\|^2}{n}. \quad (12)$$

The proof of this result can be found in Section B.2.3 of Appendix. We highlight several points concerning this theorem.

Remark 2.7. While this theorem obtains an upper bound on the difference $|\mathcal{I}^{\text{True}}(\mathbf{z}_i, \mathbf{z}_i) - \mathcal{I}^{\text{Linear}}(\mathbf{z}_i, \mathbf{z}_i)|$, our arguments presented in Appendix C.3.1 show that this upper bound is also in fact sharp, and the order of the error is in fact $\Theta_p(\frac{\|\beta^*\|^2}{n})$.

Remark 2.8. If we compare the error term $C^{\text{Linear}} \frac{\|\beta^*\|^2}{n}$ with the order of $\mathcal{I}^{\text{True}}(\mathbf{z}_i, \mathbf{z}_i)$ in Proposition 2.5 we notice that the error is very large and has the same order as the quantity that we wanted to approximate. This is consistent with the “Negative result” that we reported in the introduction.

Now to show some of the positive features of the linearization, our next theorem establishes the accuracy of $\mathcal{I}^{\text{Linear}}(\mathbf{z}_i, \mathbf{z}_{\text{new}})$ for the case that \mathbf{z}_i and \mathbf{z}_{new} are independent.

Theorem 2.9. *Under Assumptions 2.1 (formally, Assumptions B.1–B.7 in the Appendix), for any $\epsilon > 0$ such that $\|\beta^*\|^2 \leq n^{1-\epsilon}$, there exists an absolute constant $\tilde{C}^{\text{Linear}}$ such that, with probability tending to 1, the linearization error satisfies:*

$$\sup_{i \in [n]} |\mathcal{I}^{\text{True}}(\mathbf{z}_i, \mathbf{z}_{\text{new}}) - \mathcal{I}^{\text{Linear}}(\mathbf{z}_i, \mathbf{z}_{\text{new}})| \leq \tilde{C}^{\text{Linear}} \frac{\|\beta^*\|}{n^{1-\epsilon}}.$$

The proof of Theorem 2.9 is shown in Appendix B.2.4.

Remark 2.10. Again, by comparing the above theorem with Theorem 2.5, we observe that the error

$$|\mathcal{I}^{\text{True}}(\mathbf{z}_i, \mathbf{z}_{\text{new}}) - \mathcal{I}^{\text{Linear}}(\mathbf{z}_i, \mathbf{z}_{\text{new}})|$$

is of the same order as $\mathcal{I}^{\text{True}}(\mathbf{z}_i, \mathbf{z}_{\text{new}})$ itself. Consequently, this approximation does not yield quantitatively accurate

estimates of $\mathcal{I}^{\text{True}}(\mathbf{z}_i, \mathbf{z}_{\text{new}})$. This observation is consistent with the negative result highlighted in the introduction.

Remark 2.11. Despite the negative results discussed in Remarks 2.8 and 2.10, the TRAK approximation nevertheless exhibits an important positive property, as established by the second part of Theorem 2.6. Specifically, when \mathbf{z}_{new} is strongly correlated with \mathbf{z}_i , the quantity $\mathcal{I}^{\text{Linear}}(\mathbf{z}_i, \mathbf{z}_{\text{new}})$ remains large. In contrast, when a data point \mathbf{z}_j is independent of \mathbf{z}_{new} , Theorem 2.9 implies that $\mathcal{I}^{\text{Linear}}(\mathbf{z}_j, \mathbf{z}_{\text{new}})$ is of much smaller order. As a result, even though the TRAK approximation may incur substantial absolute error, it can still reliably distinguish data points with large true influence $\mathcal{I}^{\text{True}}(\mathbf{z}_i, \mathbf{z}_{\text{new}})$ from those with negligible influence. This is consistent with the “positive result” mentioned in the introduction.

2.2.4. ALO STEP

In this section, we characterize the error introduced by the ALO approximation. If we ignore the projection step of the TRAK method, the influence function produced by TRAK reduces to

$$\mathcal{I}^{\text{ALO}}(\mathbf{z}_i, \mathbf{z}_{\text{new}}) \triangleq \frac{\dot{\ell}_i(\check{\beta}) \mathbf{g}_{\text{new}}^\top \mathbf{H}^{-1} \mathbf{g}_i}{1 - \ddot{\ell}_i(\check{\beta}) \mathbf{g}_i^\top \mathbf{H}^{-1} \mathbf{g}_i}, \quad (13)$$

where $\mathbf{H} = \mathbf{G}^\top \text{diag}[\ddot{\ell}(\check{\beta})] \mathbf{G}$, $\dot{\ell}_i(\beta) = \dot{\ell}(y_i, \mathbf{g}_i^\top \beta + \mathbf{b}_i)$ and $\ddot{\ell}_i(\beta) = \ddot{\ell}(y_i, \mathbf{g}_i^\top \beta + \mathbf{b}_i)$. In this section we would like to characterize the difference between $\mathcal{I}^{\text{ALO}}(\mathbf{z}_i, \mathbf{z}_{\text{new}}) - \mathcal{I}^{\text{Linear}}(\mathbf{z}_i, \mathbf{z}_{\text{new}})$. Our first theorem shows that in case \mathbf{z}_{new} has strong correlation with \mathbf{z}_i , the error is much smaller than $\mathcal{I}^{\text{Linear}}(\mathbf{z}_i, \mathbf{z}_{\text{new}})$. Hence, the error of this step is negligible.

Theorem 2.12. *Under Assumptions 2.1 (formally, Assumptions B.1–B.7 in the Appendix), for any $\epsilon > 0$ such that $\|\beta^*\|^2 \leq n^{1-\epsilon}$, there exists an absolute constant \tilde{C}^{ALO} such that, with probability tending to 1, the ALO step error satisfies:*

$$\sup_{i \in [n]} |\mathcal{I}^{\text{Linear}}(\mathbf{z}_i, \mathbf{z}_i) - \mathcal{I}^{\text{ALO}}(\mathbf{z}_i, \mathbf{z}_i)| \leq \tilde{C}^{\text{ALO}} \frac{\|\beta^*\|^2}{n^{1.5-\epsilon}}.$$

The proof of Theorem 2.12 is postponed to Appendix B.2.5.

It turns out that the error introduced by the ALO step is negligible even in the cases where \mathbf{z}_{new} is independent of \mathbf{z}_i .

Theorem 2.13. *Let \mathbf{z}_{new} be independent of the dataset \mathbf{z}_i . Under Assumptions 2.1 (formally, Assumptions B.1–B.7 in the Appendix), for any $\epsilon > 0$ such that $\|\beta^*\|^2 \leq n^{1-\epsilon}$, there exists an absolute constant C^{ALO} such that, with probability tending to 1, the ALO step error satisfies:*

$$\sup_{i \in [n]} |\mathcal{I}^{\text{Linear}}(\mathbf{z}_i, \mathbf{z}_{\text{new}}) - \mathcal{I}^{\text{ALO}}(\mathbf{z}_i, \mathbf{z}_{\text{new}})| \leq C^{\text{ALO}} \frac{\|\beta^*\|}{n^{1.5-\epsilon}}.$$

The proof of Theorem 2.13 is postponed to Appendix B.2.6.

Combining the above two theorems we can conclude that in both cases, we have

$$\frac{\mathcal{I}^{\text{ALO}}(\mathbf{z}_i, \mathbf{z}_{\text{new}})}{\mathcal{I}^{\text{Linear}}(\mathbf{z}_i, \mathbf{z}_{\text{new}})} = 1 + o_p(1.)$$

Hence, the error introduced by the ALO step is much smaller than the magnitude of the influence, and is therefore negligible.

2.2.5. PROJECTION STEP

Finally, in this section, we study the impact of the projection step on the accuracy of the TRAK algorithm..

Theorem 2.14. *Under Assumptions 2.1 (formally, Assumptions B.1–B.7 in the Appendix), if \mathbf{z}_{new} and \mathbf{z}_i are independent, then for any $\epsilon > 0$ such that $\|\beta^*\|^2 \leq n^{1-\epsilon}$, there exists absolute constant C^{TRAK} such that, with probability tending to 1, the projection error satisfies*

$$|\mathcal{I}^{\text{TRAK}}(\mathbf{z}_{\text{new}}, \mathbf{z}_i; k)| \leq C^{\text{TRAK}} \frac{\|\beta^*\| \sqrt{k}}{n^{1-\epsilon} \sqrt{d}}.$$

Furthermore, for $\mathbf{z}_{\text{new}} = \mathbf{z}_i$, there is an absolute constant c^{TRAK} such that with probability tending to 1,

$$\left| \frac{\mathcal{I}^{\text{TRAK}}(\mathbf{z}_i, \mathbf{z}_i; k)}{\mathcal{I}^{\text{ALO}}(\mathbf{z}_i, \mathbf{z}_i; k)} \right| \geq c^{\text{TRAK}} \frac{k}{d}.$$

The proof of this result is presented in Section B.2.7 of the Appendix.

Remark 2.15. Note that according to theorem 2.4 $\mathcal{I}^{\text{ALO}}(\mathbf{z}_i, \mathbf{z}_i; k) \geq c \frac{\|\beta^*\|^2}{n}$ for some absolute constant $c > 0$. Consequently,

$$\mathcal{I}^{\text{TRAK}}(\mathbf{z}_i, \mathbf{z}_i; k) \geq c \frac{\|\beta^*\|^2 k}{nd}.$$

The key question is whether this influence is larger than $\mathcal{I}^{\text{TRAK}}(\mathbf{z}_i, \mathbf{z}_{\text{new}}; k)$ in the case where \mathbf{z}_{new} is independent of \mathbf{z}_i . If so, this separation allows us to reliably distinguish data points that are strongly dependent on \mathbf{z}_{new} , and therefore meaningfully affect the model's prediction at \mathbf{x}_{new} , from those that are effectively independent of \mathbf{z}_{new} .

In Appendix Figure 12, we further show that the obtained order is sharp. Thus according to Theorem 2.14, if $\|\beta^*\| \sqrt{k/d} \ll 1$, then $\mathcal{I}^{\text{TRAK}}(\mathbf{z}_i, \mathbf{z}_i; k)$ can become smaller than $\mathcal{I}^{\text{TRAK}}(\mathbf{z}_{\text{new}}, \mathbf{z}_i; k)$ for an independent \mathbf{z}_{new} . Hence, the TRAK method may fail to reliably detect influential data points. This observation implies that, in order for TRAK to successfully identify such points, the number of projections k must satisfy $k \gg \frac{d}{\|\beta^*\|^2}$.

Hence, Theorem 2.14 demonstrates that the projection step reduces the separation between $\mathcal{I}^{\text{TRAK}}$ values for data points that are highly dependent on the test point and those that are independent of it.

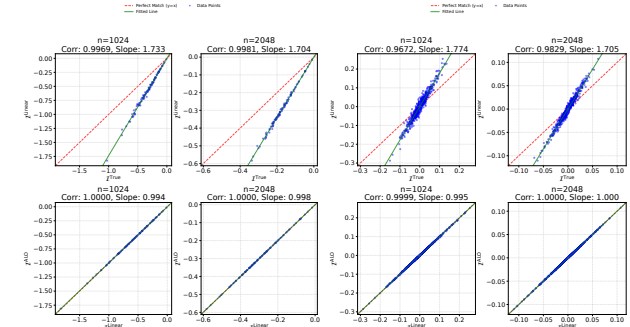


Figure 1. Experimental results for 3-class classification with $p = 100$. **Left two panels:** Results for the dependent case, where $\mathbf{z}_i = \mathbf{z}_{\text{new}}$. **Right two panels:** Results for the independent case, where \mathbf{z}_i and \mathbf{z}_{new} are independent. **Top row:** Displays $\mathcal{I}^{\text{Linear}}$ versus $\mathcal{I}^{\text{True}}$. Although the deviation from the red $y = x$ line suggests large errors between $\mathcal{I}^{\text{Linear}}$ and $\mathcal{I}^{\text{True}}$, the two quantities still exhibit strong correlation. **Bottom row:** Displays \mathcal{I}^{ALO} versus $\mathcal{I}^{\text{True}}$.

3. Simulation results

In this section, we present experiments on simulated data to evaluate the validity of our theoretical results. For linear models f , including binary classification and Poisson regression, the behavior of TRAK is considerably simpler; in particular, the linearization step incurs no error. We therefore defer simulation results for these linear settings to Appendix C.1.1 and instead focus on a multi-class classification problem, which provides a more challenging and informative testbed for analyzing TRAK.

As discussed in Appendix A.1, in the multi-class setting the model f is inherently nonlinear. Consequently, all three sources of approximation error in TRAK, namely, the linearization error, the ALO error, and the projection error, are simultaneously present. Our objective in these experiments is to empirically examine how each approximation step affects the resulting influence estimates and to compare the simulation results with the predictions of our theoretical analysis.

Setting of our simulation The feature vectors $\mathbf{x}_1^\top, \dots, \mathbf{x}_n^\top$ are sampled independently from $\mathcal{N}(\mathbf{0}, \Sigma)$, where Σ is a Toeplitz covariance matrix with $\text{cor}(X_{ij}, X_{ij'}) = 0.1^{|j-j'|}$. We consider multiclass classification problems with $K > 2$. Results for the case $K = 3$ are presented here, while results for $K = 5$ are deferred to Appendix C.1.2. The simulation outcomes are qualitatively consistent across both settings though.

We rescale β^* and Σ such that $\|\beta^*\|^2 = p$ and $\|\Sigma\| = \|\beta^*\|^{-1}$. For each trial t , we generate $(\mathbf{X}^{(t)}, y^{(t)})$ with $y^{(t)} \sim \mathcal{M}(\text{softmax}(\mathbf{X}^{(t)} \mathbf{W}^{*(t)\top}))$, where \mathcal{M} is the multinomial distribution and softmax denotes the softmax function. To ensure identifiability, we set $\mathbf{W}_K^{*(t)} = \mathbf{0}_p$. To write

the parameters of the model in the format that we adopted in this paper, we define β^* as

$$\beta^* \triangleq \text{vec}(\mathbf{W}_{[1:(K-1),:]}^{*(t)}).$$

We randomly remove 100 training points and independently sample 10 new test points \mathbf{z}_{new} . This procedure yields 1,000 realizations of $\mathcal{I}^{\text{True}}$, $\mathcal{I}^{\text{Linear}}$, and $\mathcal{I}^{\text{TRAK}}(k)$ per trial, which are aggregated in our plots. Recall that k denotes the projection dimension. To evaluate our theorems for the case of highly dependent test data, we consider $\mathbf{z}_i = \mathbf{z}_{\text{new}}$. This means that in these cases we only have 100 realizations.

Linearization step The top row of Figure 1 plots $\mathcal{I}^{\text{Linear}} = \mathbf{g}^\top (\hat{\beta}_{/i} - \hat{\beta})$ (y-axis) against $\mathcal{I}^{\text{True}} = f(\mathbf{z}, \hat{\beta}_{/i}) - f(\mathbf{z}, \hat{\beta})$ for the dependent and independent cases, respectively. The observed behavior is consistent with the predictions of Proposition 2.4 and Theorem 2.6, as well as Proposition 2.5 and Theorem 2.9. In particular, although the exact ordering of influence values differs between $\mathcal{I}^{\text{Linear}}$ and $\mathcal{I}^{\text{True}}$, the two quantities exhibit a strong correlation (exceeding 0.95 in both experiments). This is expected, since data points with large $\mathcal{I}^{\text{True}}$ tend to also have large $\mathcal{I}^{\text{Linear}}$, while those with small $\mathcal{I}^{\text{True}}$ correspondingly have small $\mathcal{I}^{\text{Linear}}$.

Moreover, when compared with the red $y = x$ reference line, the plots display a substantial vertical spread, indicating a large discrepancy between $\mathcal{I}^{\text{Linear}}$ and $\mathcal{I}^{\text{True}}$. This discrepancy is consistent with the predictions of Theorems 2.6 and 2.9.

Furthermore, the scaling range in the dependent case is much larger than that in the independent case; that is, the absolute values of the influence functions are larger when $\mathbf{z}_i = \mathbf{z}_{\text{new}}$. This observation is also consistent with the order difference in Proposition 2.4 and Proposition 2.5, as well as Theorem 2.6 and Theorem 2.9.

ALO Step The bottom row of Figure 1 evaluates the accuracy of Theorems 2.12 and 2.13 by plotting \mathcal{I}^{ALO} (y-axis) against $\mathcal{I}^{\text{Linear}}$ (x-axis). As evident from the figure, the two quantities are nearly indistinguishable, indicating that the ALO step introduces only a negligible amount of error. This empirical observation is fully consistent with the theoretical guarantees provided by these theorems.

Projection Step In the next set of simulations, we study the accuracy of the projection step and empirically evaluate the predictions of Theorem 2.14. Figure 2 plots $\mathcal{I}^{\text{TRAK}}$ against $\mathcal{I}^{\text{True}}$, where each row corresponds to a different number of projections. Specifically, the first, second, and third rows use $k = 0.75d$, $0.50d$, and $0.25d$, respectively. Throughout these experiments, we fix $p = 100$ and $d = (K-1)p = 200$.

The observed behavior is consistent with our theoretical predictions. First, the slope of the relationship between $\mathcal{I}^{\text{TRAK}}$ and $\mathcal{I}^{\text{True}}$ decreases as k decreases, in accordance with Theorem 2.14. Second, as the number of projections is reduced, data points with smaller true influence values exhibit larger relative errors. Consequently, the correlation between $\mathcal{I}^{\text{TRAK}}$ and $\mathcal{I}^{\text{True}}$ decreases as k decreases.

Additionally, as k/d becomes smaller, we observe that $\mathcal{I}^{\text{TRAK}}$ shrinks in both the dependent and independent cases, which is consistent with Theorem 2.14. Moreover, when $k/d = 0.25$ (the bottom-row setting), the difference between the left (dependent) and right (independent) cases becomes quite small. This suggests that when k is relatively small, the projection may no longer preserve a substantial discrepancy between the dependent and independent influence values.

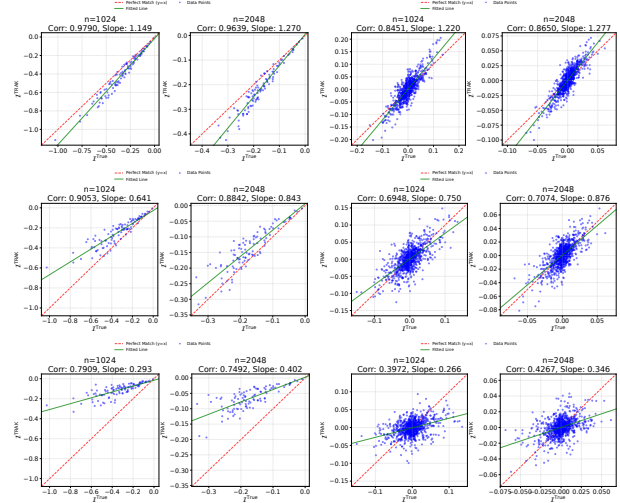


Figure 2. Experimental results for a three-class classification problem with $p = 100$ and $d = 200$. The x-axis shows $\mathcal{I}^{\text{True}}$, while the y-axis shows $\mathcal{I}^{\text{TRAK}}$ after projection. **Left two panels:** Results for the dependent case, where $\mathbf{z}_i = \mathbf{z}_{\text{new}}$. **Right two panels:** Results for the independent case, where \mathbf{z}_i and \mathbf{z}_{new} are independent. From top to bottom, the projection dimension is $k = 150$, $k = 100$, and $k = 50$, respectively. As is clear, as the number of projections decreases the correlation becomes smaller.

4. Empirical Studies

In this section, we conduct experiments on real-world datasets that may not satisfy our data-generation assumptions. The goal is to empirically assess the robustness of our theoretical conclusions to such deviations. Following Park et al. (2023), we adopt the CIFAR-10 dataset and study a multi-class classification problem. All input samples are preprocessed via channel-wise standardization to zero mean and unit variance, using statistics derived from the training partition.

We additionally construct a binary classification dataset by restricting CIFAR-10 to the *airplane* and *automobile* classes, which we refer to as CIFAR-2. Due to space constraints, we present results only for the multiclass classification setting and defer the CIFAR-2 experiments to Appendix C.4.1.

Experimental setup. We use the full CIFAR-10 dataset (10 classes, $n = 50,000$ training images). To make the calculations of $\mathcal{I}^{\text{True}}(\cdot, \cdot)$ feasible, we downsample each $32 \times 32 \times 3$ image to $8 \times 8 \times 3$ using 4×4 average pooling, yielding feature dimension $p = 192$. We train a multinomial logistic regression model (with the standard $K - 1$ parameterization), so the parameter dimension is $d = p \times (K - 1) = 192 \times 9 = 1728$. The trained model achieves a training accuracy of 42.1% and a test accuracy of 40.9%. Although this performance is lower than that of modern deep learning baselines, it is typical for models that operate directly on raw pixel inputs and lack the depth required to learn complex features. Importantly, the primary objective of this section is not to maximize predictive accuracy, but rather to assess whether our theoretical conclusions remain robust under deviations from the assumed data-generation mechanism.

Correlation analysis. We quantify approximation quality by sampling 100 test points and 100 training points (for a total of 10,000 pairs). For each pair we calculate $\mathcal{I}^{\text{True}}$, $\mathcal{I}^{\text{Linear}}$, \mathcal{I}^{ALO} . The results of our simulations are reported in Figure 3. Again our results are consistent with our main results: (i) the linearization introduces large errors; however $\mathcal{I}^{\text{Linear}}$ exhibits strong correlation with $\mathcal{I}^{\text{True}}$ ($\rho = 0.916$). (ii) The error between \mathcal{I}^{ALO} and $\mathcal{I}^{\text{Linear}}$ is negligible, and hence the correlation between the two quantities is very large $\rho = 0.999$. Hence, the results are consistent with the what we observed on simulated data in Section 3.

Rank alignment. Beyond correlation, we assess retrieval quality by comparing the top- k data points selected by $\mathcal{I}^{\text{True}}$, $\mathcal{I}^{\text{Linear}}$, and \mathcal{I}^{ALO} . We evaluate both proponents (Top- k) and opponents (Bottom- k) using two ranking-based metrics. For each test point, we compute: (i) **Exact Match Count**, defined as the number of test points (out of 100) for which the retrieved top- k list exactly matches the corresponding leave-one-out (LOO) list, including the ordering; and (ii) **Overlap Ratio**, defined as the fraction of overlap between the retrieved and exact top- k sets, averaged across test points.

The results in Table 1 indicate that exact matches become increasingly rare as k grows, reflecting the higher dimensionality and increased class complexity of the problem. Nevertheless, the overlap ratio remains stable and consistently exceeds 70% across all values of k , demonstrating that the approximate influence methods largely preserve the

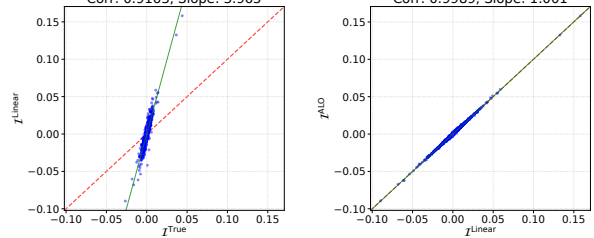


Figure 3. CIFAR-10: Correlation between $\mathcal{I}^{\text{True}}$ and $\mathcal{I}^{\text{Linear}}$, and between $\mathcal{I}^{\text{Linear}}$ and \mathcal{I}^{ALO} . Results are aggregated over 100 held-out test points and 100 training points (10,000 pairs).

Table 1. Rank alignment between exact and approximate influence rankings on CIFAR-10. We compare $\mathcal{I}^{\text{True}}$ and $\mathcal{I}^{\text{Linear}}$; $\mathcal{I}^{\text{True}}$ and \mathcal{I}^{ALO} separately. Exact Matches count the number of test points (out of 100) with identical rankings up to size- k , while Overlap Ratio is the average set overlap.

Metric	Size (k)					
	1	3	5	10	20	50
<i>Proponents (Top-k Positive Influence)</i>						
$\mathcal{I}^{\text{Linear}}$ Exact Matches	68	15	0	0	0	0
$\mathcal{I}^{\text{Linear}}$ Overlap Ratio	0.680	0.737	0.702	0.736	0.723	0.784
\mathcal{I}^{ALO} Exact Matches	67	15	0	0	0	0
\mathcal{I}^{ALO} Overlap Ratio	0.670	0.737	0.706	0.733	0.726	0.787
<i>Opponents (Bottom-k Negative Influence)</i>						
$\mathcal{I}^{\text{Linear}}$ Exact Matches	69	18	1	0	0	0
$\mathcal{I}^{\text{Linear}}$ Overlap Ratio	0.690	0.740	0.740	0.743	0.730	0.784
\mathcal{I}^{ALO} Exact Matches	70	16	1	0	0	0
\mathcal{I}^{ALO} Overlap Ratio	0.700	0.737	0.750	0.741	0.726	0.787

most influential data points even when exact rankings differ.

5. Conclusion

TRAK is a widely used data attribution method that attains scalability through three approximations: linearization, approximate leave-one-out (ALO), and projection. In this work, we theoretically analyze the errors introduced by each step. We show that the ALO approximation incurs negligible error, while the linearization step introduces substantial error but still preserves the ability to distinguish highly influential data points from unimportant ones. In contrast, the projection step can introduce significant additional error, and using too few projections may prevent TRAK from reliably identifying influential points. Overall, our results clarify both the strengths and limitations of TRAK and provide guidance for its effective use at scale.

Impact Statement

This work provides a theoretical analysis of the TRAK algorithm, a widely used method for data attribution in modern machine learning systems. By clarifying when TRAK produces reliable influence estimates and identifying regimes in

which its approximations may break down, our results help practitioners use data attribution tools more responsibly and interpret their outputs with appropriate caution. Improved understanding of data attribution methods can support transparency, debugging, and accountability in machine learning pipelines. At the same time, the techniques studied here do not introduce new capabilities for misuse, and we do not anticipate direct negative societal impacts beyond those already associated with data attribution and interpretability methods.

References

Anderson, T. W. *An Introduction to Multivariate Statistical Analysis*. Wiley, 1958.

Auddy, A., Zou, H., Rahnama Rad, K., and Maleki, A. Approximate leave-one-out cross validation for regression with l_1 regularizers. *IEEE Transactions on Information Theory*, 70(11):8040–8071, 2024.

Beirami, A., Razaviyayn, M., Shahrampour, S., and Tarokh, V. On optimal generalizability in parametric learning. *Advances in Neural Information Processing Systems*, 30, 2017.

Ghorbani, A. and Zou, J. Data shapley: Equitable valuation of data for machine learning. In *International conference on machine learning*, pp. 2242–2251. PMLR, 2019.

Guu, K., Webson, A., Pavlick, E., Dixon, L., Tenney, I., and Bolukbasi, T. Simfluence: Modeling the influence of individual training examples by simulating training runs. *arXiv preprint arXiv:2303.08114*, 2023.

Hammoudeh, Z. and Lowd, D. Identifying a training-set attack’s target using renormalized influence estimation. In *Proceedings of the 2022 ACM SIGSAC Conference on Computer and Communications Security*, pp. 1367–1381, 2022.

Hammoudeh, Z. and Lowd, D. Training data influence analysis and estimation: A survey. *Machine Learning*, 113(5):2351–2403, 2024.

Hampel, F. R. The influence curve and its role in robust estimation. *Journal of the American Statistical Association*, 69(346):383–393, 1974.

Han, X., Wallace, B. C., and Tsvetkov, Y. Explaining black box predictions and unveiling data artifacts through influence functions. *arXiv preprint arXiv:2005.06676*, 2020.

Ilyas, A., Park, S. M., Engstrom, L., Leclerc, G., and Madry, A. Datamodels: Predicting predictions from training data. In *Proceedings of the 39th International Conference on Machine Learning*, 2022.

Jia, R., Dao, D., Wang, B., Hubis, F. A., Hynes, N., Gürel, N. M., Li, B., Zhang, C., Song, D., and Spanos, C. J. Towards efficient data valuation based on the shapley value. In *The 22nd International Conference on Artificial Intelligence and Statistics*, pp. 1167–1176. PMLR, 2019.

Jin, C., Netrapalli, P., Ge, R., Kakade, S. M., and Jordan, M. I. A short note on concentration inequalities for random vectors with subgaussian norm. *arXiv preprint arXiv:1902.03736*, 2019.

Koh, P. W. and Liang, P. Understanding black-box predictions via influence functions. In Precup, D. and Teh, Y. W. (eds.), *Proceedings of the 34th International Conference on Machine Learning*, volume 70 of *Proceedings of Machine Learning Research*, pp. 1885–1894. PMLR, 2017.

Park, S. M., Georgiev, K., Ilyas, A., Leclerc, G., and Madry, A. TRAK: Attributing model behavior at scale. In *Proceedings of the 40th International Conference on Machine Learning (ICML)*, pp. 27074–27113. PMLR, 2023.

Rad, K. R. and Maleki, A. A scalable estimate of the extra-sample prediction error via approximate leave-one-out. *Journal of the Royal Statistical Society Series B: Statistical Methodology*, 82(4):965–996, 2020.

Sagun, L., Evci, U., Güney, V. U., Dauphin, Y. N., and Bottou, L. Empirical analysis of the Hessian of overparametrized neural networks. In *Proceedings of the 6th International Conference on Learning Representations (ICLR) Workshop Track*, 2018.

Vershynin, R. *High-dimensional probability*, 2009.

Wang, J. T., Mittal, P., Song, D., and Jia, R. Data shapley in one training run. *arXiv preprint arXiv:2406.11011*, 2024.

Xia, M., Malladi, S., Gururangan, S., Arora, S., and Chen, D. Less: Selecting influential data for targeted instruction tuning. *arXiv preprint arXiv:2402.04333*, 2024.

Ye, H., Liu, T., Zhang, A., Hua, W., and Jia, W. Cognitive mirage: A review of hallucinations in large language models. *arXiv preprint arXiv:2309.06794*, 2023.

Yeh, C.-K., Hsieh, C.-Y., Suggala, A., Inouye, D. I., and Ravikumar, P. K. On the (in)fidelity and sensitivity of explanations. *Advances in Neural Information Processing Systems*, 32, 2019.

Appendix

Organization of the Appendix

- **Section A** summarizes additional methodological details. In particular, in Section A.1 we discuss how to transform a multi-class classification problem into a nonlinear scalar-output function $f(\cdot, \cdot)$.
- **Section B** summarizes all theoretical and technical details of the paper. Section B.1 collects all assumptions used throughout the paper. We further verify that these assumptions hold for common GLM loss functions in Section B.4, and show that they are satisfied by linear models and one-layer neural networks in Section B.5. All proofs are provided in Section B.2, and all technical lemmas are collected in Section B.3. A roadmap of our main theorems is summarized in Table 2.
- **Section C** presents additional simulation results that further verify our theoretical findings. Sections C.1 and C.2 summarize results for the independent case: Section C.1 focuses on correlation-based analyses, while Section C.2 focuses on magnitude-based analyses. Section C.3 reports simulation results for the dependent case $\mathbf{z}_i = \mathbf{z}_{\text{new}}$. Finally, Section C.4 presents results on real-world empirical datasets.

Table 2. Roadmap of theoretical results in the Appendix.

Influence Function Approximation				
	True Influence	Linearization Step	ALO Step	Projection Step
Theorem	$\mathbf{z}_i = \mathbf{z}_{\text{new}}$	Theorem 2.4	Theorem 2.6	Theorem 2.12
	Independent	Theorem 2.5	Theorem 2.9	Theorem 2.13
Proof	$\mathbf{z}_i = \mathbf{z}_{\text{new}}$	Appendix B.2.1	Appendix B.2.3	Appendix B.2.5
	Independent	Appendix B.2.2	Appendix B.2.4	Appendix B.2.6
				Appendix B.2.7

A. More Details

A.1. Multi-class Classification Extension

The goal of this section is to extend our analysis to the multiclass classification setting. We consider a dataset with K classes and employ the standard cross-entropy loss,

$$\mathcal{L}_{\text{CE}}(\mathbf{z}, \boldsymbol{\beta}) = -\log p_y(\mathbf{z}, \boldsymbol{\beta}),$$

where $p_y(\mathbf{z}, \boldsymbol{\beta})$ denotes the model's predicted probability for the true class label y associated with the data point \mathbf{z} . Since we consider a multiclass classification problem, the model must produce class probabilities for all K classes. Even in the simplest setting, the model parameters therefore take the form

$$\mathbf{W} = (\mathbf{W}_1, \dots, \mathbf{W}_{K-1}, \mathbf{W}_K)^\top,$$

where each $\mathbf{W}_k \in \mathbb{R}^p$ corresponds to the weight vector for class k . For identifiability, we fix $\mathbf{W}_K = \mathbf{0}_p$. We then define

$$\boldsymbol{\beta} := \text{vec}(\mathbf{W}_{[1:(K-1),:]}) \in \mathbb{R}^d,$$

where the parameter dimension is $d = (K-1)p > p$; thus, this model is no longer a simple linear model, unlike the binary classification case. To address this complexity, we employ a method similar to that used in (Park et al., 2023). Specifically, we define:

$$f(\mathbf{z}, \boldsymbol{\beta}) = \log \left(\frac{p(\mathbf{z}, \boldsymbol{\beta})}{1 - p(\mathbf{z}, \boldsymbol{\beta})} \right), \quad p(\mathbf{z}, \boldsymbol{\beta}) = \frac{e^{\mathbf{W}_y^\top \mathbf{x}}}{\sum_{j=1}^K e^{\mathbf{W}_j^\top \mathbf{x}}},$$

where we set $\mathbf{W}_K = \mathbf{0}_p$. The loss function can then be expressed as:

$$\mathcal{L}_{\text{CE}}(\mathbf{z}, \boldsymbol{\beta}) = \log(1 + e^{-f(\mathbf{z}, \boldsymbol{\beta})}) = l(f(\mathbf{z}, \boldsymbol{\beta})),$$

where $l(s) = \log(1 + e^{-s})$. We can further express the gradient as:

$$\mathbf{g} = \nabla_{\boldsymbol{\beta}} f(\mathbf{z}, \hat{\boldsymbol{\beta}}) = \frac{(\mathbf{1}_y - \mathbf{p}(\mathbf{z}, \hat{\boldsymbol{\beta}}))}{1 - p(\mathbf{z}, \hat{\boldsymbol{\beta}})} \otimes \mathbf{x},$$

where $\mathbf{1}_y$ is a vector of length $K-1$ with entries $\mathbf{1}_{y[k]} = 1$ if $y = k$ and 0 otherwise (note that if $y = K$, $\mathbf{1}_y$ is a zero vector). Similarly, $\mathbf{p}(\mathbf{z}, \boldsymbol{\beta}) = \left(\frac{\exp(\mathbf{W}_1^\top \mathbf{x})}{\sum_{j=1}^K \exp(\mathbf{W}_j^\top \mathbf{x})}, \dots, \frac{\exp(\mathbf{W}_{K-1}^\top \mathbf{x})}{\sum_{j=1}^K \exp(\mathbf{W}_j^\top \mathbf{x})} \right)^\top$ is also a vector of length $K-1$. Finally, we obtain $\mathbf{g} \in \mathbb{R}^d$ with $d = (K-1)p$.

B. Proofs

B.1. Notations and Assumptions

B.1.1. NOTATIONS AND DEFINITIONS

Let $\sigma_{\min}(A)$ and $\sigma_{\max}(A)$ denote the minimum and maximum eigenvalues of a matrix A , respectively. A random vector $\mathbf{x} \in \mathbb{R}^d$ is called norm-subGaussian with parameter σ , denoted as $nSG(\sigma)$, if there exists $\sigma > 0$ such that

$$\mathbb{P}(\|\mathbf{x} - \mathbb{E}\mathbf{x}\| \geq t) \leq 2e^{-\frac{t^2}{2\sigma^2}} \quad \text{for all } t \geq 0,$$

as defined in Jin et al. (2019).

B.1.2. DETAILED MODELING ASSUMPTIONS

In this section, we provide the formal statements of the assumptions summarized in Section 2.1.

Assumption B.1 (Sub-Gaussian design). The rows of $\mathbf{X}_n \in \mathbb{R}^{n \times p}$ are independent zero-mean sub-Gaussian random vectors with covariance matrix $\boldsymbol{\Sigma}_p$. We assume $\boldsymbol{\Sigma}_p$ is well conditioned, i.e., $\rho_{\max} \asymp \rho_{\min} \asymp \Theta(1/\|\boldsymbol{\beta}^*\|^2)$, where ρ_{\max} and ρ_{\min} denote the extremal eigenvalues.

Justification of Scaling. When $d > p$ and $\beta^* = \text{vec}(\mathbf{W})$ with $\mathbf{W} \in \mathbb{R}^{h \times p}$, we typically have $f(\mathbf{x}, \beta^*) \asymp \|\mathbf{W}\mathbf{x}\| = O_p(1)$. Assuming that both $\mathbf{W}^\top \mathbf{W}$ and Σ are well-conditioned, we obtain

$$\|\mathbf{W}\mathbf{x}\|^2 \asymp \frac{\|\mathbf{W}\|_F^2}{p} \|\mathbf{x}\|^2 \asymp \frac{\|\mathbf{W}\|_F^2}{p} \cdot p \|\Sigma\| = \|\mathbf{W}\|_F^2 \|\Sigma\|,$$

which implies $\|\Sigma\| \asymp 1/\|\beta^*\|^2$.

Assumption B.2 (Regularity conditions on ∇f). Define $\beta_1 = t_1 \check{\beta} + t_2 \check{\beta}_{/i} + (1 - t_1 - t_2)\beta^*$ and $\beta_2 = t_1 \hat{\beta} + t_2 \hat{\beta}_{/i} + (1 - t_1 - t_2)\beta^*$. For $j = 1, 2$ and \mathbf{x} ranging over all $\mathbf{x}_{\text{new}}, \mathbf{x}_1, \dots, \mathbf{x}_n$, there exists a constant $C_1 = O(1)$ such that with probability at least $1 - q_n$ (where $q_n \rightarrow 0$):

$$\sup_{i \in [n]} \sup_{\substack{t_1, t_2 \in [0, 1] \\ t_1 + t_2 \leq 1}} \|\nabla f(\mathbf{x}, \beta_j)\| \leq C_1 \cdot \text{poly}(\log n).$$

Assumption B.3 (Regularity conditions on \mathbf{G} and empirical Hessian). Recall $\mathbf{G}(\beta)$ from Eq. (5). Define $\beta_1 = t_1 \check{\beta} + t_2 \check{\beta}_{/i} + (1 - t_1 - t_2)\beta^*$ and $\beta_2 = t_1 \hat{\beta} + t_2 \hat{\beta}_{/i} + (1 - t_1 - t_2)\beta^*$. For $j = 1, 2$, there exist constants $C_2, c_1 = \Theta(1)$ such that with probability at least $1 - q_n$:

$$\begin{aligned} \frac{1}{n} \sigma_{\max}(\mathbf{G}(\hat{\beta})^\top \mathbf{G}(\hat{\beta})) &\leq C_2 \|\beta^*\|^{-2}, \\ \inf_{i \in [n]} \inf_{\substack{t_1, t_2 \in [0, 1] \\ t_1 + t_2 \leq 1}} \frac{1}{n} \sigma_{\min}(\mathbf{G}(\beta_j)^\top \mathbf{G}(\beta_j)) &\geq c_1 \|\beta^*\|^{-2}, \\ \inf_{i \in [n]} \inf_{\substack{t_1, t_2 \in [0, 1] \\ t_1 + t_2 \leq 1}} \frac{1}{n} \sigma_{\min} \left(\sum_{i=1}^n \nabla^2 \ell(y_i, f(\mathbf{x}_i, \beta_j)) \right) &\geq c_1 \|\beta^*\|^{-2}, \\ \sup_{i \in [n]} \sup_{\substack{t_1, t_2 \in [0, 1] \\ t_1 + t_2 \leq 1}} \frac{1}{n} \sigma_{\max} \left(\sum_{i=1}^n \nabla^2 \ell(y_i, f(\mathbf{x}_i, \beta_j)) \right) &\leq \tilde{c}_1 \|\beta^*\|^{-2}. \end{aligned}$$

Assumption B.4 (Regularity conditions on $\nabla^2 f$). There exists a constant $C_2 = O(1)$ such that with probability at least $1 - q_n$:

$$\sup_{i \in [n]} \sup_{\substack{t_1, t_2 \in [0, 1] \\ t_1 + t_2 \leq 1}} \|\nabla^2 f(\mathbf{x}_{\text{new}}, t_1 \hat{\beta}_{/i} + t_2 \hat{\beta} + (1 - t_1 - t_2)\beta^*)\| \leq C_2 \|\beta^*\|^{-2}.$$

Assumption B.5 (Regularity conditions on ℓ). There exist constants $\tilde{C}_1, \tilde{C}_2 = O(1)$, and $\mu > 0$ such that with probability at least $1 - q_n$:

$$\begin{aligned} \sup_{i \in [n]} \sup_{t \in [0, 1]} |\dot{\ell}(y_i, f(\mathbf{x}_i, \hat{\beta}_{/i}))| &\leq \tilde{C}_1 \cdot \text{poly}(\log n), \\ \sup_{i \in [n]} \sup_{t \in [0, 1]} |\ddot{\ell}(y_i, f(\mathbf{x}_i, \beta^*))| &\leq \tilde{C}_1 \cdot \text{poly}(\log n), \\ \sup_{i \in [n]} \sup_{t \in [0, 1]} |\ddot{\ell}(y_i, f(\mathbf{x}_i, \hat{\beta}))| &\leq \tilde{C}_1 \cdot \text{poly}(\log n), \\ \inf_{i \in [n]} \inf_{t \in [0, 1]} \ddot{\ell}(y_i, f(\mathbf{x}_i, (1 - t)\hat{\beta}_{/i} + t\hat{\beta})) &\geq \mu. \end{aligned}$$

Additionally, the Hessian of the loss satisfies the following Lipschitz-like conditions. Define $\beta_1 = t_1 \check{\beta} + t_2 \check{\beta}_{/i} + (1 - t_1 - t_2)\beta^*$ and $\beta_2 = t_1 \hat{\beta} + t_2 \hat{\beta}_{/i} + (1 - t_1 - t_2)\beta^*$. For $j = 1, 2$ and \mathbf{x} ranging over all $\mathbf{x}_{\text{new}}, \mathbf{x}_1, \dots, \mathbf{x}_n$:

$$\begin{aligned} \sup_{i \in [n]} \sup_{t \in [0, 1]} \frac{\|\ddot{\ell}_{/i}((1 - t)\check{\beta}_{/i} + t\check{\beta}) - \ddot{\ell}_{/i}(\check{\beta})\|_2}{\|\check{\beta} - \check{\beta}_{/i}\|_2} &\leq \tilde{C}_2 \frac{\sqrt{n}}{\|\beta^*\|} \sqrt{\text{poly}(\log n)}, \\ \sup_{i \in [n]} \sup_{t \in [0, 1]} \frac{\|\ddot{\ell}_{/i}((1 - t)\check{\beta}_{/i} + t\check{\beta}) - \ddot{\ell}_{/i}(\beta^*)\|_2}{\|\check{\beta} - \beta^*\|_2} &\leq \tilde{C}_2 \frac{\sqrt{n}}{\|\beta^*\|} \sqrt{\text{poly}(\log n)}, \\ \sup_{i \in [n]} \sup_{t \in [0, 1]} \frac{\|\ddot{\ell}_{/i}(y_j, f(\mathbf{x}_j, (1 - t)\hat{\beta}_{/i} + t\hat{\beta})) - \ddot{\ell}_{/i}(y_j, f(\mathbf{x}_j, \beta^*))\|_2}{\|\hat{\beta} - \beta^*\|_2} &\leq \tilde{C}_2 \frac{\sqrt{n}}{\|\beta^*\|} \sqrt{\text{poly}(\log n)}. \end{aligned}$$

Assumption B.6 (Unique minimizer). For $\mathbf{g}_i = \nabla f(\mathbf{x}_i, \hat{\beta})$, the function $\sum_{j=1}^n \ell(y_j, \mathbf{g}_j^\top \beta + \mathbf{b}_j) \mathbf{g}_j$ has a unique minimizer.

Assumption B.7 (Normed-Subgaussian Gradients). Let $\mathbf{g}_{i,*} = \nabla f(\mathbf{x}_i, \beta^*)$. We assume that for $i \in [n]$, there exists $\sigma > 0$ such that $\mathbf{g}_{i,*} \stackrel{\text{iid}}{\sim} \text{nSG}(\sigma)$. Moreover, denote $\Sigma_g^* = \mathbb{E}[\mathbf{g}_{i,*} \mathbf{g}_{i,*}^\top]$, $\lambda_{\max}(\Sigma_g^*) \asymp \lambda_{\min}(\Sigma_g^*) = O(\|\beta^*\|^{-2})$.

The following assumption is only relevant if we want to prove the lower bound in Proposition 2.4 and 2.6.

Assumption B.8 (Uniform Lower Bounds). There exists a constant D_1 such that

$$\|\nabla f(\mathbf{x}_i; \beta^*)\|_2^2 \geq D_1,$$

and

$$|\dot{\ell}(y_i, f(\mathbf{x}_i, \beta^*))| \geq D_1.$$

B.2. Proofs of Theorems

B.2.1. PROOF OF PROPOSITION 2.4

By using the mean value theorem we have

$$\mathcal{I}^{\text{True}}(\mathbf{z}_i, \mathbf{z}_{\text{new}}) \triangleq f(\mathbf{x}_{\text{new}}; \hat{\beta}_{/i}) - f(\mathbf{x}_{\text{new}}; \hat{\beta}) = \nabla^\top f(\mathbf{x}_{\text{new}}, \tilde{\beta})(\hat{\beta}_{/i} - \hat{\beta}), \quad (14)$$

where $\tilde{\beta}$ is a point on the line segment that connects $\hat{\beta}_{/i}$ and $\hat{\beta}$. Using the first order optimality conditions for $\hat{\beta}$ and $\hat{\beta}_{/i}$ we have

$$\begin{aligned} 0 &= \frac{1}{n} \sum_{j \neq i} \nabla l(y_j, f(\mathbf{x}_j, \hat{\beta}_{/i})) \\ &= \frac{1}{n} \sum_{j \neq i} \nabla l(y_j, f(\mathbf{x}_j, \hat{\beta})) + \frac{1}{n} \nabla l(y_i, f(\mathbf{x}_i, \hat{\beta})). \end{aligned} \quad (15)$$

Hence, by using the integral form of the mean value theorem we have

$$(\hat{\beta}_{/i} - \hat{\beta}) = \left(\int_{t=0}^1 \frac{1}{n} \sum_{j \neq i} \nabla^2 l(y_j, f(\mathbf{x}_j, t\hat{\beta}_{/i} + (1-t)\hat{\beta})) dt \right)^{-1} \left(\frac{1}{n} \nabla l(y_i, f(\mathbf{x}_i, \hat{\beta})) \right). \quad (16)$$

By combining (14) and (16) we obtain

$$\mathcal{I}^{\text{True}}(\mathbf{z}_i, \mathbf{z}_{\text{new}}) = \nabla^\top f(\mathbf{x}_{\text{new}}, \tilde{\beta}) \left(\int_{t=0}^1 \frac{1}{n} \sum_{j \neq i} \nabla^2 l(y_j, f(\mathbf{x}_j, t\hat{\beta}_{/i} + (1-t)\hat{\beta})) dt \right)^{-1} \left(\frac{1}{n} \nabla l(y_i, f(\mathbf{x}_i, \hat{\beta})) \right). \quad (17)$$

Therefore we can use the Cauchy-Schwartz inequality and Assumption B.3 to prove

$$|\mathcal{I}^{\text{True}}(\mathbf{z}_i, \mathbf{z}_{\text{new}})| \leq \frac{\|\beta^*\|^2}{c_1 n} \|\nabla f(\mathbf{x}_{\text{new}}, \tilde{\beta})\| \|\nabla l(y_i, f(\mathbf{x}_i, \hat{\beta}))\| = O_P\left(\frac{\text{poly}(\log n) \|\beta^*\|^2}{n}\right), \quad (18)$$

where to obtain the last equality we have used Assumptions B.2 and B.5.

To prove the second part of the theorem, i.e. (9), again we use (17). Note that

$$\begin{aligned} \mathcal{I}^{\text{True}}(\mathbf{z}_i, \mathbf{z}_i) &= \nabla^\top f(\mathbf{x}_{\text{new}}, \tilde{\beta}) \left(\int_{t=0}^1 \frac{1}{n} \sum_{j \neq i} \nabla^2 l(y_j, f(\mathbf{x}_j, t\hat{\beta}_{/i} + (1-t)\hat{\beta})) dt \right)^{-1} \left(\frac{1}{n} \nabla l(y_i, f(\mathbf{x}_i, \hat{\beta})) \right) \\ &= \nabla^\top f(\mathbf{x}_{\text{new}}, \beta^*) \left(\int_{t=0}^1 \frac{1}{n} \sum_{j \neq i} \nabla^2 l(y_j, f(\mathbf{x}_j, t\hat{\beta}_{/i} + (1-t)\hat{\beta})) dt \right)^{-1} \frac{1}{n} \nabla l(y_i, f(\mathbf{x}_i, \hat{\beta})) \\ &+ \left(\nabla^\top f(\mathbf{x}_{\text{new}}, \hat{\beta}) - \nabla^\top f(\mathbf{x}_{\text{new}}, \beta^*) \right) \left(\int_{t=0}^1 \frac{1}{n} \sum_{j \neq i} \nabla^2 l(y_j, f(\mathbf{x}_j, t\hat{\beta}_{/i} + (1-t)\hat{\beta})) dt \right)^{-1} \frac{1}{n} \nabla l(y_i, f(\mathbf{x}_i, \hat{\beta})) \\ &= \nabla^\top f(\mathbf{x}_{\text{new}}, \beta^*) \left(\int_{t=0}^1 \frac{1}{n} \sum_{j \neq i} \nabla^2 l(y_j, f(\mathbf{x}_j, t\hat{\beta}_{/i} + (1-t)\hat{\beta})) dt \right)^{-1} \frac{1}{n} \nabla l(y_i, f(\mathbf{x}_i, \hat{\beta})) + O_P\left(\frac{\|\beta^*\|^2}{n^{1.5-\epsilon}}\right), \end{aligned} \quad (19)$$

where to obtain the last inequality we have used the Cauchy-Schwartz inequality and Lemma B.10. With a similar reasoning we can further simplify (19) in the following way:

$$\begin{aligned} \mathcal{I}^{\text{True}}(\mathbf{z}_i, \mathbf{z}_i) &= \nabla^\top f(\mathbf{x}_{\text{new}}, \boldsymbol{\beta}^*) \left(\int_{t=0}^1 \frac{1}{n} \sum_{j \neq i} \nabla^2 l(y_j, f(\mathbf{x}_j, t\hat{\boldsymbol{\beta}}_{/i} + (1-t)\hat{\boldsymbol{\beta}})) dt \right)^{-1} \frac{1}{n} \dot{\ell}(y_i, f(\mathbf{x}_i, \boldsymbol{\beta}^*) \nabla f(\mathbf{x}_i, \boldsymbol{\beta}^*)) \\ &+ O_P \left(\frac{\|\boldsymbol{\beta}^*\|^2}{n^{1.5-\epsilon}} \right). \end{aligned} \quad (20)$$

Furthermore, using Assumption B.3 we have

$$|\mathcal{I}^{\text{True}}(\mathbf{z}_i, \mathbf{z}_i)| \geq \frac{\|\boldsymbol{\beta}^*\|^2}{\tilde{c}_2 n} |\nabla^\top f(\mathbf{x}_i, \boldsymbol{\beta}^*) \nabla f(\mathbf{x}_i, \boldsymbol{\beta}^*)| |\dot{\ell}(y_i, f(\mathbf{x}_i, \boldsymbol{\beta}^*))| - O_P \left(\frac{\|\boldsymbol{\beta}^*\|^2}{n^{1.5-\epsilon}} \right). \quad (21)$$

Assumption B.8 then implies (9).

B.2.2. PROOF OF PROPOSITION 2.5

First note that

$$\begin{aligned} |f(\mathbf{x}_{\text{new}}, \hat{\boldsymbol{\beta}}_{/i}) - f(\mathbf{x}_{\text{new}}, \hat{\boldsymbol{\beta}})| &\leq \sup_{t \in [0,1]} \|\mathbf{g}_{\text{new}}^\top(\hat{\boldsymbol{\beta}}_{/i} - \hat{\boldsymbol{\beta}}) + (\hat{\boldsymbol{\beta}}_{/i} - \hat{\boldsymbol{\beta}})^\top \nabla^2 f(\mathbf{x}_{\text{new}}, (1-t)\hat{\boldsymbol{\beta}}_{/i} + t\hat{\boldsymbol{\beta}})(\hat{\boldsymbol{\beta}}_{/i} - \hat{\boldsymbol{\beta}})\| \\ &\leq \sup_{t \in [0,1]} \|\nabla^2 f(\mathbf{x}_{\text{new}}, (1-t)\hat{\boldsymbol{\beta}}_{/i} + t\hat{\boldsymbol{\beta}})\| \|\hat{\boldsymbol{\beta}}_{/i} - \hat{\boldsymbol{\beta}}\|^2 + \|\mathbf{g}_{\text{new},*}^\top(\hat{\boldsymbol{\beta}}_{/i} - \hat{\boldsymbol{\beta}})\| + \|(\mathbf{g}_{\text{new}} - \mathbf{g}_{\text{new},*})(\hat{\boldsymbol{\beta}}_{/i} - \hat{\boldsymbol{\beta}})\| \\ &\leq C_2 \|\boldsymbol{\beta}^*\|^{-2} \|\hat{\boldsymbol{\beta}}_{/i} - \hat{\boldsymbol{\beta}}\|^2 + \|\mathbf{g}_{\text{new},*}^\top(\hat{\boldsymbol{\beta}}_{/i} - \hat{\boldsymbol{\beta}})\| + \|\mathbf{g}_{\text{new}} - \mathbf{g}_{\text{new},*}\| \|\hat{\boldsymbol{\beta}}_{/i} - \hat{\boldsymbol{\beta}}\|. \end{aligned}$$

The first inequality follows from the mean value theorem. The second inequality uses the triangle inequality. The third inequality follows from Assumption B.4 and the Cauchy-Schwarz inequality. Thus, it suffices to bound the three terms in the last expression.

1. Bounding $\|\hat{\boldsymbol{\beta}}_{/i} - \hat{\boldsymbol{\beta}}\|$. Using the mean value theorem and the first-order optimality conditions in (1) and (3), we have:

$$\begin{aligned} 0 &= \frac{1}{n} \sum_{j=1}^n \nabla l(y_j, f(\mathbf{x}_j, \hat{\boldsymbol{\beta}}_{/i})) - \frac{1}{n} \nabla l(y_i, f(\mathbf{x}_i, \hat{\boldsymbol{\beta}}_{/i})) \\ &= \frac{1}{n} \sum_{j=1}^n \nabla l(y_j, f(\mathbf{x}_j, \hat{\boldsymbol{\beta}})) + \frac{1}{n} \sum_{j=1}^n \nabla^2 l(y_j, f(\mathbf{x}_j, \tilde{\boldsymbol{\beta}}_{/i}))(\hat{\boldsymbol{\beta}}_{/i} - \hat{\boldsymbol{\beta}}) - \frac{1}{n} \nabla l(y_i, f(\mathbf{x}_i, \hat{\boldsymbol{\beta}}_{/i})) \\ &= \frac{1}{n} \sum_{j=1}^n \nabla^2 l(y_j, f(\mathbf{x}_j, \tilde{\boldsymbol{\beta}}_{/i}))(\hat{\boldsymbol{\beta}}_{/i} - \hat{\boldsymbol{\beta}}) - \frac{1}{n} \nabla l(y_i, f(\mathbf{x}_i, \hat{\boldsymbol{\beta}}_{/i})), \end{aligned}$$

where $\tilde{\boldsymbol{\beta}}_{/i} = (1-t_i)\hat{\boldsymbol{\beta}}_{/i} + t_i\hat{\boldsymbol{\beta}}$ for some $t_i \in [0, 1]$. This implies:

$$\begin{aligned} \sup_{i \in [n]} \|\hat{\boldsymbol{\beta}}_{/i} - \hat{\boldsymbol{\beta}}\| &= \sup_{i \in [n]} \left\| \left(\frac{1}{n} \sum_{j=1}^n \nabla^2 l(y_j, f(\mathbf{x}_j, \tilde{\boldsymbol{\beta}}_{/i})) \right)^{-1} \frac{1}{n} \nabla l(y_i, f(\mathbf{x}_i, \hat{\boldsymbol{\beta}}_{/i})) \right\| \\ &\leq \sup_{i \in [n]} \sigma_{\max} \left(\frac{1}{n} \sum_{j=1}^n \nabla^2 l(y_j, f(\mathbf{x}_j, \tilde{\boldsymbol{\beta}}_{/i})) \right)^{-1} \sup_{i \in [n]} \left\| \frac{1}{n} \nabla l(y_i, f(\mathbf{x}_i, \hat{\boldsymbol{\beta}}_{/i})) \right\| \\ &\leq \frac{\tilde{C}_1 \|\boldsymbol{\beta}^*\|^2 \text{poly}(\log n)}{c_1 n}, \quad \text{with probability } \geq 1 - q_n, \end{aligned} \quad (22)$$

where to obtain the last inequality we use Assumption B.2 and B.5.

2. Bounding $\|\mathbf{g}_{\text{new}} - \mathbf{g}_{\text{new},*}\|$. From Lemma B.10, for any $\epsilon > 0$, with probability at least $1 - q_n - n^{-\epsilon}$, there exists an absolute constant s_g^* such that

$$\|\mathbf{g}_{\text{new}} - \mathbf{g}_{\text{new},*}\| \leq s_g^* (\log n)^{0.5} n^{\epsilon-0.5}. \quad (23)$$

3. Bounding $\|\mathbf{g}_{\text{new},*}^\top(\hat{\beta}_{/i} - \hat{\beta})\|$. By Assumption B.7, $\mathbf{g}_{\text{new},*}$ is sub-Gaussian. Using (22) and the independence of $\mathbf{g}_{\text{new},*}$ from $\hat{\beta}$, $\hat{\beta}_{/i}$, $\check{\beta}$, and $\check{\beta}_{/i}$, there exists an absolute constant s_g such that $\mathbf{g}_{\text{new},*}^\top(\hat{\beta}_{/i} - \hat{\beta})$ is a $s_g \frac{\|\beta^*\| \text{poly}(\log n)}{n}$ -sub-Gaussian random variable. Hence, for any $\epsilon > 0$, with probability at least $1 - 2n^{-\epsilon}$, there exists an absolute constant \hat{s}_g such that

$$\|\mathbf{g}_{\text{new},*}^\top(\hat{\beta}_{/i} - \hat{\beta})\| \leq \hat{s}_g \frac{\|\beta^*\|}{n^{1-\epsilon}}. \quad (24)$$

Final bound. Combining the bounds above, there exists a constant s_1 such that, for any $\epsilon > 0$,

$$|f(\mathbf{x}_{\text{new}}, \hat{\beta}_{/i}) - f(\mathbf{x}_{\text{new}}, \hat{\beta})| \leq s_1 \left(\frac{\|\beta^*\|^2}{n^2} \text{poly}(\log n) + \frac{\|\beta^*\|^2}{n^{1.5-\epsilon}} + \frac{\|\beta^*\|}{n^{1-\epsilon}} \right),$$

with probability at least $1 - 3(q_n + n^{-\epsilon})$. The final result follows from $\|\beta^*\|^2 \ll n^{1-\epsilon}$.

B.2.3. PROOF OF THEOREM 2.6

By the first-order optimality conditions, we have:

$$\begin{aligned} \sum_{j=1}^n \dot{\ell}(y_j, \mathbf{g}_j^\top \hat{\beta} + \mathbf{b}_j) \mathbf{g}_j &= 0, \\ \sum_{j=1}^n \dot{\ell}(y_j, \mathbf{g}_j^\top \check{\beta} + \mathbf{b}_j) \mathbf{g}_j &= 0. \end{aligned}$$

Under Assumption B.6, $\sum_{j=1}^n \ell(y_j, \mathbf{g}_j^\top \beta + \mathbf{b}_j) \mathbf{g}_j$ has a unique minimizer. Therefore, we conclude that $\hat{\beta} = \check{\beta}$.

Next, we bound the difference:

$$\begin{aligned} |f(\mathbf{x}_i, \hat{\beta}_{/i}) - (\mathbf{g}_i^\top \check{\beta}_{/i} + \mathbf{b}_i)| &= |f(\mathbf{x}_i, \hat{\beta}_{/i}) - f(\mathbf{x}_i, \hat{\beta})| + |\mathbf{g}_i^\top(\hat{\beta} - \check{\beta})| + |\mathbf{g}_i^\top(\check{\beta} - \check{\beta}_{/i})| \\ &\leq \sup_{t \in [0,1]} \|\mathbf{g}_i^\top(\hat{\beta}_{/i} - \hat{\beta}) + (\hat{\beta}_{/i} - \hat{\beta})^\top \left(\int_{t=0}^1 \nabla^2 f(\mathbf{x}_i, (1-t)\hat{\beta}_{/i} + t\hat{\beta}) dt \right) (\hat{\beta}_{/i} - \hat{\beta})\| \\ &\quad + |\mathbf{g}_i^\top(\hat{\beta} - \check{\beta})| + |\mathbf{g}_i^\top(\check{\beta} - \check{\beta}_{/i})| \\ &\leq \sup_{t \in [0,1]} \|\nabla^2 f(\mathbf{x}_i, (1-t)\hat{\beta}_{/i} + t\hat{\beta})\| \|\hat{\beta}_{/i} - \hat{\beta}\|^2 \\ &\quad + \|\mathbf{g}_{i,*}^\top(\hat{\beta}_{/i} - \hat{\beta})\| + \|\mathbf{g}_{i,*}^\top(\check{\beta} - \check{\beta}_{/i})\| \\ &\quad + \|(\mathbf{g}_i - \mathbf{g}_{i,*})(\hat{\beta}_{/i} - \hat{\beta})\| + \|(\mathbf{g}_i - \mathbf{g}_{i,*})(\check{\beta} - \check{\beta}_{/i})\| \\ &\leq C_2 \|\beta^*\|^{-2} \|\hat{\beta}_{/i} - \hat{\beta}\|^2 \\ &\quad + \|\mathbf{g}_{i,*}^\top(\hat{\beta}_{/i} - \hat{\beta})\| + \|\mathbf{g}_{i,*}^\top(\check{\beta} - \check{\beta}_{/i})\| \\ &\quad + \|\mathbf{g}_i - \mathbf{g}_{i,*}\| \|\hat{\beta}_{/i} - \hat{\beta}\| + \|\mathbf{g}_i - \mathbf{g}_{i,*}\| \|\check{\beta} - \check{\beta}_{/i}\|. \end{aligned}$$

The first inequality follows from the mean value theorem and the fact that $\check{\beta} = \hat{\beta}$. The second inequality uses the triangle and Cauchy-Schwarz inequalities. The third inequality follows from Assumption B.4 and Cauchy-Schwarz. Thus, it suffices to bound the three terms in the last three lines. Using the same method as the one used in deriving (22) we have

$$\sup_{i \in [n]} \|\check{\beta}_{/i} - \check{\beta}\| = O_P \left(\frac{\|\beta^*\|^2 \text{poly}(\log n)}{n} \right).$$

Furthermore, using the mean value theorem we have

$$\begin{aligned} \mathbf{g}_{i,*}^\top(\check{\beta}_{/i} - \check{\beta}) &= \dot{\ell}_i(\check{\beta}) \mathbf{g}_{i,*}^\top \left(\int_{t=0}^1 \mathbf{G}_{/i}^\top \text{diag}[\check{\ell}_{/i}(\check{\beta}_{/i} - t\check{\Delta}_{/i})] \mathbf{G}_{/i} dt \right)^{-1} \mathbf{g}_i \\ &= \dot{\ell}_i(\check{\beta}) \mathbf{g}_{i,*}^\top \left(\int_{t=0}^1 \mathbf{G}_{/i}^\top \text{diag}[\check{\ell}_{/i}(\check{\beta}_{/i} - t\check{\Delta}_{/i})] \mathbf{G}_{/i} dt \right)^{-1} \mathbf{g}_{i,*} + O_P \left(\frac{\|\beta^*\|^2}{n^{1.5-\epsilon}} \right), \end{aligned} \quad (25)$$

where to obtain the last equality we used an argument similar to the one we used for deriving (21). Hence, we have

$$|\mathbf{g}_{i,*}^\top(\check{\beta}_{/i} - \check{\beta})| \leq \frac{\|\beta^*\|^2}{C_2 n} |\dot{\ell}_i(\check{\beta})| \mathbf{g}_{i,*}^\top \mathbf{g}_{i,*} + O_P\left(\frac{\|\beta^*\|^2}{n^{1.5-\epsilon}}\right) = O_P\left(\frac{\text{poly}(\log n)\|\beta^*\|^2}{n}\right).$$

Similarly, we have

$$|\mathbf{g}_{i,*}^\top(\check{\beta} - \check{\beta}_{/i})| = O_P\left(\frac{\text{poly}(\log n)\|\beta^*\|^2}{n}\right).$$

Now we aim to bound the term $\|\mathbf{g}_i - \mathbf{g}_{i,*}\| \|\hat{\beta}_{/i} - \hat{\beta}\|$. According to (23) we have with high probability,

$$\|\mathbf{g}_i - \mathbf{g}_{i,*}\| \leq s_g^*(\log n)^{0.5} n^{\epsilon-0.5}. \quad (26)$$

Therefore,

$$\|\mathbf{g}_i - \mathbf{g}_{i,*}\| \|\hat{\beta}_{/i} - \hat{\beta}\| = O_P\left(\frac{\|\beta^*\|^2}{n^{1.5-\epsilon}}\right). \quad (27)$$

Combining all the calculation above we can conclude that

$$|f(\mathbf{x}_{\text{new}}, \hat{\beta}_{/i}) - (\mathbf{g}_{\text{new}}^\top \check{\beta}_{/i} + \mathbf{b}_{\text{new}})| = O_P\left(\frac{\|\beta^*\|^2 \text{poly}(\log n)}{n}\right).$$

Now we turn our attention to proving (12). First note that using the same argument as the one presented above we have

$$\begin{aligned} \mathcal{I}^{\text{Linear}}(\mathbf{z}_i, \mathbf{z}_i) &= \nabla f(\mathbf{z}_i, \hat{\beta})^\top (\check{\beta}_{/i} - \check{\beta}) = \nabla f(\mathbf{z}_i, \beta^*)^\top (\check{\beta}_{/i} - \check{\beta}) + O_P\left(\frac{\|\beta^*\|^2 \text{poly}(\log n)}{n^{1.5-\epsilon}}\right) \\ &= \dot{\ell}_i(\check{\beta}) \mathbf{g}_{i,*}^\top \left(\int_{t=0}^1 \mathbf{G}_{/i}^\top \text{diag}[\ddot{\ell}_i(\check{\beta}_{/i} - t\check{\Delta}_{/i})] \mathbf{G}_{/i} dt \right)^{-1} \mathbf{g}_i + O_P\left(\frac{\|\beta^*\|^2 \text{poly}(\log n)}{n^{1.5-\epsilon}}\right) \\ &= \dot{\ell}_i(\check{\beta}) \mathbf{g}_{i,*}^\top \left(\int_{t=0}^1 \mathbf{G}_{/i}^\top \text{diag}[\ddot{\ell}_i(\check{\beta}_{/i} - t\check{\Delta}_{/i})] \mathbf{G}_{/i} dt \right)^{-1} \mathbf{g}_{i,*} + O_P\left(\frac{\|\beta^*\|^2}{n^{1.5-\epsilon}}\right), \end{aligned} \quad (28)$$

Using (36) we can conclude that with high probability we have that

$$|\dot{\ell}_i(\check{\beta}) \mathbf{g}_{i,*}^\top \left(\int_{t=0}^1 \mathbf{G}_{/i}^\top \text{diag}[\ddot{\ell}_i(\check{\beta}_{/i} - t\check{\Delta}_{/i})] \mathbf{G}_{/i} dt \right)^{-1} \mathbf{g}_{i,*}| \geq |\dot{\ell}_i(\check{\beta})| \mathbf{g}_{i,*}^\top \mathbf{g}_{i,*} \frac{2\|\beta^*\|^2}{c_1 \mu n}. \quad (29)$$

Combing this results with Assumption B.8 establishes (12).

B.2.4. PROOF OF THEOREM 2.9

By the first-order optimality conditions for $\hat{\beta}$ and $\check{\beta}$, we have:

$$\begin{aligned} \sum_{j=1}^n \dot{\ell}(y_j, \mathbf{g}_j^\top \hat{\beta} + \mathbf{b}_j) \mathbf{g}_j &= 0, \\ \sum_{j=1}^n \dot{\ell}(y_j, \mathbf{g}_j^\top \check{\beta} + \mathbf{b}_j) \mathbf{g}_j &= 0. \end{aligned}$$

Under Assumption B.6, $\sum_{j=1}^n \ell(y_j, \mathbf{g}_j^\top \beta + \mathbf{b}_j) \mathbf{g}_j$ has a unique minimizer; therefore, we conclude that $\hat{\beta} = \check{\beta}$.

Next, we bound the difference:

$$\begin{aligned}
 |f(\mathbf{x}_{\text{new}}, \hat{\beta}_{/i}) - (\mathbf{g}_{\text{new}}^\top \check{\beta}_{/i} + \mathbf{b}_{\text{new}})| &= |f(\mathbf{x}_{\text{new}}, \hat{\beta}_{/i}) - f(\mathbf{x}_{\text{new}}, \hat{\beta})| + |\mathbf{g}_{\text{new}}^\top (\hat{\beta} - \check{\beta})| + |\mathbf{g}_{\text{new}}^\top (\check{\beta} - \check{\beta}_{/i})| \\
 &\leq \sup_{t \in [0,1]} \|\mathbf{g}_{\text{new}}^\top (\hat{\beta}_{/i} - \hat{\beta}) + (\hat{\beta}_{/i} - \hat{\beta})^\top \nabla^2 f(\mathbf{x}_{\text{new}}, (1-t)\hat{\beta}_{/i} + t\hat{\beta})(\hat{\beta}_{/i} - \hat{\beta})\| \\
 &\quad + |\mathbf{g}_{\text{new}}^\top (\hat{\beta} - \check{\beta})| + |\mathbf{g}_{\text{new}}^\top (\check{\beta} - \check{\beta}_{/i})| \\
 &\leq \sup_{t \in [0,1]} \|\nabla^2 f(\mathbf{x}_{\text{new}}, (1-t)\hat{\beta}_{/i} + t\hat{\beta})\| \|\hat{\beta}_{/i} - \hat{\beta}\|^2 \\
 &\quad + \|\mathbf{g}_{\text{new},*}^\top (\hat{\beta}_{/i} - \hat{\beta})\| + \|\mathbf{g}_{\text{new},*}^\top (\check{\beta} - \check{\beta}_{/i})\| \\
 &\quad + \|(\mathbf{g}_{\text{new}} - \mathbf{g}_{\text{new},*})(\hat{\beta}_{/i} - \hat{\beta})\| + \|(\mathbf{g}_{\text{new}} - \mathbf{g}_{\text{new},*})(\check{\beta} - \check{\beta}_{/i})\| \\
 &\leq C_2 \|\beta^*\|^{-2} \|\hat{\beta}_{/i} - \hat{\beta}\|^2 \\
 &\quad + \|\mathbf{g}_{\text{new},*}^\top (\hat{\beta}_{/i} - \hat{\beta})\| + \|\mathbf{g}_{\text{new},*}^\top (\check{\beta} - \check{\beta}_{/i})\| \\
 &\quad + \|\mathbf{g}_{\text{new}} - \mathbf{g}_{\text{new},*}\| \|\hat{\beta}_{/i} - \hat{\beta}\| + \|\mathbf{g}_{\text{new}} - \mathbf{g}_{\text{new},*}\| \|\check{\beta} - \check{\beta}_{/i}\|.
 \end{aligned}$$

The first inequality follows from the mean value theorem and the fact that $\check{\beta} = \hat{\beta}$. The second inequality uses the triangle and Cauchy-Schwarz inequalities. The third inequality follows from Assumption B.4 and Cauchy-Schwarz. Thus, it suffices to bound the three terms in the last three lines. Using the same method as (22) and (24), we can get the bounds

$$\sup_{i \in [n]} \|\check{\beta}_{/i} - \check{\beta}\| = O\left(\frac{\|\beta^*\|^2 \text{poly}(\log n)}{n}\right), \text{ with probability } \geq 1 - q_n, \quad (30)$$

$$\|\mathbf{g}_{\text{new},*}^\top (\check{\beta}_{/i} - \check{\beta})\| = O\left(\frac{\|\beta^*\|}{n^{1-\epsilon}}\right), \text{ with probability } \geq 1 - 2n^{-\epsilon}. \quad (31)$$

Combining (23), we conclude that there exists a constant s_1 such that, for any $\epsilon > 0$,

$$|f(\mathbf{x}_{\text{new}}, \hat{\beta}_{/i}) - (\mathbf{g}_{\text{new}}^\top \check{\beta}_{/i} + \mathbf{b}_{\text{new}})| \leq s_1 \left(\frac{\|\beta^*\|^2}{n^2} \text{poly}(\log n) + \frac{\|\beta^*\|^2}{n^{1.5-\epsilon}} + \frac{\|\beta^*\|}{n^{1-\epsilon}} \right),$$

with probability at least $1 - 3(q_n + n^{-\epsilon})$. The final result follows from $\|\beta^*\|^2 \ll n^{1-\epsilon}$.

B.2.5. PROOF OF THEOREM 2.12

First, define $\check{\Delta}_{/i} := \check{\beta}_{/i} - \check{\beta}$ and the Jacobian compactly as

$$\mathbf{J}_{/i}(\boldsymbol{\theta}) = \mathbf{G}_{/i}^\top \text{diag}(\ddot{\ell}_{/i}(\boldsymbol{\theta})) \mathbf{G}_{/i}.$$

Also define the estimated and exact leave- i -out perturbation vectors as

$$\hat{\Delta}_{/i} \triangleq \dot{\ell}_i(\check{\beta}) [\mathbf{J}_{/i}(\check{\beta}_{/i} - \check{\Delta}_{/i})]^{-1} \mathbf{g}_i.$$

Applying the Woodbury matrix identity yields

$$\begin{aligned}
 \mathbf{g}_i^\top \hat{\Delta}_{/i} &= \dot{\ell}_i(\check{\beta}) \mathbf{g}_i^\top \left(\mathbf{G}_{/i}^\top \text{diag}[\ddot{\ell}_{/i}(\check{\beta}_{/i} - \check{\Delta}_{/i})] \mathbf{G}_{/i} \right)^{-1} \mathbf{g}_i \\
 &= \frac{\dot{\ell}_i(\check{\beta}) \mathbf{g}_i^\top (\mathbf{G}^\top \text{diag}[\ddot{\ell}(\check{\beta})] \mathbf{G})^{-1} \mathbf{g}_i}{1 - \dot{\ell}_i(\check{\beta}) \mathbf{g}_i^\top (\mathbf{G}^\top \text{diag}[\ddot{\ell}(\check{\beta})] \mathbf{G})^{-1} \mathbf{g}_i}.
 \end{aligned}$$

By the multivariate mean-value theorem, there exists $t \in [0, 1]$ such that

$$\check{\Delta}_{/i} = \dot{\ell}_i(\check{\beta}) \left(\mathbf{J}_{/i}(\check{\beta}_{/i} - (1-t)\check{\Delta}_{/i}) \right)^{-1} \mathbf{g}_i.$$

Introduce

$$\gamma_{\delta_{/i}}(\boldsymbol{\theta}) \triangleq \ddot{\ell}_{/i}(\boldsymbol{\theta} + \boldsymbol{\delta}) - \ddot{\ell}_{/i}(\boldsymbol{\theta}),$$

so that

$$\mathbf{J}_{/i}(\boldsymbol{\theta} + \boldsymbol{\delta}) = \mathbf{J}_{/i}(\boldsymbol{\theta}) + \mathbf{G}_{/i}^\top \text{diag}[\boldsymbol{\gamma}_{\delta/i}(\boldsymbol{\theta})] \mathbf{G}_{/i}.$$

Note that $\mathbf{J}_{/i}(\boldsymbol{\theta} + \boldsymbol{\delta})$ remains positive definite for all $t \in [0, 1]$, with $\boldsymbol{\theta} = \check{\boldsymbol{\beta}}_{/i}$ and $\boldsymbol{\delta} = -(1-t)\check{\boldsymbol{\Delta}}_{/i}$.

Using the notation above, we now bound the error. With high probability, we obtain

$$\begin{aligned} & \left| \left| \mathbf{g}_i^\top \check{\boldsymbol{\Delta}}_{/i} - \mathbf{g}_i^\top \hat{\boldsymbol{\Delta}}_{/i} \right| - \left| \mathbf{g}_{i*}^\top \check{\boldsymbol{\Delta}}_{/i} - \mathbf{g}_{i*}^\top \hat{\boldsymbol{\Delta}}_{/i} \right| \right| \\ & \leq \left| \mathbf{g}_i^\top \check{\boldsymbol{\Delta}}_{/i} - \mathbf{g}_i^\top \hat{\boldsymbol{\Delta}}_{/i} - (\mathbf{g}_{i*}^\top \check{\boldsymbol{\Delta}}_{/i} - \mathbf{g}_{i*}^\top \hat{\boldsymbol{\Delta}}_{/i}) \right| \\ & \leq \|\mathbf{g}_i - \mathbf{g}_{i*}\| \|\check{\boldsymbol{\Delta}}_{/i} - \hat{\boldsymbol{\Delta}}_{/i}\| \leq n^{\epsilon-0.5} \|\check{\boldsymbol{\Delta}}_{/i} - \hat{\boldsymbol{\Delta}}_{/i}\| \text{poly}(\log n), \end{aligned} \quad (32)$$

where we use Lemma B.10 and triangle inequality.

Also, since we know that

$$\left| \mathbf{g}_{i*}^\top \check{\boldsymbol{\Delta}}_{/i} - \mathbf{g}_{i*}^\top \hat{\boldsymbol{\Delta}}_{/i} \right| \leq \|\mathbf{g}_{i*}\| \|\check{\boldsymbol{\Delta}}_{/i} - \hat{\boldsymbol{\Delta}}_{/i}\|,$$

then we know that

$$\left| \mathbf{g}_i^\top \check{\boldsymbol{\Delta}}_{/i} - \mathbf{g}_i^\top \hat{\boldsymbol{\Delta}}_{/i} \right| \leq O_p(\|\check{\boldsymbol{\Delta}}_{/i} - \hat{\boldsymbol{\Delta}}_{/i}\| \text{poly}(\log n)), \quad (33)$$

where we use (34). Next, we consider $\|\check{\boldsymbol{\Delta}}_{/i} - \hat{\boldsymbol{\Delta}}_{/i}\|$. Using Assumption B.4, we decompose it as

$$\|\check{\boldsymbol{\Delta}}_{/i} - \hat{\boldsymbol{\Delta}}_{/i}\| \leq \tilde{C}_1 \text{poly}(\log n) (\|((A_i + \Delta_i)^{-1} - A_i^{-1})\mathbf{g}_{i*}\| + \|((A_i + \Delta_i)^{-1} - A_i^{-1})(\mathbf{g}_i - \mathbf{g}_{i*})\|),$$

where $A_i = \mathbf{G}_{/i}^\top \mathbf{D} \mathbf{G}_{/i}$, $\Delta_i = \mathbf{G}_{/i}^\top \boldsymbol{\Gamma} \mathbf{G}_{/i}$, $\boldsymbol{\Gamma} = \text{diag}[\boldsymbol{\gamma}_{\boldsymbol{\beta}}(\check{\boldsymbol{\beta}})]$, and $\mathbf{D} = \text{diag}(\check{\boldsymbol{\ell}}_{/i}(\check{\boldsymbol{\beta}}))$.

Part 1: $\|((A_i + \Delta_i)^{-1} - A_i^{-1})\mathbf{g}_{i*}\|$ First, we bound $\|((A_i + \Delta_i)^{-1} - A_i^{-1})\mathbf{g}_{i*}\|$. Denote $\mathbf{S} = (A_i + \Delta_i)^{-1} - A_i^{-1}$. Using Lemma B.9, we know that there exists a constant M_0 such that

$$\|\mathbf{S}\mathbf{g}_{i*}\| \leq M_0 \|A_i^{-1} \Delta_i A_i^{-1} \mathbf{g}_{i*}\|.$$

Note that

$$\|A_i^{-1} \Delta_i A_i^{-1} \mathbf{g}_{i*}\| \leq \|A_i^{-1} \mathbf{G}_{/i}\| \|\boldsymbol{\Gamma}\|_F \|\mathbf{G}_{/i} A_i^{-1} \mathbf{g}_{i*}\|_\infty.$$

Note that By independence of \mathbf{g}_{i*} and $A_i^{-1} \Delta_i A_i^{-1}$, for a subgaussian vector $\mathbf{G}_{/i} A_i^{-1} \mathbf{g}_{i*}$, we can get that

$$\|\mathbf{G}_{/i} A_i^{-1} \mathbf{g}_{i*}\|_\infty \leq \frac{1}{\|\boldsymbol{\beta}^*\|} \|\mathbf{G}_{/i}\| \|A_i^{-1}\|,$$

then

$$\|A_i^{-1} \Delta_i A_i^{-1} \mathbf{g}_{i*}\| \leq \|\mathbf{G}_{/i}\|^2 \|A_i^{-1}\|^2 \|\boldsymbol{\Gamma}\|_F \frac{1}{\|\boldsymbol{\beta}^*\|}$$

we next bound $\|A_i^{-1}\| = \|(\mathbf{G}_{/i}^\top \mathbf{D} \mathbf{G}_{/i})^{-1}\|$ and $\|\mathbf{G}_{/i} \mathbf{G}_{/i}^\top\|$. By Assumption B.7 and Lemma 2(1) of (Jin et al., 2019), we have

$$\sup_{i \in [n]} \|\mathbf{g}_{i*}\|^2 \leq M \log n, \quad \text{with probability } \geq 1 - 2n^{-M}, \quad \forall M > 0. \quad (34)$$

Combining Lemma B.10 and Assumption B.3, for any $\epsilon > 0$ such that $n^{1-\epsilon} \gg \|\boldsymbol{\beta}^*\|^2$, and setting $M = \epsilon$, we obtain that with probability at least $1 - q_n - 2n^{-\epsilon}$ and for sufficiently large n ,

$$\begin{aligned} \sigma_{\max}(\mathbf{G}_{/i}^\top \mathbf{G}_{/i}) & \leq \sigma_{\max}(\mathbf{G}^\top \mathbf{G}) + \mathbf{g}_i^\top \mathbf{g}_i \leq \frac{C_2 n}{\|\boldsymbol{\beta}^*\|^2} + 2 \left(C_g \sqrt{\frac{\log n}{n^{1-2\epsilon}}} \right)^2 + \epsilon \log n \leq \frac{2C_2 n}{\|\boldsymbol{\beta}^*\|^2}, \\ \sigma_{\min}(\mathbf{G}_{/i}^\top \mathbf{G}_{/i}) & \geq \sigma_{\min}(\mathbf{G}^\top \mathbf{G}) - \mathbf{g}_i^\top \mathbf{g}_i \geq \frac{c_1 n}{\|\boldsymbol{\beta}^*\|^2} - 2 \left(C_g \sqrt{\frac{\log n}{n^{1-2\epsilon}}} \right)^2 - \epsilon \log n \geq \frac{c_1 n}{2\|\boldsymbol{\beta}^*\|^2}. \end{aligned} \quad (35)$$

Combining this with Assumption B.5, we obtain

$$\|A_i^{-1}\| = \|(\mathbf{G}_{/i}^\top \mathbf{D} \mathbf{G}_{/i})^{-1}\| \leq \frac{2\|\boldsymbol{\beta}^*\|^2}{c_1 \mu n}, \quad \text{with probability } \geq 1 - q_n - 2n^{-\epsilon}. \quad (36)$$

Next, we bound $\|\Gamma\|_F$, simplify notation as $\Gamma := \text{diag}(\gamma)$. By Assumption B.5 and (30), with probability at least $1 - q_n$, we have

$$\|\gamma\|_2 \leq O\left(\|\check{\beta}_{/i} - \check{\beta}\| \frac{n^{1/2}}{\|\beta^*\|} \text{poly}(\log n)\right) = O\left(\frac{\|\beta^*\|}{n^{1/2}} \text{poly}(\log n)\right). \quad (37)$$

And hence combining these terms, we get

$$\|S\mathbf{g}_{i,*}\| \leq \frac{\|\beta^*\|^2}{n^{3/2-\epsilon}}.$$

Part 2: $\|((A_i + \Delta_i)^{-1} - A_i^{-1})(\mathbf{g}_i - \mathbf{g}_{i,*})\|$. Denote $T_i = A_i^{-1} \Delta_i A_i^{-1}$, then using Lemma B.9:

$$\begin{aligned} \|((A_i + \Delta_i)^{-1} - A_i^{-1})(\mathbf{g}_i - \mathbf{g}_{i,*})\| &\leq M_0 \|T_i T_i^\top\| \|\mathbf{g}_i - \mathbf{g}_{i,*}\| \\ &\preceq \frac{\|\beta^*\|^6}{n^3} \cdot n^{\epsilon-1/2} \text{poly}(\log n) \\ &\asymp \frac{\|\beta^*\|^2}{n^{3/2-\epsilon}} \cdot \frac{\|\beta^*\|^4}{n^2} \preceq \|((A_i + \Delta_i)^{-1} - A_i^{-1})\mathbf{g}_{i,*}\|, \end{aligned}$$

where the second inequality uses the fact that $\|\Gamma\| \leq \|\Gamma\|_F$ and (37). Therefore,

$$\|\check{\Delta}_{/i} - \hat{\Delta}_{/i}\| \preceq \frac{\|\beta^*\|^2}{n^{3/2-\epsilon}}. \quad (38)$$

Returning to (33), we conclude that with high probability,

$$\left| \mathbf{g}_i^\top \check{\Delta}_{/i} - \mathbf{g}_i^\top \hat{\Delta}_{/i} \right| = O\left(\frac{\|\beta^*\|^2}{n^{3/2-\epsilon}}\right).$$

This completes the proof.

B.2.6. PROOF OF THEOREM 2.13

First, define $\check{\Delta}_{/i} := \check{\beta}_{/i} - \check{\beta}$ and the Jacobian compactly as

$$\mathbf{J}_{/i}(\boldsymbol{\theta}) = \mathbf{G}_{/i}^\top \text{diag}(\check{\ell}_{/i}(\boldsymbol{\theta})) \mathbf{G}_{/i}.$$

Also define the estimated and exact leave- i -out perturbation vectors as

$$\hat{\Delta}_{/i} \triangleq \check{\ell}_i(\check{\beta}) [\mathbf{J}_{/i}(\check{\beta}_{/i} - \check{\Delta}_{/i})]^{-1} \mathbf{g}_i.$$

Applying the Woodbury matrix identity yields

$$\begin{aligned} \mathbf{g}_{\text{new}}^\top \hat{\Delta}_{/i} &= \check{\ell}_i(\check{\beta}) \mathbf{g}_{\text{new}}^\top \left(\mathbf{G}_{/i}^\top \text{diag}[\check{\ell}_{/i}(\check{\beta}_{/i} - \check{\Delta}_{/i})] \mathbf{G}_{/i} \right)^{-1} \mathbf{g}_i \\ &= \frac{\check{\ell}_i(\check{\beta}) \mathbf{g}_{\text{new}}^\top (\mathbf{G}^\top \text{diag}[\check{\ell}(\check{\beta})] \mathbf{G})^{-1} \mathbf{g}_i}{1 - \check{\ell}_i(\check{\beta}) \mathbf{g}_i^\top (\mathbf{G}^\top \text{diag}[\check{\ell}(\check{\beta})] \mathbf{G})^{-1} \mathbf{g}_i}. \end{aligned}$$

From (30), we know that there exists an absolute constant s_Δ^* such that

$$\|\check{\Delta}_{/i}\|_2 \leq s_\Delta^* \frac{\|\beta^*\|^2 \text{poly}(\log n)}{n}, \quad \text{with probability } \geq 1 - q_n. \quad (39)$$

By the multivariate mean-value theorem, there exists $t \in [0, 1]$ such that

$$\check{\Delta}_{/i} = \check{\ell}_i(\check{\beta}) \left(\mathbf{J}_{/i}(\check{\beta}_{/i} - (1-t)\check{\Delta}_{/i}) \right)^{-1} \mathbf{g}_i.$$

Introduce

$$\gamma_{\delta/i}(\boldsymbol{\theta}) \triangleq \ddot{\ell}_{/i}(\boldsymbol{\theta} + \boldsymbol{\delta}) - \ddot{\ell}_{/i}(\boldsymbol{\theta}),$$

so that

$$\mathbf{J}_{/i}(\boldsymbol{\theta} + \boldsymbol{\delta}) = \mathbf{J}_{/i}(\boldsymbol{\theta}) + \mathbf{G}_{/i}^\top \text{diag}[\gamma_{\delta/i}(\boldsymbol{\theta})] \mathbf{G}_{/i}.$$

Note that $\mathbf{J}_{/i}(\boldsymbol{\theta} + \boldsymbol{\delta})$ remains positive definite for all $t \in [0, 1]$, with $\boldsymbol{\theta} = \check{\boldsymbol{\beta}}_{/i}$ and $\boldsymbol{\delta} = -(1-t)\check{\boldsymbol{\Delta}}_{/i}$.

Using the notation above, we now bound the error. With high probability, we obtain

$$\begin{aligned} & \left| \mathbf{g}_{\text{new}}^\top \check{\boldsymbol{\Delta}}_{/i} - \mathbf{g}_{\text{new}}^\top \hat{\boldsymbol{\Delta}}_{/i} \right| \\ & \leq \left| \mathbf{g}_{\text{new}*}^\top (\check{\boldsymbol{\Delta}}_{/i} - \hat{\boldsymbol{\Delta}}_{/i}) \right| + \|\mathbf{g}_{\text{new}*} - \mathbf{g}_i\| \|\check{\boldsymbol{\Delta}}_{/i} - \hat{\boldsymbol{\Delta}}_{/i}\| \\ & \leq (\|\boldsymbol{\beta}^*\|^{-1} + n^{\epsilon-0.5}) \|\check{\boldsymbol{\Delta}}_{/i} - \hat{\boldsymbol{\Delta}}_{/i}\| \text{poly}(\log n), \end{aligned} \quad (40)$$

where we use that $\mathbf{g}_{\text{new}*}$ is independent of $\check{\boldsymbol{\Delta}}_{/i} - \hat{\boldsymbol{\Delta}}_{/i}$, along with Assumption B.7 and Lemma B.10.

Next, we consider $\|\check{\boldsymbol{\Delta}}_{/i} - \hat{\boldsymbol{\Delta}}_{/i}\|$. As we have get in (38),

$$\|\check{\boldsymbol{\Delta}}_{/i} - \hat{\boldsymbol{\Delta}}_{/i}\| \preceq \frac{\|\boldsymbol{\beta}^*\|^2}{n^{3/2-\epsilon}}.$$

Returning to (40), we conclude that with high probability,

$$\left| \mathbf{g}_{\text{new}}^\top \check{\boldsymbol{\Delta}}_{/i} - \mathbf{g}_{\text{new}}^\top \hat{\boldsymbol{\Delta}}_{/i} \right| = O\left(\frac{\|\boldsymbol{\beta}^*\|}{n^{3/2-\epsilon}}\right).$$

This completes the proof.

B.2.7. PROOF OF THEOREM 2.14

By Equation (13), we have

$$\mathcal{I}^{\text{ALO}}(\mathbf{z}_i, \mathbf{z}_{\text{new}}) = \frac{\dot{\ell}_i(\check{\boldsymbol{\beta}}) \mathbf{g}_{\text{new}}^\top (\mathbf{G}^\top \text{diag}[\ddot{\ell}(\check{\boldsymbol{\beta}})] \mathbf{G})^{-1} \mathbf{g}_i}{1 - \dot{\ell}_i(\check{\boldsymbol{\beta}}) \mathbf{g}_i^\top (\mathbf{G}^\top \text{diag}[\ddot{\ell}(\check{\boldsymbol{\beta}})] \mathbf{G})^{-1} \mathbf{g}_i}.$$

Using the Woodbury identity, we obtain

$$\mathcal{I}^{\text{ALO}}(\mathbf{z}_i, \mathbf{z}_{\text{new}}) = \dot{\ell}_i(\check{\boldsymbol{\beta}}) \mathbf{g}_{\text{new}}^\top (\mathbf{G}_{/i}^\top \text{diag}[\ddot{\ell}_{/i}(\check{\boldsymbol{\beta}})] \mathbf{G}_{/i})^{-1} \mathbf{g}_i.$$

Similarly, from Equation (6), we have

$$\mathcal{I}^{\text{TRAK}}(\mathbf{z}_i, \mathbf{z}_{\text{new}}) = \dot{\ell}_i(\check{\boldsymbol{\beta}}) \boldsymbol{\phi}_{\text{new}}^\top (\boldsymbol{\Phi}_{/i}^\top \text{diag}[\ddot{\ell}_{/i}(\check{\boldsymbol{\beta}})] \boldsymbol{\Phi}_{/i})^{-1} \boldsymbol{\phi}_i.$$

We ignore the k in $\mathcal{I}^{\text{TRAK}}(\mathbf{z}_i, \mathbf{z}_{\text{new}}; k)$ for simplicity. Recall that for the projection matrix $\mathbf{S} \in \mathbb{R}^{k \times d}$, TRAK defines the feature map $\boldsymbol{\phi}(\mathbf{x}) = \mathbf{S}^\top \mathbf{g}(\mathbf{x})$, where $\mathbf{g}(\mathbf{x}) = \nabla f(\mathbf{x}, \hat{\boldsymbol{\beta}})$. Accordingly, we define $\boldsymbol{\Phi} = (\boldsymbol{\phi}_1, \dots, \boldsymbol{\phi}_n)^\top \in \mathbb{R}^{n \times k}$ with $\boldsymbol{\phi}_i = \mathbf{S}^\top \mathbf{g}_i$ and $\boldsymbol{\phi}_{\text{new}} = \mathbf{S}^\top \mathbf{g}_{\text{new}}$. The entries \mathbf{S}_{ij} for $i \in [k], j \in [d]$ are i.i.d. $\mathcal{N}(0, 1)$.

By Equation (35) and Theorem B.5, with probability at least $1 - q_n - 2n^{-\epsilon}$,

$$\frac{n}{\|\boldsymbol{\beta}^*\|^2} \preceq \sigma_{\min}(\mathbf{G}_{/i}^\top \text{diag}[\ddot{\ell}_{/i}(\check{\boldsymbol{\beta}})] \mathbf{G}_{/i}) \preceq \sigma_{\max}(\mathbf{G}_{/i}^\top \text{diag}[\ddot{\ell}_{/i}(\check{\boldsymbol{\beta}})] \mathbf{G}_{/i}) \preceq \frac{n \text{poly}(\log n)}{\|\boldsymbol{\beta}^*\|^2}. \quad (41)$$

We denote κ as the condition number of $\mathbf{G}_{/i}^\top \text{diag}[\ddot{\ell}_{/i}(\check{\boldsymbol{\beta}})] \mathbf{G}_{/i}$ and $\kappa = O_p(\text{poly}(\log n))$ by Assumption B.5. Then we split $\mathcal{I}^{\text{ALO}}(\mathbf{z}_i, \mathbf{z}_{\text{new}})$ and $\mathcal{I}^{\text{TRAK}}(\mathbf{z}_i, \mathbf{z}_{\text{new}})$ as

$$\mathcal{I}^{\text{ALO}}(\mathbf{z}_i, \mathbf{z}_{\text{new}}) = \dot{\ell}_i(\check{\boldsymbol{\beta}}) \mathbf{g}_{\text{new}*}^\top (\mathbf{G}_{/i}^\top \text{diag}[\ddot{\ell}_{/i}(\check{\boldsymbol{\beta}})] \mathbf{G}_{/i})^{-1} \mathbf{g}_i + \dot{\ell}_i(\check{\boldsymbol{\beta}}) (\mathbf{g}_{\text{new}} - \mathbf{g}_{\text{new}*})^\top (\mathbf{G}_{/i}^\top \text{diag}[\ddot{\ell}_{/i}(\check{\boldsymbol{\beta}})] \mathbf{G}_{/i})^{-1} \mathbf{g}_i.$$

$$\mathcal{I}^{\text{TRAK}}(\mathbf{z}_i, \mathbf{z}_{\text{new}}) = \dot{\ell}_i(\check{\boldsymbol{\beta}}) \boldsymbol{\phi}_{\text{new}*}^\top (\boldsymbol{\Phi}_{/i}^\top \text{diag}[\ddot{\ell}_{/i}(\check{\boldsymbol{\beta}})] \boldsymbol{\Phi}_{/i})^{-1} \boldsymbol{\phi}_i + \dot{\ell}_i(\check{\boldsymbol{\beta}}) (\boldsymbol{\phi}_{\text{new}} - \boldsymbol{\phi}_{\text{new}*})^\top (\boldsymbol{\Phi}_{/i}^\top \text{diag}[\ddot{\ell}_{/i}(\check{\boldsymbol{\beta}})] \boldsymbol{\Phi}_{/i})^{-1} \boldsymbol{\phi}_i.$$

We denote the first terms in $\mathcal{I}_{*}^{\text{ALO}}(\mathbf{z}_i, \mathbf{z}_{\text{new}})$ and $\mathcal{I}_{*}^{\text{TRAK}}(\mathbf{z}_i, \mathbf{z}_{\text{new}})$ as $\mathcal{I}_{*}^{\text{ALO}}(\mathbf{z}_i, \mathbf{z}_{\text{new}})$ and $\mathcal{I}_{*}^{\text{TRAK}}(\mathbf{z}_i, \mathbf{z}_{\text{new}})$, and the last terms as $\mathcal{D}_{*}^{\text{ALO}}(\mathbf{z}_i, \mathbf{z}_{\text{new}})$ and $\mathcal{D}_{*}^{\text{TRAK}}(\mathbf{z}_i, \mathbf{z}_{\text{new}})$.

First, we consider the case when $\mathbf{z}_i = \mathbf{z}_{\text{new}}$. By our Theorem 2.13 and Theorem B.10, we get that

$$\mathcal{I}_{*}^{\text{ALO}}(\mathbf{z}_i, \mathbf{z}_i) \geq O_p\left(\frac{\|\beta^*\|^2}{n}\right), \quad \mathcal{D}_{*}^{\text{ALO}}(\mathbf{z}_i, \mathbf{z}_i) \leq O_p\left(\frac{\|\beta^*\|^3}{n^{1.5-\epsilon}}\right).$$

Then, by the assumption $\|\beta^*\| \leq n^{0.5-\epsilon}$, we obtain that with high probability, for sufficiently large n and p ,

$$\frac{\mathcal{D}_{*}^{\text{ALO}}(\mathbf{z}_i, \mathbf{z}_i)}{\mathcal{I}_{*}^{\text{ALO}}(\mathbf{z}_i, \mathbf{z}_i)} \leq \frac{1}{2}.$$

Thus,

$$\begin{aligned} \frac{\mathcal{I}_{*}^{\text{TRAK}}(\mathbf{z}_i, \mathbf{z}_i)}{\mathcal{I}_{*}^{\text{ALO}}(\mathbf{z}_i, \mathbf{z}_i)} &= \frac{\mathcal{I}_{*}^{\text{TRAK}}(\mathbf{z}_i, \mathbf{z}_i) + \mathcal{D}_{*}^{\text{TRAK}}(\mathbf{z}_i, \mathbf{z}_i)}{\mathcal{I}_{*}^{\text{ALO}}(\mathbf{z}_i, \mathbf{z}_i) + \mathcal{D}_{*}^{\text{ALO}}(\mathbf{z}_i, \mathbf{z}_i)} \\ &\geq \frac{\mathcal{I}_{*}^{\text{TRAK}}(\mathbf{z}_i, \mathbf{z}_i)}{\mathcal{I}_{*}^{\text{ALO}}(\mathbf{z}_i, \mathbf{z}_i) + \mathcal{D}_{*}^{\text{ALO}}(\mathbf{z}_i, \mathbf{z}_i)} \geq \frac{\mathcal{I}_{*}^{\text{TRAK}}(\mathbf{z}_i, \mathbf{z}_i)}{\mathcal{I}_{*}^{\text{ALO}}(\mathbf{z}_i, \mathbf{z}_i)} \frac{1}{1 + \frac{\mathcal{D}_{*}^{\text{ALO}}(\mathbf{z}_i, \mathbf{z}_i)}{\mathcal{I}_{*}^{\text{ALO}}(\mathbf{z}_i, \mathbf{z}_i)}}. \end{aligned}$$

We now focus on the ratio $\frac{\mathcal{I}_{*}^{\text{TRAK}}(\mathbf{z}_i, \mathbf{z}_i)}{\mathcal{I}_{*}^{\text{ALO}}(\mathbf{z}_i, \mathbf{z}_i)}$. From Theorem B.12, we get that with probability greater than $1 - C \exp(-c\epsilon^2 k)$,

$$\frac{1}{\kappa}(1-\epsilon)\frac{k}{d} \leq \frac{\mathcal{I}_{*}^{\text{TRAK}}(\mathbf{z}_i, \mathbf{z}_i)}{\mathcal{I}_{*}^{\text{ALO}}(\mathbf{z}_i, \mathbf{z}_i)} \leq \min\left(\kappa(1+\epsilon)\frac{k}{d}, 1\right). \quad (42)$$

Hence, there exists a constant $c^{\text{TRAK}} > 0$ such that with high probability,

$$\frac{\mathcal{I}_{*}^{\text{TRAK}}(\mathbf{z}_i, \mathbf{z}_i)}{\mathcal{I}_{*}^{\text{ALO}}(\mathbf{z}_i, \mathbf{z}_i)} \geq c^{\text{TRAK}} \frac{k}{d}.$$

Next, we consider the case when \mathbf{z}_i and \mathbf{z}_{new} are independent. Define

$$\mathbf{u}_i := (\mathbf{G}_{/i}^{\top} \text{diag}[\ddot{\ell}_{/i}(\check{\beta})] \mathbf{G}_{/i})^{-1} \mathbf{g}_i \quad \text{and} \quad \mathbf{u}_{i*} := (\mathbf{G}_{/i}^{\top} \text{diag}[\ddot{\ell}_{/i}(\check{\beta})] \mathbf{G}_{/i})^{-1} \mathbf{g}_{i,*}.$$

$$\mathbf{v}_i := S^{\top} (S \mathbf{G}_{/i}^{\top} \text{diag}[\ddot{\ell}_{/i}(\check{\beta})] \mathbf{G}_{/i} S^{\top})^{-1} S \mathbf{g}_i \quad \text{and} \quad \mathbf{v}_{i*} := S^{\top} (S \mathbf{G}_{/i}^{\top} \text{diag}[\ddot{\ell}_{/i}(\check{\beta})] \mathbf{G}_{/i} S^{\top})^{-1} S \mathbf{g}_{i,*}.$$

Note that our goal is to calculate an upper bound for $\mathbf{g}_{\text{new}}^{\top} \mathbf{v}_i$. Using Assumption B.7 and the independence of $\mathbf{g}_{\text{new},*}$ and \mathbf{v}_i we have $\mathbf{g}_{\text{new},*}^{\top} \mathbf{v}_i$ is $\frac{\|\mathbf{v}_{i*}\| \text{poly}(\log(n))}{\|\beta^*\|}$ -subGaussian. Thus,

$$|\mathbf{g}_{\text{new},*}^{\top} \mathbf{v}_i| = O_P\left(\frac{\|\mathbf{v}_{i*}\| \text{poly}(\log(n))}{\|\beta^*\|}\right). \quad (43)$$

Now, by Theorem B.10, for any $\epsilon > 0$, $\mathbf{g}_i = \mathbf{g}_{i,*} + (\mathbf{g}_i - \mathbf{g}_{i,*}) = \mathbf{g}_{i,*} + O_P\left(\sqrt{\frac{\log n}{n^{1-2\epsilon}}}\right)$. Consequently,

$$|(\mathbf{g}_{\text{new}} - \mathbf{g}_{\text{new},*})^{\top} \mathbf{v}_i| = O_P\left(\frac{\text{poly}(\log n)}{n^{0.5-\epsilon}} \|\mathbf{v}_{i*}\|\right) = O_P\left(\frac{\|\beta^*\|}{n^{0.5-\epsilon}} \frac{\|\mathbf{v}_{i*}\| \text{poly}(\log(n))}{\|\beta^*\|}\right). \quad (44)$$

Hence we have

$$|\mathbf{g}_{\text{new}}^{\top} \mathbf{v}_i| = |\mathbf{g}_{\text{new},*}^{\top} \mathbf{v}_i| + O_P\left(\frac{\|\beta^*\|}{n^{0.5-\epsilon}} \frac{\|\mathbf{v}_{i*}\| \text{poly}(\log(n))}{\|\beta^*\|}\right) = O_P\left(\frac{\|\mathbf{v}_{i*}\| \text{poly}(\log(n))}{\|\beta^*\|}\right), \quad (45)$$

where to get the last equality we have used (43). To bound $\|\mathbf{v}_{i*}\|^2$ note that

$$\begin{aligned} &\sigma_{\min}((S H_i S^{\top})^{-0.5} S S^{\top} (S H_i S^{\top})^{-0.5}) \mathbf{g}_i^{\top} S^{\top} (S H_i S^{\top})^{-1} S \mathbf{g}_i \leq \|\mathbf{v}_{i*}\|^2 \\ &\leq \sigma_{\max}((S H_i S^{\top})^{-0.5} S S^{\top} (S H_i S^{\top})^{-0.5}) \mathbf{g}_i^{\top} S^{\top} (S H_i S^{\top})^{-1} S \mathbf{g}_i \end{aligned}$$

where we denote $H_i = \mathbf{G}_{/i}^\top \text{diag}[\ddot{\ell}_{/i}(\check{\beta})] \mathbf{G}_{/i}$. Observe that $\sigma_{\max}((SH_i S^\top)^{-0.5} S S^\top (SH_i S^\top)^{-0.5}) \leq \sigma_{\min}(H_i)^{-1}$ and $\sigma_{\min}((SH_i S^\top)^{-0.5} S S^\top (SH_i S^\top)^{-0.5}) \geq \sigma_{\max}(H_i)^{-1}$. Hence,

$$\sigma_{\max}(H^{-1}) \mathbf{g}_i^\top S^\top (SH_i S^\top)^{-1} S \mathbf{g}_i \leq \|\mathbf{v}_{i*}\|^2 \leq \sigma_{\min}(H^{-1}) \mathbf{g}_i^\top S^\top (SH_i S^\top)^{-1} S \mathbf{g}_i$$

Further we can show that

$$\sigma_{\min}(H_i^{-1}) \mathbf{g}_i^\top H_i^{-1} \mathbf{g}_i \leq \|\mathbf{u}_{i*}\|^2 \leq \sigma_{\max}(H_i^{-1}) \mathbf{g}_i^\top H_i^{-1} \mathbf{g}_i \quad (46)$$

Combining these two equations with Theorem B.12, we finally get with high probability,

$$\frac{1}{\kappa^2} (1 - \epsilon) \frac{k}{d} \leq \frac{\|\mathbf{v}_{i*}\|^2}{\|\mathbf{u}_{i*}\|^2} \leq \min\left(\kappa(1 + \epsilon) \frac{k}{d}, 1\right) \kappa.$$

Combining this bound with (45) leads to

$$|\mathbf{g}_{\text{new}}^\top \mathbf{v}_i| = O_P\left(\frac{\|\mathbf{u}_{i*}\| \text{poly}(\log(n))}{\|\beta^*\| \sqrt{k}} \sqrt{\frac{k}{d}}\right).$$

Since

$$\|\mathbf{u}_{i*}\| = O_P\left(\frac{\|\beta^*\|^2}{n^{1-\epsilon}}\right),$$

and with $\kappa = O_P(\text{poly}(\log n))$, we obtain

$$|\mathbf{g}_{\text{new}}^\top \mathbf{v}_i| = O_P\left(\frac{\|\beta^*\| \sqrt{k}}{n^{1-\epsilon} \sqrt{d}} \text{poly}(\log(n))\right).$$

B.3. Technical Lemmas

Lemma B.9. Assume that $\mathbf{G}^\top (\mathbf{D} + \mathbf{\Gamma}) \mathbf{G}$ and $\mathbf{G}^\top \mathbf{D} \mathbf{G}$ are positive definite, and both \mathbf{D} and $\mathbf{\Gamma}$ are diagonal matrices. Let \mathbf{g} be a vector independent of \mathbf{G} , $\mathbf{\Gamma}$, and \mathbf{D} . If $\|(\mathbf{G}^\top \mathbf{D} \mathbf{G})^{-1}(\mathbf{G}^\top \mathbf{\Gamma} \mathbf{G})\| < 1$, then there exists an absolute constant M_0 such that

$$\|((\mathbf{G}^\top (\mathbf{D} + \mathbf{\Gamma}) \mathbf{G})^{-1} - (\mathbf{G}^\top \mathbf{D} \mathbf{G})^{-1}) \mathbf{g}\| \leq M_0 \|(\mathbf{G}^\top \mathbf{D} \mathbf{G})^{-1} \mathbf{G}^\top \mathbf{\Gamma} \mathbf{G} (\mathbf{G}^\top \mathbf{D} \mathbf{G})^{-1} \mathbf{g}\|.$$

Proof of Lemma B.9. Let $A = \mathbf{G}^\top \mathbf{D} \mathbf{G}$ and $\Delta = \mathbf{G}^\top \mathbf{\Gamma} \mathbf{G}$. By the Neumann series expansion, since $\|A^{-1} \Delta\| < 1$,

$$(A + \Delta)^{-1} = A^{-1} - A^{-1} \Delta A^{-1} + A^{-1} \Delta A^{-1} \Delta A^{-1} - \dots.$$

Thus,

$$(A + \Delta)^{-1} - A^{-1} = -A^{-1} \Delta A^{-1} + A^{-1} \Delta A^{-1} \Delta A^{-1} - \dots.$$

Multiplying by \mathbf{g} and taking norms,

$$\begin{aligned} \|((A + \Delta)^{-1} - A^{-1}) \mathbf{g}\| &\leq \|A^{-1} \Delta A^{-1} \mathbf{g}\| + \|A^{-1} \Delta A^{-1} \Delta A^{-1} \mathbf{g}\| + \dots \\ &\leq \|A^{-1} \Delta A^{-1} \mathbf{g}\| (1 + \|A^{-1} \Delta\| + \|A^{-1} \Delta\|^2 + \dots) \\ &= \|A^{-1} \Delta A^{-1} \mathbf{g}\| \cdot \frac{1}{1 - \|A^{-1} \Delta\|}. \end{aligned}$$

Since $\|A^{-1} \Delta\| < 1$ by assumption, the geometric series converges. Taking $M_0 = \frac{1}{1 - \|A^{-1} \Delta\|}$ completes the proof. \square

Lemma B.10. Suppose Assumptions B.7 hold. Then for all $\epsilon > 0$, with probability at least $1 - q_n - n^{-\epsilon}$, there exists a constant $C_\beta, C_g > 0$, independent of n, p and d , and

$$\|\hat{\beta}_n - \beta^*\| \leq C_\beta \|\beta^*\|^2 \sqrt{\frac{\log(n)}{n^{1-2\epsilon}}},$$

and

$$\|\mathbf{g}_i - \mathbf{g}_{i*}\| \leq C_g \sqrt{\frac{\log(n)}{n^{1-2\epsilon}}},$$

Proof of Lemma B.10. Denote $\dot{\ell}_{i*} = \dot{\ell}(y_i, f(\mathbf{x}_i, \boldsymbol{\beta}^*))$. By Assumption B.5, we know that $\max_{i \in [n]} |\dot{\ell}_{i*}| \leq \tilde{C}_1 \log n$. Also, using Lemma 2(1) in Jin et al. (2019), we know that $\mathbb{E}\|\mathbf{g}_{i,*}\|^2 \leq 2\sigma^2$, then using $\mathbb{E}[\dot{\ell}_{i*}\mathbf{g}_{i,*}] = 0$ and $\{\dot{\ell}_{i*}\mathbf{g}_{i,*}\}_{i \in [n]}$ are independent, we get that

$$\mathbb{E}\left\|\frac{1}{n} \sum_{i=1}^n \dot{\ell}_{i*}\mathbf{g}_{i,*}\right\|^2 = \frac{1}{n^2} \mathbb{E} \sum_{i=1}^n \dot{\ell}_{i*}^2 \mathbf{g}_{i,*}^\top \mathbf{g}_{i,*} \leq \frac{2\tilde{C}_1\sigma^2 \log n}{n}.$$

Then using moment inequality, we get that

$$\mathbb{P}\left(\left\|\frac{1}{n} \sum_{i=1}^n \dot{\ell}_{i*}\mathbf{g}_{i,*}\right\|^2 \geq t\right) \leq \frac{2\tilde{C}_1\sigma^2 \log n}{nt^2}.$$

Thus we can say that for all $\epsilon > 0$, $t = \frac{\sqrt{\log n}}{n^{\frac{1}{2}-\epsilon}}$, when n big enough, then with probability $\geq 1 - n^{-\epsilon}$, there exists a constant C_g such that

$$\left\|\frac{1}{n} \sum_{i=1}^n \dot{\ell}_{i*}\mathbf{g}_{i,*}\right\| \leq C_g \frac{\log^{\frac{1}{2}}(n)}{n^{\frac{1}{2}-\epsilon}}. \quad (47)$$

Using Mean-Value Theorem, denote $\dot{\ell}_i = \dot{\ell}(y_i, f(\mathbf{x}_i, \hat{\boldsymbol{\beta}}))$, we know that there exists $\bar{\boldsymbol{\beta}} = t\boldsymbol{\beta}^* + (1-t)\hat{\boldsymbol{\beta}}$ where $t \in [0, 1]$, such that

$$0 = \frac{1}{n} \sum_{i=1}^n \dot{\ell}_i \mathbf{g}_i = \frac{1}{n} \sum_{i=1}^n \dot{\ell}_{i*} \mathbf{g}_{i,*} + \frac{1}{n} \sum_{i=1}^n \nabla^2 \ell(y_i, f(x_i, \bar{\boldsymbol{\beta}}))(\hat{\boldsymbol{\beta}} - \boldsymbol{\beta}^*),$$

then

$$\|\hat{\boldsymbol{\beta}} - \boldsymbol{\beta}^*\| \leq \left\| \left(\frac{1}{n} \sum_{i=1}^n \nabla^2 \ell(y_i, f(x_i, \bar{\boldsymbol{\beta}})) \right)^{-1} \right\| \left\| \frac{1}{n} \sum_{i=1}^n \dot{\ell}_{i*} \mathbf{g}_{i,*} \right\|,$$

by Assumption B.3, we know that with probability $\geq 1 - q_n$,

$$\sigma_{\min}\left(\frac{1}{n} \sum_{i=1}^n \nabla^2 \ell(y_i, f(x_i, \bar{\boldsymbol{\beta}}))\right) \geq c_1 \|\boldsymbol{\beta}^*\|^{-2},$$

combining (47), we know that

$$\|\hat{\boldsymbol{\beta}} - \boldsymbol{\beta}^*\| \leq \frac{C_g \log^{\frac{1}{2}}(n) \|\boldsymbol{\beta}^*\|^2}{c_1 n^{\frac{1}{2}-\epsilon}} := C_{\boldsymbol{\beta}} \frac{\log^{\frac{1}{2}}(n) \|\boldsymbol{\beta}^*\|^2}{n^{\frac{1}{2}-\epsilon}}$$

Finally, using Assumption B.4, note that there also $\bar{\boldsymbol{\beta}}' = t'\boldsymbol{\beta}^* + (1-t')\hat{\boldsymbol{\beta}}$ where $t' \in [0, 1]$, such that

$$\|\mathbf{g}_i - \mathbf{g}_{i,*}\| \leq \|\nabla^2 f(\mathbf{x}_i, \bar{\boldsymbol{\beta}})\| \|\boldsymbol{\beta}^* - \hat{\boldsymbol{\beta}}\| \leq C_2 \|\boldsymbol{\beta}^*\|^{-2} \|\boldsymbol{\beta}^* - \hat{\boldsymbol{\beta}}\| \leq C_2 C_{\boldsymbol{\beta}} \frac{\log^{\frac{1}{2}}(n)}{n^{\frac{1}{2}-\epsilon}} := C_{\mathbf{g}} \frac{\log^{\frac{1}{2}}(n)}{n^{\frac{1}{2}-\epsilon}}.$$

□

Lemma B.11. Denote $\mathbf{X} = (\mathbf{x}_1, \dots, \mathbf{x}_n)^\top \in \mathbb{R}^{n \times p}$, denote

$$\omega_{\max} \triangleq \sigma_{\max}(\mathbf{X} \mathbf{X}^\top), \quad (48)$$

$$\nu_{\min} \triangleq \sigma_{\min}(\mathbf{J}), \quad (49)$$

where \mathbf{x} is independent of the symmetric matrix $\mathbf{J} \in \mathbb{R}^{p \times p}$ and $\mathbf{X} \in \mathbb{R}^{n \times p}$, and \mathbf{x} a mean-zero sub-Gaussian random vectors with covariance $\boldsymbol{\Sigma}$, and $\rho_{\max} := \sigma_{\max}(\boldsymbol{\Sigma})$, then

$$\Pr\left[\|\mathbf{X} \mathbf{J}^{-1} \mathbf{x}\|_4^2 \geq 2(1+c) \left(\frac{\rho_{\max}}{\nu_{\min}^2} \omega_{\max}\right) \sqrt{n} \log n\right] < \frac{2}{n^c}. \quad (50)$$

Proof of Lemma B.11. First, we prove

$$\Pr \left[\|\mathbf{x}\|_\infty > \rho_{\max} \sqrt{2(1+c) \log p} \right] \leq \frac{2}{p^c} \quad (51)$$

where $\rho_{\max} = \sigma_{\max}(\Sigma)$. The proof strategy below is taken from (Rad & Maleki, 2020).

$$\Pr [\|\mathbf{x}\|_\infty > t] \leq \sum_{i=1}^p \Pr [|x_i| > t] \leq 2 \sum_{i=1}^p e^{-\frac{t^2}{2\Sigma_{ii}}} \leq 2p e^{-\frac{t^2}{2\max_{i=1,\dots,p} \Sigma_{ii}}} \leq 2e^{\log p - \frac{t^2}{2\rho_{\max}}},$$

where $t = \rho_{\max} \sqrt{2(1+c) \log p}$ and $\max_{i=1,\dots,p} \Sigma_{ii} \leq \rho_{\max}$. Second, we prove

$$\Pr [\|\mathbf{x}\|_4^2 > 2(1+c)\rho_{\max} \sqrt{p} \log p] \leq \frac{2}{p^c} \quad (52)$$

in the following way:

$$\begin{aligned} \Pr \left[\left(\sum_{i=1}^p x_i^4 \right)^{\frac{1}{4}} > t \right] &= \Pr \left[\sum_{i=1}^p x_i^4 > t^4 \right] \leq \Pr \left[p \max_{i=1,\dots,p} x_i^4 > t^4 \right] \\ &\leq \Pr \left[\|\mathbf{x}\|_\infty > \left(\frac{t^4}{p} \right)^{1/4} \right] \leq 2e^{\log p - \frac{t^2}{2\rho_{\max} \sqrt{p}}}, \end{aligned} \quad (53)$$

where $t^2 = 2(1+c)\rho_{\max} \sqrt{p} \log p$ yields the desired result.

Let $\mathbf{u} \triangleq \mathbf{X}\mathbf{J}^{-1}\mathbf{x}$, then \mathbf{u} is zero mean Gaussian with covariance $\Sigma_{\mathbf{u}} = \mathbf{X}\mathbf{J}^{-1}\Sigma\mathbf{J}^{-1}\mathbf{X}^\top$ by independence, leading to

$$\sigma_{\max}(\Sigma_{\mathbf{u}}) = \sigma_{\max}(\mathbf{X}\mathbf{J}^{-1}\Sigma\mathbf{J}^{-1}\mathbf{X}^\top) \leq \frac{\rho_{\max}}{\nu_{\min}^2} \omega_{\max}. \quad (54)$$

Therefore, using (52), we have

$$\begin{aligned} \Pr \left[\|\mathbf{X}\mathbf{J}^{-1}\mathbf{x}\|_4^2 > 2(1+c) \left(\frac{\rho_{\max}}{\nu_{\min}^2} \omega_{\max} \right) \sqrt{n \log n} \right] \\ \leq \Pr \left[\|\mathbf{X}\mathbf{J}^{-1}\mathbf{x}\|_4^2 > 2(1+c)\sigma_{\max}(\Sigma_{\mathbf{u}}) \sqrt{n \log n} \right] \leq \frac{2}{n^c}. \end{aligned}$$

□

Lemma B.12. Let $S \in \mathbb{R}^{k \times d}$ be such that $\forall i \in [k], j \in [d], S_{ij} \stackrel{i.i.d.}{\sim} N(0, 1)$. Let A in $\mathbb{R}^{d \times d}$ be a symmetric positive definite matrix with condition number $\left(\frac{\lambda_{\max}(A)}{\lambda_{\min}(A)} \right)$ upper bounded by $\kappa > 0$. Here $\lambda_{\max}(A)$ and $\lambda_{\min}(A)$ are the extremal eigenvalues of A . Let $u \in \mathbb{R}^d$. Then with probability greater than $1 - C \exp(-c\epsilon^2 k)$, where $C, c > 0$ are absolute constants,

$$\frac{1}{\kappa}(1-\epsilon)\frac{k}{d} \leq \frac{u^T S^\top (SAS^\top)^{-1} S u}{u^T A^{-1} u} \leq \min(\kappa(1+\epsilon)\frac{k}{d}, 1) \quad (55)$$

Proof of Lemma B.12. Define,

$$\begin{aligned} P &:= A^{1/2} S^\top (SAS^\top)^{-1} S A^{1/2} \\ \hat{A}^{-1} &:= S^\top (SAS^\top)^{-1} S \\ w &:= A^{-1/2} u \end{aligned}$$

See that P is an orthogonal projection matrix, i.e. for any $l \in \mathbb{R}^d$,

$$\|l\|^2 = \|Pl\|^2 + \|(I-P)l\|^2 \quad (56)$$

Also since $P^2 = P$, $\|Pw\|^2 = w^T Pw$. See also now,

$$\begin{aligned} u^T S^\top (SAS^\top)^{-1} Su &= u^\top \hat{A}^{-1} u = w^T Pw = \|Pw\|^2 \\ u^T A^{-1} u &= \|w\|^2 \end{aligned}$$

Thus, in Theorem B.12, we are now trying to derive a concentration for $\frac{\|Pw\|^2}{\|w\|^2}$. Consider the eigenvalue decomposition of A , $A = Q\Lambda Q^\top$, $\Lambda = \text{diag}(\lambda_1, \lambda_2, \dots, \lambda_d)$, where $\lambda_1 > \lambda_2 > \dots > \lambda_d > 0$. Define $V := Q^\top S^\top$. Since Q is orthogonal, we again have $\forall i \in [d], j \in [k], V_{ij} \stackrel{i.i.d.}{\sim} N(0, 1)$, and $V^T V$ is almost surely positive definite. See,

$$\begin{aligned} P &= A^{1/2} S^\top (SAS^\top)^{-1} S A^{1/2} \\ &= Q \Lambda^{1/2} V (V^\top \Lambda V)^{-1} V^\top \Lambda^{1/2} Q^\top = Q P_V Q^\top, \end{aligned}$$

where $P_V := \Lambda^{1/2} V (V^\top \Lambda V)^{-1} V^\top \Lambda^{1/2}$. It is easy to see that P_V is an orthogonal projection matrix satisfying Equation (56) if we replace P by P_V . Define,

$$\Pi := V (V^\top V)^{-1} V^\top; \quad h := \Lambda^{1/2} w$$

We will first show that, almost surely,

$$\frac{1}{\kappa} \frac{\|\Pi h\|^2}{\|h\|^2} \leq \frac{\|P_V w\|^2}{\|w\|^2} \leq \kappa \frac{\|\Pi h\|^2}{\|h\|^2} \quad (57)$$

By definition of Λ , we have,

$$\begin{aligned} \lambda_d I &\preceq \Lambda \preceq \lambda_1 I \\ \xrightarrow{(i)} \lambda_d V^T V &\preceq V^\top \Lambda V \preceq \lambda_1 V^T V \\ \implies \frac{1}{\lambda_1} (V^T V)^{-1} &\preceq (V^\top \Lambda V)^{-1} \preceq \frac{1}{\lambda_d} (V^T V)^{-1}, \end{aligned}$$

where (i) is since for $B, C, D \in \mathbb{R}^{d \times d}$ and any $j \in \mathbb{R}^d$, $B \preceq C \implies j^\top (C - B)j \geq 0 \implies j^\top D^\top (C - B)Dj \geq 0$. Thus we have almost surely,

$$\frac{1}{\lambda_1} \|\Pi h\|^2 \leq \|P_V w\|^2 \leq \frac{1}{\lambda_d} \|\Pi h\|^2 \quad (58)$$

Also it is clear that we have the following bounds for $\|h\|^2 = w^\top \Lambda w$, $\lambda_d \|w\|^2 \leq \|h\|^2 \leq \lambda_1 \|w\|^2$. Combining with Equation (58), we have shown Equation (57) \square

Using the fact that the quadratic forms of a Gaussian vector projected onto an independent random subspace follow a Beta distribution, Chapter 7 (Anderson, 1958), we have $\frac{\|\Pi h\|^2}{\|h\|^2} \sim \text{Beta}(k/2, (d-k)/2)$. By concentration of Beta distribution (using standard concentration inequalities from (Vershynin, 2009)), we have,

$$P \left(\left| \frac{\|\Pi h\|^2}{\|h\|^2} - \frac{k}{d} \right| > \epsilon \right) \leq C \exp(-ck\epsilon^2) \quad (59)$$

By Equation (57), we have almost surely $\frac{1}{\kappa} \frac{\|\Pi Q^\top h\|^2}{\|Q^\top h\|^2} \leq \frac{\|P_V Q^\top w\|^2}{\|Q^\top w\|^2} \leq \kappa \frac{\|\Pi Q^\top h\|^2}{\|Q^\top h\|^2}$. Thus since $P = Q P_V Q^\top$ and by Equation (59), we have shown Theorem B.12.

B.4. Confirming our assumptions on the loss function

In this section, we examine Assumption B.5 in the context of logistic regression, linear regression, and Poisson regression. Our goal is to justify that the orders are reasonable.

B.4.1. LOGISTIC REGRESSION

Since

$$\dot{\ell}_i(\beta) = -y_i + \frac{e^{\mathbf{g}_i^\top \beta}}{1 + e^{\mathbf{g}_i^\top \beta}}, \quad \ddot{\ell}_i(\beta) = \frac{e^{\mathbf{g}_i^\top \beta}}{\left(1 + e^{\mathbf{g}_i^\top \beta}\right)^2}, \quad \dddot{\ell}_i(\beta) = \frac{e^{\mathbf{g}_i^\top \beta} \left(1 - e^{\mathbf{g}_i^\top \beta}\right)}{\left(1 + e^{\mathbf{g}_i^\top \beta}\right)^3},$$

using simple algebra, it is straightforward to show that for any β , we have

$$\|\dot{\ell}(\beta)\|_\infty \leq 1, \quad \|\ddot{\ell}(\beta)\|_\infty \leq \frac{1}{4}, \quad \|\dddot{\ell}(\beta)\|_\infty \leq \frac{1}{10}.$$

Hence, the first inequality of Assumption B.5 holds. Note that we can assume $\mathbf{g}_i^\top \beta = O_p(1)$, so the second inequality of Assumption B.5 also holds. Moreover,

$$\|\ddot{\ell}_{/i}(\beta + \delta) - \ddot{\ell}_{/i}(\beta)\|_2 \leq \|\ddot{\ell}(\beta + \delta) - \ddot{\ell}(\beta)\|_2 = \sqrt{\sum_i \left(\ddot{\ell}_i(\beta + \delta) - \ddot{\ell}_i(\beta)\right)^2}.$$

Using the mean-value theorem, where $\epsilon_i \in [0, \delta_i]$, we have

$$= \sqrt{\sum_i \ddot{\ell}_i(\beta + \epsilon_i)^2 (\mathbf{g}_i^\top \delta)^2} \leq \sqrt{\delta^\top \mathbf{G}^\top \mathbf{G} \delta} \leq \sqrt{\sigma_{\max}(\mathbf{G}^\top \mathbf{G})} \|\delta\|_2.$$

Based on the inequality above, we obtain

$$\sup_{t \in [0,1]} \frac{\|\ddot{\ell}_{/i}((1-t)\hat{\beta}_{/i} + t\hat{\beta}) - \ddot{\ell}_{/i}(\hat{\beta})\|_2}{\|\hat{\beta}_{/i} - \hat{\beta}\|_2} \leq \sup_{t \in [0,1]} \frac{(1-t)\|\hat{\beta}_{/i} - \hat{\beta}\|_2 \sqrt{\sigma_{\max}(\mathbf{G}^\top \mathbf{G})}}{\|\hat{\beta}_{/i} - \hat{\beta}\|_2} \leq \sqrt{\sigma_{\max}(\mathbf{G}^\top \mathbf{G})}.$$

By Assumption B.3, we know that $\sigma_{\max}(\mathbf{G}^\top \mathbf{G}) = O_p(n/\|\beta^*\|^2)$, thus the third inequality in Assumption B.5 holds.

B.4.2. LINEAR REGRESSION

Considering $\ell(y | \mathbf{x}^\top \beta) = \frac{1}{2}(y - \mathbf{x}^\top \beta)^2$, we have $\dot{\ell}_i(\beta) = -(y_i - \mathbf{g}_i^\top \beta)$ and $\ddot{\ell}_i(\beta) = 1$. Therefore, the second and third inequalities in Assumption B.5 hold directly. Moreover, since $y \sim \mathcal{N}(\mathbf{x}^\top \beta^*, \sigma_\epsilon^2)$, by properties of sub-Gaussian random variables we obtain

$$\max_{i \in [n]} |\dot{\ell}_i(\beta)| \preceq \sqrt{\log n}.$$

Hence, the first inequality in Assumption B.5 holds.

B.4.3. POISSON REGRESSION

Consider

$$\ell(y | \mathbf{x}^\top \beta) = h(\mathbf{x}^\top \beta) - y \log h(\mathbf{x}^\top \beta) + \log y!,$$

with the conditional mean $\mathbb{E}[y | \mathbf{x}, \beta] = h(\mathbf{x}^\top \beta)$ where $h(s) = \log(1 + e^s)$. Then the first and second derivatives of the loss with respect to $s := \mathbf{x}^\top \beta$ are

$$\dot{\ell}(y, s) = h'(s) \left(1 - \frac{y}{h(s)}\right) = \sigma(s) \left(1 - \frac{y}{h(s)}\right),$$

and

$$\ddot{\ell}(y, s) = \sigma(s) \left(1 - \sigma(s)\right) \left(1 - \frac{y}{h(s)}\right) + y \frac{\sigma(s)^2}{h(s)^2}.$$

By Lemma 8 of Rad & Maleki (2020), we have

$$\sup_{t \in [0,1]} \frac{\|\ddot{\ell}_{/i}((1-t)\hat{\beta}_{/i} + t\hat{\beta}) - \ddot{\ell}_{/i}(\hat{\beta})\|_2}{\|\hat{\beta}_{/i} - \hat{\beta}\|_2} \leq (1 + 6\|y\|_\infty) \sqrt{\sigma_{\max}(\mathbf{G}^\top \mathbf{G})},$$

and

$$\|\dot{\ell}(\beta)\|_\infty \leq 1 + \|y\|_\infty.$$

where σ is sigmoid function. Since $\mathbf{x}_i^\top \beta \sim \mathcal{N}(0, \beta^\top \Sigma \beta)$, we have $\max_{i \in [n]} |\mathbf{x}_i^\top \beta| = O(\log n)$ and $\|y\|_\infty = O(\text{poly log } n)$, both holding with high probability. Therefore, using Assumption B.3, the three inequalities in Assumption B.5 hold.

B.5. Confirming our assumptions on the nonlinear function $f(\cdot, \cdot)$

B.5.1. VERIFICATION OF EXAMPLE 2.2.

Consider the GLM where $f(\mathbf{x}, \beta) = \mathbf{x}^\top \beta$. We verify Assumptions B.2, B.3, B.4, and B.7.

First, note that $p = d$ and $\nabla f(\mathbf{x}, \beta) = \mathbf{x}$. Since we assume $|\beta_i^*| = O(1)$, we have $p \asymp \|\beta^*\|^2$. Combined with Assumption B.1, this implies that Assumptions B.2 and B.7 hold, due to standard properties of sub-Gaussian vectors. Next, because $\nabla^2 f = 0$, Assumption B.4 holds automatically.

Furthermore, since

$$\mathbf{G}(\beta)^\top \mathbf{G}(\beta) = \mathbf{X}^\top \mathbf{X},$$

and $\sigma_{\max}(\Sigma) \asymp \sigma_{\min}(\Sigma) \asymp O_p(1/p)$ with $p \asymp \|\beta^*\|^2$, and the vectors \mathbf{x}_i , $i \in [n]$, are independent sub-Gaussian, we obtain

$$\sigma_{\max}(\mathbf{X}^\top \mathbf{X}) \asymp \sigma_{\min}(\mathbf{X}^\top \mathbf{X}) \asymp O_p\left(\frac{1}{\|\beta^*\|^2}\right),$$

which verifies Assumption B.3.

B.5.2. VERIFICATION OF EXAMPLE 2.3.

Setting and Assumptions. We verify Assumptions B.2, B.3, B.4, and B.7 in a linear-layer setting. Let the parameter vector be

$$\beta = (\text{vec}(\mathbf{W})^\top, \mathbf{v}^\top)^\top,$$

where $\mathbf{W} \in \mathbb{R}^{h \times p}$ satisfies

$$\sigma_{\min}(\mathbf{W}^\top \mathbf{W}) \asymp \sigma_{\max}(\mathbf{W}^\top \mathbf{W}).$$

We further assume $|v_l| = O(1)$; that is, there exist constants $v, V > 0$ such that

$$v \leq |v_l| \leq V, \quad \forall l \in [h].$$

We also assume the initialization satisfies

$$p\|\mathbf{v}\|^2 \asymp \|\mathbf{W}\|_F^2,$$

which holds for common isotropic initializations.

Let σ be an activation function with

$$0 \leq \sigma'(x) \leq E.$$

For $\mathbf{x} \in \mathbb{R}^p$, define $\sigma(\mathbf{x})$ element-wise. Define the function

$$f(\mathbf{x}, \mathbf{W}, \mathbf{v}) = \mathbf{v}^\top \sigma(\mathbf{W}\mathbf{x}).$$

The gradients are given by

$$\nabla_{\mathbf{v}} f(\mathbf{x}, \mathbf{W}, \mathbf{v}) = \sigma(\mathbf{W}\mathbf{x}) \in \mathbb{R}^h,$$

$$\nabla_{\mathbf{W}} f(\mathbf{x}, \mathbf{W}, \mathbf{v}) = \text{diag}(\sigma'(\mathbf{W}\mathbf{x})) \mathbf{v} \mathbf{x}^\top \in \mathbb{R}^{h \times p}.$$

For notational convenience, for $l \in [h]$ and $i \in B \subset [n]$, define

$$A_{li}^B = \sigma'(\mathbf{W}_l^\top \mathbf{x}_i), \quad D_{li}^B = v_l \sigma'(\mathbf{W}_l^\top \mathbf{x}_i).$$

Then the relationship between the Gram matrices is

$$D^B(D^B)^\top = \text{diag}(\mathbf{v}) A^B (A^B)^\top \text{diag}(\mathbf{v}).$$

Assume that for any $B \subset [n]$ with $|B| \gg h$, with high probability we can find constants $\underline{\alpha}, \bar{\alpha} > 0$ such that

$$\bar{\alpha}|B| \geq \lambda_{\max}(A^B A^{B,\top}) \geq \lambda_{\min}(A^B A^{B,\top}) \geq \underline{\alpha}|B|.$$

Intuitively, if for all $l \in [h]$,

$$\sum_{i \in B} \sigma'^2(\mathbf{W}_l^\top \mathbf{x}_i) \asymp |B|,$$

then

$$\text{tr}(A^B A^{B,\top}) = \sum_{l=1}^h \sum_{i \in B} \sigma'^2(\mathbf{W}_l^\top \mathbf{x}_i) \asymp h|B|.$$

If $A^B A^{B,\top}$ is well-conditioned, this implies the eigenvalue bounds above. Consequently, utilizing the bounds on v_l ,

$$V^2 \bar{\alpha} |B| \geq \lambda_{\max}(D^B D^{B,\top}) \geq \lambda_{\min}(D^B D^{B,\top}) \geq v^2 \underline{\alpha} |B|.$$

We denote $A^{[n]} = A$ and $D^{[n]} = D$ for simplicity.

We further assume $n > d$ and $n \gg h^2$. Intuitively, if $n < d$ where d is the parameter dimension, the empirical Fisher

$$\mathbf{G}^\top \mathbf{G} = \sum_{i=1}^n \mathbf{g}_i \mathbf{g}_i^\top$$

cannot be invertible. Similarly, in very wide networks, the sample size must dominate the width to obtain stable approximations.

Verification of Assumption B.2. First, we verify Assumption B.2. Note that

$$\|\nabla_{\mathbf{v}} f(\mathbf{x}, \mathbf{W}, \mathbf{v})\| = \|\sigma(\mathbf{W}\mathbf{x})\| \leq E\|\mathbf{W}\mathbf{x}\| = O_{\text{HP}}(\sqrt{\text{tr}(\mathbf{W}\Sigma\mathbf{W}^\top)}) = O_{\text{HP}}(\sqrt{\|\mathbf{W}\|_F^2/\|\beta^*\|^2}) = O_{\text{HP}}(1).$$

$$\|\nabla_{\mathbf{W}} f(\mathbf{x}, \mathbf{W}, \mathbf{v})\|_F^2 \leq E^2 \|\mathbf{v}\|^2 \|\mathbf{x}\|^2 = O_{\text{HP}}\left(\frac{p\|\mathbf{v}\|^2}{\|\beta^*\|^2}\right) = O_{\text{HP}}(1),$$

using the scaling assumption $p\|\mathbf{v}\|^2 \asymp \|\mathbf{W}\|_F^2$.

Verification of Assumption B.3. Next, we verify Assumption B.3. For simplicity, we consider

$$\mathbf{g}_i = \text{vec}(\nabla_{\mathbf{W}} f(\mathbf{x}_i, \mathbf{W}, \mathbf{v})) = c_i \otimes \mathbf{x}_i,$$

where $c_i = D_{:,i}$ is the i -th column of D . Denoting $\mathbf{G} = (\mathbf{g}_1, \dots, \mathbf{g}_n)$, we know that

$$M := \frac{1}{n} \mathbf{G}^\top \mathbf{G} = \frac{1}{n} \sum_{i=1}^n \mathbf{g}_i \mathbf{g}_i^\top = \frac{1}{n} \sum_{i=1}^n c_i c_i^\top \otimes \mathbf{x}_i \mathbf{x}_i^\top = \frac{1}{n} \sum_{i=1}^n (c_i \otimes \mathbf{x}_i) (c_i \otimes \mathbf{x}_i)^\top.$$

To analyze the eigenvalues of M , consider any $q \in \mathbb{R}^{ph}$ such that $q = \text{vec}(Q)$ and $\|q\| = \|Q\|_F = 1$. We only need to bound

$$q^\top M q = q^\top \left(\frac{1}{n} \sum_{i=1}^n (c_i \otimes \mathbf{x}_i) (c_i \otimes \mathbf{x}_i)^\top \right) q = \frac{1}{n} \sum_{i=1}^n (\mathbf{x}_i^\top Q c_i)^2.$$

Note that $Q \in \mathbb{R}^{p \times h}$. We consider two cases separately: $\text{rank}(Q) = 1$ and $\text{rank}(Q) > 1$.

First, consider the case when $\text{rank}(Q) = 1$. There exist $a \in \mathbb{R}^p$ and $b \in \mathbb{R}^h$ such that $Q = ab^\top$. WLOG, assume $\|a\|^2 = \|b\|^2 = 1$. Then we have:

$$\begin{aligned} q^\top Mq &= a^\top \left[\frac{1}{n}(\mathbf{x}_1, \dots, \mathbf{x}_n) \text{diag}((b^\top c_1)^2, \dots, (b^\top c_n)^2)(\mathbf{x}_1, \dots, \mathbf{x}_n)^\top \right] a \\ &\geq \|a\|^2 \lambda_{\min} \left(\frac{1}{n}(\mathbf{x}_1, \dots, \mathbf{x}_n) \text{diag}((b^\top c_1)^2, \dots, (b^\top c_n)^2)(\mathbf{x}_1, \dots, \mathbf{x}_n)^\top \right). \end{aligned} \quad (60)$$

For any $b \in \mathbb{R}^h$ with $\|b\| = 1$, denote $S_b = \{i : (b^\top c_i)^2 \geq \frac{\underline{\alpha}v^2}{2}\}$ and let $S_b^c = [n] \setminus S_b$. We know that

$$\begin{aligned} \|b\|^2 \underline{\alpha}nv^2 &\leq b^\top DD^\top b = \sum_{i=1}^n (b^\top c_i)^2 = \sum_{i \in S_b} (b^\top c_i)^2 + \sum_{i \notin S_b} (b^\top c_i)^2 \\ &\leq \|b\|^2 E^2 V^2 h |S_b| + (n - |S_b|) \frac{\underline{\alpha}v^2}{2} \\ &= \left(E^2 V^2 h - \frac{\underline{\alpha}v^2}{2} \right) |S_b| + \frac{\underline{\alpha}v^2}{2} n, \end{aligned}$$

where in the second inequality we used $|c_i|^2 \leq E^2 V^2 h$. Thus, we get

$$|S_b| \geq \frac{\underline{\alpha}v^2}{2E^2 V^2 h - \underline{\alpha}v^2} n \gg h,$$

using $n \gg h^2$. We can further refine the inequality:

$$\begin{aligned} \|b\|^2 \underline{\alpha}nv^2 &\leq b^\top DD^\top b = \sum_{i=1}^n (b^\top c_i)^2 = \sum_{i \in S_b} (b^\top c_i)^2 + \sum_{i \notin S_b} (b^\top c_i)^2 \\ &\leq \|b\|^2 \bar{\alpha}V^2 |S_b| + (n - |S_b|) \frac{\underline{\alpha}v^2}{2} \\ &= \frac{\underline{\alpha}v^2}{2} n + |S_b| \left(\bar{\alpha}V^2 - \frac{\underline{\alpha}v^2}{2} \right), \end{aligned}$$

where we used $b^\top D^{S_b} D^{S_b, \top} b \leq \|b\|^2 |S_b| \bar{\alpha}V^2$ for $|S_b| \gg h$. Then we obtain

$$|S_b| \geq \frac{\underline{\alpha}v^2}{2\bar{\alpha}V^2 - \underline{\alpha}v^2} n := C(\underline{\alpha}, \bar{\alpha}, v, V) n.$$

Returning to (60), we have

$$\begin{aligned} q^\top Mq &\geq \lambda_{\min} \left(\frac{1}{n}(\mathbf{x}_1, \dots, \mathbf{x}_n) \text{diag}((b^\top c_1)^2, \dots, (b^\top c_n)^2)(\mathbf{x}_1, \dots, \mathbf{x}_n)^\top \right) \\ &\geq \lambda_{\min} \left(\frac{1}{n} \sum_{i \in S_b} \mathbf{x}_i \mathbf{x}_i^\top (b^\top c_i)^2 \right) \geq \lambda_{\min} \left(\frac{1}{n} \sum_{i \in S_b} \mathbf{x}_i \mathbf{x}_i^\top \frac{\underline{\alpha}v^2}{2} \right) \\ &= \frac{\underline{\alpha}v^2}{2} \frac{|S_b|}{n} \lambda_{\min} \left(\frac{1}{|S_b|} \sum_{i \in S_b} \mathbf{x}_i \mathbf{x}_i^\top \right). \end{aligned}$$

By the sub-Gaussianity of i.i.d \mathbf{x}_i , we have

$$\lambda_{\min} \left(\frac{1}{|S_b|} \sum_{i \in S_b} \mathbf{x}_i \mathbf{x}_i^\top \right) - \lambda_{\min}(\Sigma) \left(1 - \sqrt{\frac{p}{|S_b|}} \right)^2 \rightarrow 0, \quad \text{a.s.},$$

where $\lambda_{\min}(\Sigma) (1 - \sqrt{\frac{p}{|S_b|}})^2 \asymp \|\beta^*\|^{-2}$. Finally, we get

$$q^\top Mq \succeq \|\beta^*\|^{-2}, \quad \text{a.s.}.$$

Next, we consider the upper bound in the rank-1 case. Similar to (60), we get

$$\begin{aligned} q^\top M q &= a^\top \left[\frac{1}{n} (\mathbf{x}_1, \dots, \mathbf{x}_n) \operatorname{diag}((b^\top c_1)^2, \dots, (b^\top c_n)^2) (\mathbf{x}_1, \dots, \mathbf{x}_n)^\top \right] a \\ &\leq \|a\|^2 \lambda_{\max} \left(\frac{1}{n} (\mathbf{x}_1, \dots, \mathbf{x}_n) \operatorname{diag}((b^\top c_1)^2, \dots, (b^\top c_n)^2) (\mathbf{x}_1, \dots, \mathbf{x}_n)^\top \right). \end{aligned} \quad (61)$$

Define $T_b = \{i : (b^\top c_i)^2 \geq ph\}$. We know that

$$\|b\|^2 \bar{\alpha} n V^2 \geq b^\top D D^\top b = \sum_{i=1}^n (b^\top c_i)^2 = \sum_{i \in T_b} (b^\top c_i)^2 + \sum_{i \notin T_b} (b^\top c_i)^2 \geq |T_b| ph.$$

So we get $|T_b| \leq \frac{\bar{\alpha} V^2}{ph} n$. Note that

$$\begin{aligned} &\lambda_{\max} \left(\frac{1}{n} (\mathbf{x}_1, \dots, \mathbf{x}_n) \operatorname{diag}((b^\top c_1)^2, \dots, (b^\top c_n)^2) (\mathbf{x}_1, \dots, \mathbf{x}_n)^\top \right) \\ &\leq \lambda_{\max} \left(\frac{1}{n} \sum_{i \in T_b} \mathbf{x}_i \mathbf{x}_i^\top (b^\top c_i)^2 \right) + \lambda_{\max} \left(\frac{1}{n} \sum_{i \notin T_b} \mathbf{x}_i \mathbf{x}_i^\top (b^\top c_i)^2 \right). \end{aligned}$$

We consider these two parts. For the first part:

$$\lambda_{\max} \left(\frac{1}{n} \sum_{i \in T_b} \mathbf{x}_i \mathbf{x}_i^\top (b^\top c_i)^2 \right) \preceq \frac{|T_b|}{n} \frac{p}{\|\beta^*\|^2} E^2 V^2 h \|b\|^2 \leq \frac{\bar{\alpha} V^2}{ph} \frac{p h E^2 V^2}{\|\beta\|^2} \asymp \|\beta^*\|^{-2},$$

with high probability. For the second part:

$$\begin{aligned} \lambda_{\max} \left(\frac{1}{n} \sum_{i \notin T_b} \mathbf{x}_i \mathbf{x}_i^\top (b^\top c_i)^2 \right) &\leq \frac{n - |T_b|}{n} \lambda_{\max} \left(\frac{1}{n - |T_b|} \sum_{i \notin T_b} \mathbf{x}_i \mathbf{x}_i^\top (b^\top c_i)^2 \right) \\ &\leq \lambda_{\max}(\Sigma) \left(1 + \sqrt{\frac{p}{n - |T_b|}} \right)^2 \asymp \|\beta^*\|^{-2}, \end{aligned}$$

with high probability, where we used that $\|\mathbf{x}_i \mathbf{x}_i^\top\|_2 = \mathbf{x}_i^\top \mathbf{x}_i = O_{\text{HP}}(\frac{p}{\|\beta^*\|^2})$ and $|T_b| \leq \frac{\bar{\alpha} V^2}{ph} n$. Thus,

$$q^\top M q \preceq \|\beta^*\|^{-2}, \quad \text{with high probability.}$$

This concludes the rank-1 case.

Next, we consider the case when $\operatorname{rank}(Q) = R > 1$. We can write $Q = \sum_{r=1}^R a_r b_r^\top$, where $\{a_r\}_{r \in [R]}$ and $\{b_r\}_{r \in [R]}$ are orthogonal sets respectively. WLOG, assume $\|b_r\| = 1$ for $r = 1, \dots, R$. Since $\|Q\|_F^2 = 1$, we have $\sum_{r=1}^R \|a_r\|^2 = 1$. Note that

$$q^\top M q \approx \sum_{r=1}^R a_r^\top \left[\frac{1}{n} (\mathbf{x}_1, \dots, \mathbf{x}_n) \operatorname{diag}((b_r^\top c_1)^2, \dots, (b_r^\top c_n)^2) (\mathbf{x}_1, \dots, \mathbf{x}_n)^\top \right] a_r.$$

Using results from Case 1, we already know that for each r :

$$\begin{aligned} &\lambda_{\min} \left(\frac{1}{n} (\mathbf{x}_1, \dots, \mathbf{x}_n) \operatorname{diag}((b_r^\top c_1)^2, \dots, (b_r^\top c_n)^2) (\mathbf{x}_1, \dots, \mathbf{x}_n)^\top \right) \\ &\asymp \lambda_{\max} \left(\frac{1}{n} (\mathbf{x}_1, \dots, \mathbf{x}_n) \operatorname{diag}((b_r^\top c_1)^2, \dots, (b_r^\top c_n)^2) (\mathbf{x}_1, \dots, \mathbf{x}_n)^\top \right) \asymp \|\beta^*\|^{-2}. \end{aligned}$$

We then obtain

$$q^\top M q \asymp \sum_{r=1}^R \|a_r\|^2 \|\beta^*\|^{-2} \asymp \|\beta^*\|^{-2}.$$

Verification of Assumption B.7. For simplicity, we consider $\sigma(x) = x$. We have

$$\mathbf{g}_{i,*} = \begin{pmatrix} \mathbf{W} \\ \mathbf{v} \otimes \mathbb{I}_p \end{pmatrix} \mathbf{x}_i,$$

and

$$\left\| \begin{pmatrix} \mathbf{W} \\ \mathbf{v} \otimes \mathbb{I}_p \end{pmatrix} \right\| = \sqrt{\lambda_{\max}(\mathbf{W}^\top \mathbf{W}) + \|\mathbf{v}\|^2} \leq \sqrt{\frac{2\|\mathbf{W}\|_F^2}{p}} \asymp \frac{\|\beta^*\|}{\sqrt{p}},$$

where for the first inequality we use the assumption that $\lambda_{\min}(\mathbf{W}^\top \mathbf{W}) \asymp \lambda_{\max}(\mathbf{W}^\top \mathbf{W})$.

Using $\mathbf{x}_i \sim$ zero-mean sub-Gaussian with covariance Σ , where $\|\Sigma\| \asymp \|\beta^*\|^{-2}$, we know that $\frac{\|\beta^*\|}{\sqrt{p}} \mathbf{x}_i$ is zero-mean sub-Gaussian with covariance Σ' such that $\|\Sigma'\| \asymp \frac{1}{p}$. Thus $\frac{\|\beta^*\|}{\sqrt{p}} \mathbf{x}_i \sim \text{nSG}(\sigma)$ for some $\sigma > 0$. Then

$$\begin{aligned} \mathbb{P}\left(\left\| \begin{pmatrix} \mathbf{W} \\ \mathbf{v} \otimes \mathbb{I}_p \end{pmatrix} \mathbf{x}_i - \mathbb{E} \begin{pmatrix} \mathbf{W} \\ \mathbf{v} \otimes \mathbb{I}_p \end{pmatrix} \mathbf{x}_i \right\| \geq t\right) &\leq \mathbb{P}\left(\left\| \begin{pmatrix} \mathbf{W} \\ \mathbf{v} \otimes \mathbb{I}_p \end{pmatrix} \right\| \|\mathbf{x}_i - \mathbb{E}\mathbf{x}_i\| \geq t\right) \\ &\asymp \mathbb{P}\left(\frac{\|\beta^*\|}{\sqrt{p}} \|\mathbf{x}_i - \mathbb{E}\mathbf{x}_i\| \geq t\right) \\ &\leq 2 \exp\left(-\frac{t^2}{2\sigma^2}\right). \end{aligned}$$

Therefore,

$$\mathbf{g}_{i,*} \stackrel{i.i.d.}{\sim} \text{nSG}(\sigma).$$

C. More empirical results

C.1. Correlation-Based Simulations

C.1.1. VANILLA LINEAR MODELS

We first consider the linear case where $f(\mathbf{x}, \beta^*) = \mathbf{x}^\top \beta^*$ and focus on binary classification and Poisson regression as representative examples.

In this setting, the linearization error is exactly zero; thus, only the ALO step and the projection step need to be evaluated.

We generate the rows $\mathbf{x}_1^\top, \dots, \mathbf{x}_n^\top$ of the design matrix \mathbf{X} independently from a mean-zero multivariate normal distribution with covariance matrix Σ . Here, Σ is a Toeplitz matrix satisfying

$$\text{corr}(X_{ij}, X_{ij'}) = 0.1^{|j-j'|}.$$

We rescale β^* and Σ such that $\|\beta^*\|^2 = p$ and $\beta^{*\top} \Sigma \beta^* = 1$, ensuring that our theoretical assumptions are satisfied.

Binary Classification For binary classification, we randomly select 100 training points to remove. To reduce variability, we independently sample 10 new test points \mathbf{z}_{new} from the same distribution. For each test point, we compute its influence with respect to each removed training point. This procedure yields 1,000 realizations of $\mathcal{I}^{\text{True}}$, \mathcal{I}^{ALO} , and $\mathcal{I}^{\text{TRAK}}(k)$, where k denotes the projection dimension.

ALO Step Figure 4 validates Theorem 2.13. As shown, $\mathcal{I}^{\text{True}}$ and \mathcal{I}^{ALO} are nearly identical, with fitted slopes close to one. This confirms that the ALO step introduces only negligible magnitude error, consistent with our theoretical guarantee.

Projection Step Figure 5 shows the correlation between $\mathcal{I}^{\text{True}}$ and $\mathcal{I}^{\text{TRAK}}$ for $k = 0.75d, 0.50d$, and $0.25d$, where $d = p = 100$. Two observations stand out: first, the slope is not 1 and decreases as k decreases, validating Theorem 2.14; second, as k decreases, the correlation also decreases, validating Theorem 2.14 that the probability of ranking failure decreases as k increases. Nevertheless, the correlation remains noisy, and precise rankings are not preserved.

Poisson Regression We next consider Poisson regression with a softplus mean function. As shown in Figure 4 and Figure 6, we observe trends similar to those in binary classification, further validating Theorems 2.13 and 2.14.

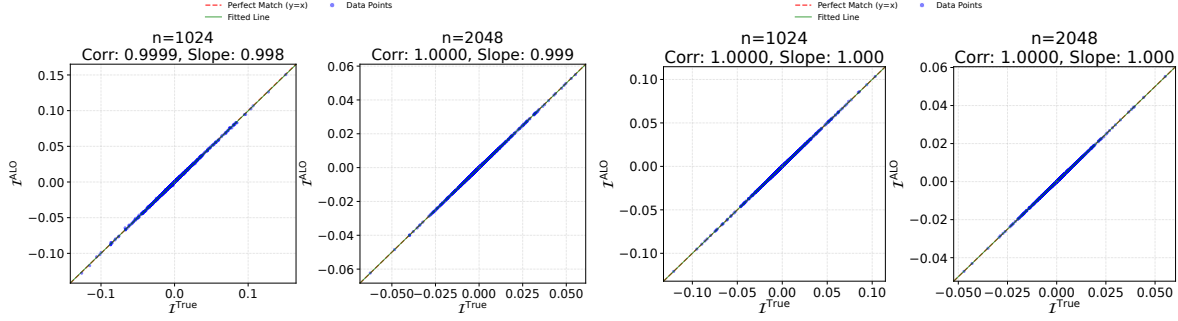


Figure 4. **Left two panels:** Binary logistic regression with $p = 100$, $n = 1024$ and $n = 2048$. The x-axis shows $\mathcal{I}^{\text{True}}$; the y-axis shows \mathcal{I}^{ALO} . **Right two panels:** Poisson regression under the same p and n settings.

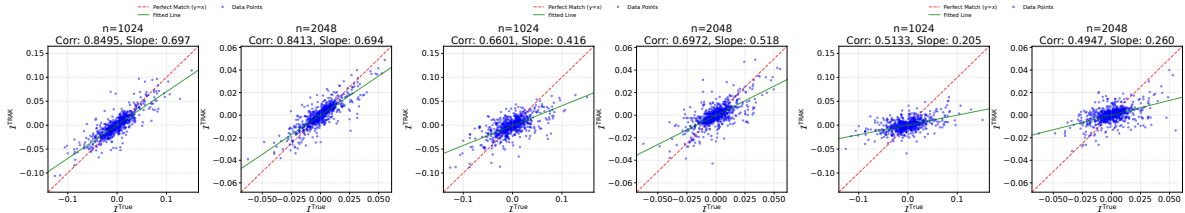


Figure 5. Binary logistic regression with projection ($p = 100$, $n = 1024$ and $n = 2048$). The x-axis is $\mathcal{I}^{\text{True}}$; the y-axis is $\mathcal{I}^{\text{TRAK}}$. From left to right, projection dimensions are $k = 75, 50$, and 25 .

C.1.2. NONLINEAR CASE

Here we present results for 5-class classification, which can be compared with Figure 1 and Figure 2 in the main text.

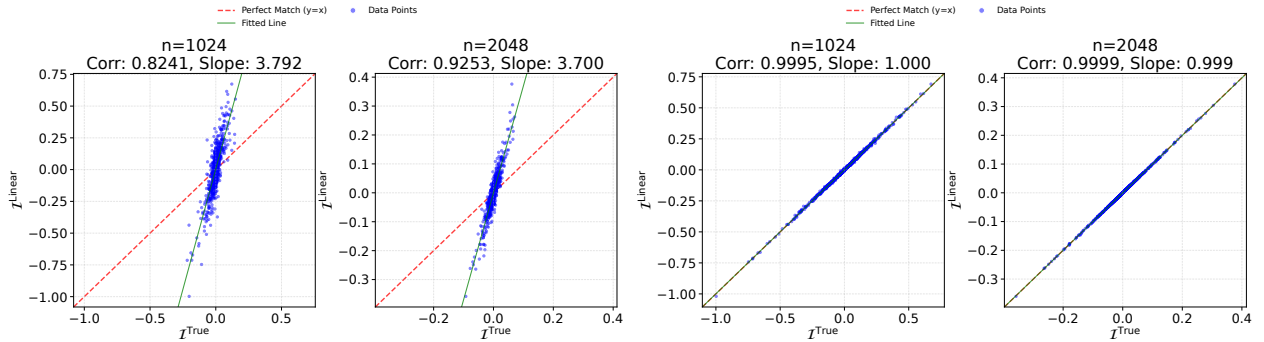


Figure 7. Correlation analysis for 5-class classification with $p = 100$. **Left two panels:** Linearization step: x-axis is $\mathcal{I}^{\text{True}}$, y-axis is $\mathcal{I}^{\text{Linear}}$. **Right two panels:** ALO step: x-axis is $\mathcal{I}^{\text{True}}$, y-axis is \mathcal{I}^{ALO} .

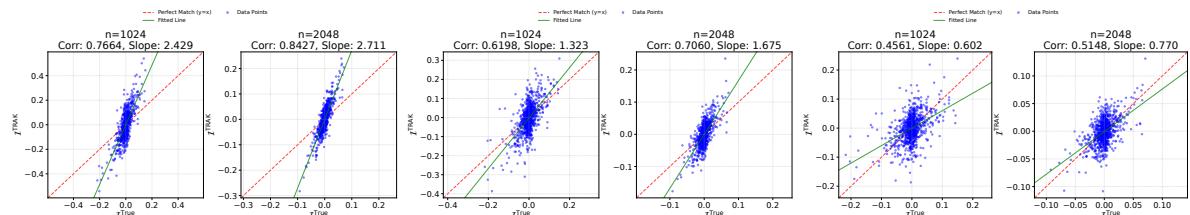


Figure 8. 5-class classification with projection ($p = 100$, $n = 1024$ and $n = 2048$). The x-axis is $\mathcal{I}^{\text{True}}$; the y-axis is $\mathcal{I}^{\text{TRAK}}$. From left to right, projection dimensions are $k = 75, 50$, and 25 .

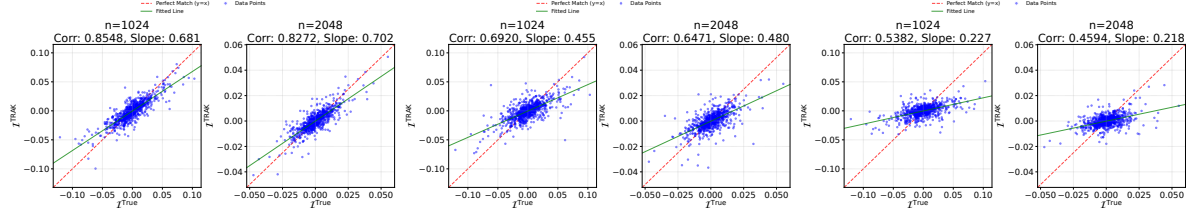


Figure 6. Poisson regression with projection. Settings are identical to Figure 5.

C.2. Magnitude-Based Simulations

C.2.1. SIMULATIONS FOR VANILLA LINEAR MODELS

We first consider the linear model $f(\mathbf{x}, \beta^*) = \mathbf{x}^\top \beta^*$. Here, the linearization error is identically zero, so only the ALO approximation error must be examined.

We generate the rows $\mathbf{x}_1^\top, \dots, \mathbf{x}_n^\top$ of \mathbf{X} independently from a mean-zero Gaussian distribution with covariance Σ , where Σ is Toeplitz with $\text{cor}(X_{ij}, X_{ij'}) = 0.1^{|j-j'|}$. We rescale β^* and Σ such that $\|\beta^*\|^2 = p$ and $\beta^{*\top} \Sigma \beta^* = 1$, satisfying the assumptions of Section C.2.1.

For each trial t , we generate a dataset $\mathbf{X}^{(t)} \in \mathbb{R}^{n \times p}$ with responses $y^{(t)} \in \mathbb{R}^n$. We repeat for 100 independent trials. In each trial, we independently sample 10 new test points and randomly remove 10 training points. Applying Theorem 2.13, this produces 100 error realizations per trial, yielding 10,000 realizations overall, which we use to construct empirical confidence intervals and median errors.

Binary Logistic Regression We first consider binary classification.

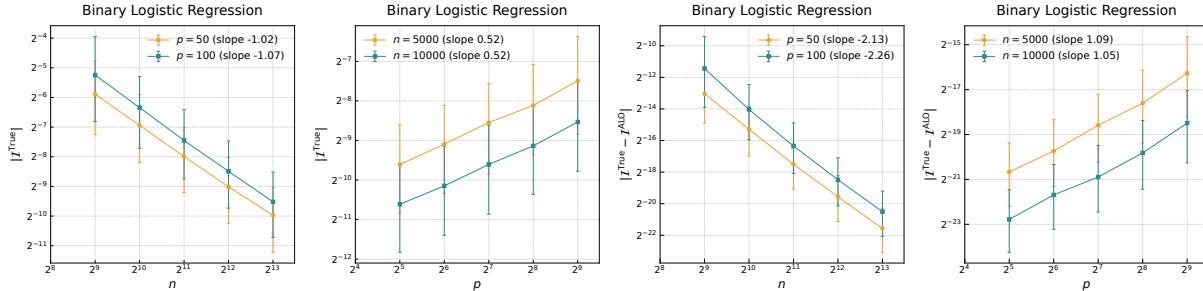


Figure 9. Binary logistic regression. **Left two panels:** $|\mathcal{I}^{\text{True}}|$. **Right two panels:** $|\mathcal{I}^{\text{True}} - \mathcal{I}^{\text{ALO}}|$. Both axes are log-transformed. Medians are plotted; error bars show first and third quartiles.

Figure 9 reports the magnitude of $|\mathcal{I}^{\text{True}}|$ and the approximation error $|\mathcal{I}^{\text{True}} - \mathcal{I}^{\text{ALO}}|$ for varying n and p (log scale). The left panels show that $|\mathcal{I}^{\text{True}}|$ scales approximately as $p^{1/2}/n$, matching Proposition 2.5 and demonstrating that the bound is essentially sharp under our normalization ($\|\beta^*\|^2 = p$).

The right panels show that $|\mathcal{I}^{\text{True}} - \mathcal{I}^{\text{ALO}}|$ decays roughly as p/n^2 when $p \ll n$, which is smaller than the general upper bound $p^{1/2}/n^{3/2}$ from Theorem 2.13. When $p \asymp n$, the two rates coincide. This suggests the bound in Theorem 2.13 could be sharpened under stronger assumptions; nevertheless, it suffices to conclude that the ALO error is negligible in magnitude.

Poisson Regression We next consider Poisson regression with a softplus mean function. Figure 10 presents the corresponding results. The scaling of both $|\mathcal{I}^{\text{True}}|$ and $|\mathcal{I}^{\text{True}} - \mathcal{I}^{\text{ALO}}|$ closely mirrors the binary logistic case, further confirming Proposition 2.5 and Theorem 2.13 for linear models beyond logistic regression.

C.2.2. SIMULATIONS FOR MULTI-CLASS CLASSIFICATION

We now consider nonlinear functions, using multi-class classification ($K = 3$ and $K = 5$) as an example. In short, we obtain similar scaling for $|\mathcal{I}^{\text{True}}|$ and $|\mathcal{I}^{\text{True}} - \mathcal{I}^{\text{ALO}}|$ as in the linear case, and we further validate the order of $|\mathcal{I}^{\text{True}} - \mathcal{I}^{\text{Linear}}|$.

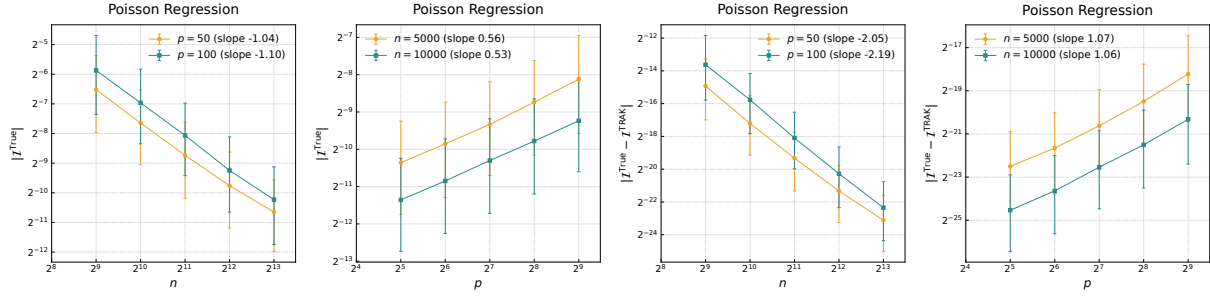


Figure 10. Poisson regression. **Left two panels:** $|\mathcal{I}^{\text{True}}|$. **Right two panels:** $|\mathcal{I}^{\text{True}} - \mathcal{I}^{\text{ALO}}|$. Both axes are log-transformed. Medians are plotted; error bars show first and third quartiles.

The experimental setup matches Section C.2.1. As shown in Figure 11, the orders in n and p of $|\mathcal{I}^{\text{True}}|$ and $|\mathcal{I}^{\text{Linear}} - \mathcal{I}^{\text{ALO}}|$

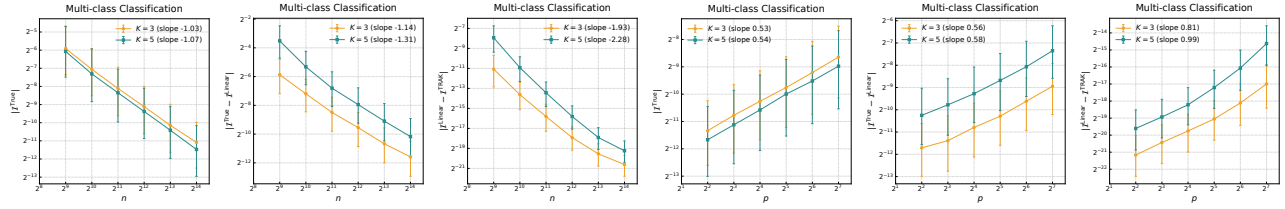


Figure 11. Multi-class classification. **Left:** $|\mathcal{I}^{\text{True}}|$. **Middle:** $|\mathcal{I}^{\text{True}} - \mathcal{I}^{\text{Linear}}|$. **Right:** $|\mathcal{I}^{\text{Linear}} - \mathcal{I}^{\text{ALO}}|$. Both axes are log-transformed. Medians are plotted; error bars show first and third quartiles.

are consistent with those described in Section C.2.1. For $|\mathcal{I}^{\text{True}} - \mathcal{I}^{\text{Linear}}|$, the order is approximately \sqrt{p}/n , validating both the correctness and sharpness of Theorem 2.9.

Finally, we examine the order of the projection step in Figure 12. In the top row of Figure 12, we present the independent case, where \mathbf{z}_i and \mathbf{z}_{new} are independent. The first panel fixes $p = 100$ and varies n , while the second panel fixes $n = 5,000$ and varies p . In both cases, the magnitude of $\mathcal{I}^{\text{TRAK}}$ scales as $\propto n^{-1}p^{1/2}$, which matches the order of \mathcal{I}^{ALO} in the independent setting. Moreover, the second and fourth panels show that the magnitude of $\mathcal{I}^{\text{TRAK}}$ scales as $\propto k^{1/2}$, which validates the sharpness of the bound in Theorem 2.14 for the independent case.

C.3. From Independence to Dependence

In this section, we present results for the case where the test point \mathbf{z}_{new} is dependent on the training point \mathbf{z}_i . Specifically, we study the magnitude and correlation properties of $\mathcal{I}^{\text{True}}(\mathbf{z}_i, \mathbf{z}_i)$, $\mathcal{I}^{\text{Linear}}(\mathbf{z}_i, \mathbf{z}_i)$, and $\mathcal{I}^{\text{ALO}}(\mathbf{z}_i, \mathbf{z}_i)$.

C.3.1. MAGNITUDE-BASED RESULTS

In Figure 13, we select 100 training datapoints as \mathbf{z}_i for each n and p , then plot the corresponding influence functions. As shown in Figure 13, we plot the magnitudes of $|\mathcal{I}^{\text{True}}(\mathbf{z}_i, \mathbf{z}_i)|$, $|\mathcal{I}^{\text{True}}(\mathbf{z}_i, \mathbf{z}_i) - \mathcal{I}^{\text{Linear}}(\mathbf{z}_i, \mathbf{z}_i)|$, and $|\mathcal{I}^{\text{Linear}}(\mathbf{z}_i, \mathbf{z}_i) - \mathcal{I}^{\text{ALO}}(\mathbf{z}_i, \mathbf{z}_i)|$ as one of n and p varies while the other is held fixed. Using a similar experimental setting as in Section C.2.2, we observe that the empirical orders of $|\mathcal{I}^{\text{True}}(\mathbf{z}_i, \mathbf{z}_i)|$ and $|\mathcal{I}^{\text{True}}(\mathbf{z}_i, \mathbf{z}_i) - \mathcal{I}^{\text{Linear}}(\mathbf{z}_i, \mathbf{z}_i)|$ are approximately $\frac{p}{n}$. This observation validates Theorem 2.4 and Theorem 2.6.

For $|\mathcal{I}^{\text{Linear}}(\mathbf{z}_i, \mathbf{z}_i) - \mathcal{I}^{\text{ALO}}(\mathbf{z}_i, \mathbf{z}_i)|$, the empirical order is even smaller than $\frac{p^{1.5}}{n^2}$, which is below the bound established in Theorem 2.12. As discussed previously in Appendix C.2.1, although the bound in Theorem 2.12 may not be sharp, it is already sufficient to demonstrate that the ALO step is benign and preserves the magnitude of the influence function.

Finally, we examine the order of the projection step in Figure 12. In the bottom row of Figure 12, we present the dependent case, where $\mathbf{z}_i = \mathbf{z}_{\text{new}}$. The first panel fixes $p = 100$ and varies n , while the second panel fixes $n = 5,000$ and varies p . In both cases, the magnitude of $\mathcal{I}^{\text{TRAK}}$ scales as $\propto n^{-1}p^1$, which matches the order of \mathcal{I}^{ALO} in the dependent setting.

Moreover, the second and fourth panels show that the magnitude of $\mathcal{I}^{\text{TRAK}}$ scales as $\propto k$, which validates the sharpness of the bound in Theorem 2.14 for the dependent case.

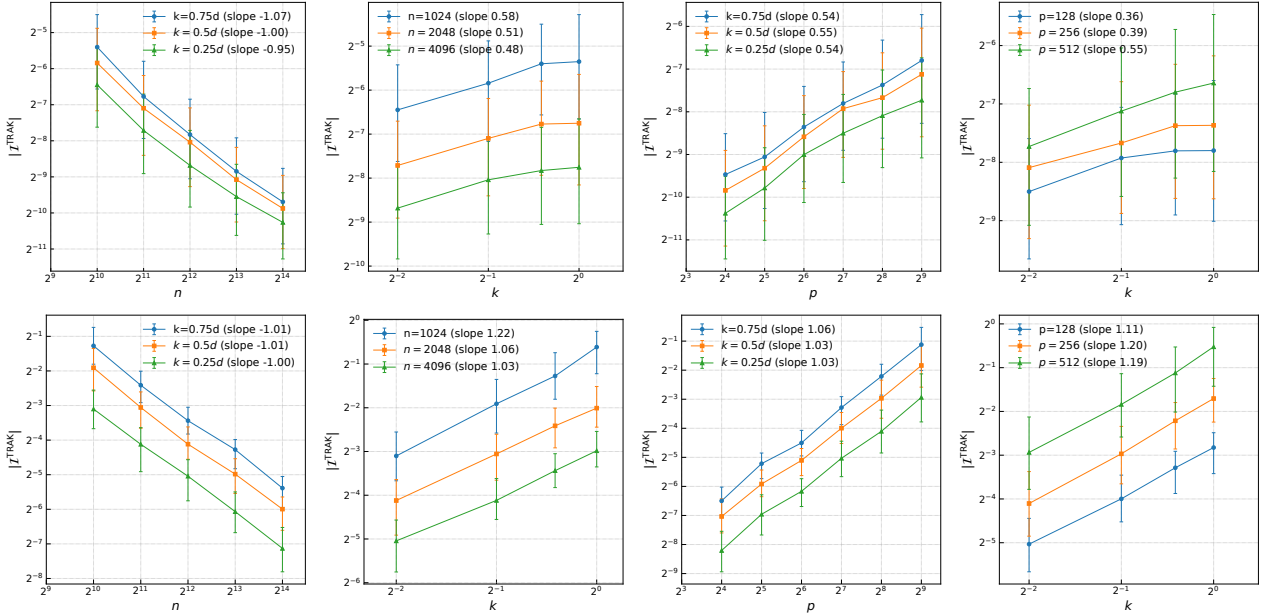


Figure 12. 3-class classification: projection magnitude order check. **Left two panels:** p is fixed at 100; **Right two panels:** n is fixed at 5,000; **Top row:** the independent case where \mathbf{z}_i and \mathbf{z}_{new} are independent; **Bottom row:** the dependent case $\mathbf{z}_i = \mathbf{z}_{\text{new}}$.

C.3.2. CORRELATION-BASED RESULTS

In Figure 14, we select 100 training datapoints as \mathbf{z}_i and plot the corresponding influence functions. The results are consistent with our theoretical findings. For the linearization step, the slope deviates substantially from 1, indicating a large magnitude error, in agreement with Theorem 2.6. Nevertheless, the linearization exhibits a clear linear trend and retains a relatively high correlation. For the ALO step, the magnitude error is much smaller, which aligns with Theorem 2.12.

Another notable observation arises from comparing the dependent and independent settings. Specifically, comparing the left two panels of Figure 14 with Figure 8, we find that both the linearization error and the ALO error are substantially larger in the dependent case. This phenomenon is predicted by Theorem 2.6 versus Theorem 2.9, as well as Theorem 2.12 versus Theorem 2.13. In particular, in the dependent setting, $|\mathcal{I}^{\text{True}}(\mathbf{z}_i, \mathbf{z}_i)|$, $|\mathcal{I}^{\text{True}}(\mathbf{z}_i, \mathbf{z}_i) - \mathcal{I}^{\text{Linear}}(\mathbf{z}_i, \mathbf{z}_i)|$, and $|\mathcal{I}^{\text{Linear}}(\mathbf{z}_i, \mathbf{z}_i) - \mathcal{I}^{\text{ALO}}(\mathbf{z}_i, \mathbf{z}_i)|$ can all be of strictly higher order than in the independent case.

C.4. More Empirical Studies

C.4.1. BINARY CLASSIFICATION ON CIFAR2

Experimental setup. We present results on CIFAR-2, constructed by taking the 5,000 airplane and 5,000 automobile images from CIFAR-10, yielding $n = 10,000$ training points. We use the same downsampling procedure as in Section 4 (from $32 \times 32 \times 3$ to $8 \times 8 \times 3$ via 4×4 average pooling), resulting in $p = 192$ features. We train a (binary) logistic regression model, obtaining 81.8% training accuracy and 81.2% test accuracy ($n_{\text{test}} = 2,000$).

Correlation analysis. We sample 100 test points and 100 training points (totaling 10,000 pairs) and compute the exact LOO influence and our approximation. As shown in Figure 15, the Pearson correlation is consistently close to 1, empirically confirming the high fidelity of the ALO approximation, consistent with Theorem 2.13.

Rank alignment. We further evaluate top- k ranking alignment using two metrics: (i) **Exact Match Count**: the number of test points (out of 100) where the retrieved top- k list matches the exact LOO list exactly (order preserved), and (ii) **Overlap Ratio**: the average fraction of overlap between retrieved and exact top- k sets. As reported in Table 3, exact matches decrease as k increases, while the overlap ratio remains very close to one, indicating that the approximation preserves local neighborhoods of influential examples.

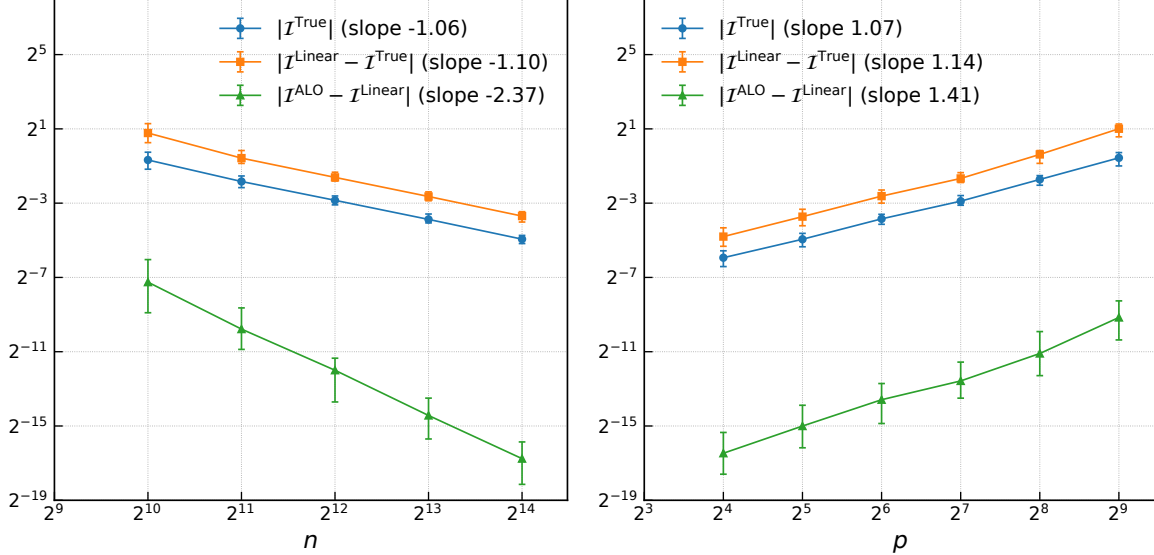


Figure 13. 5-class classification. Both axes are log-transformed. Medians are plotted, and error bars indicate the first and third quartiles. The left panel fixes $p = 100$, while the right panel fixes $n = 5000$.

Qualitative visualization. Figure 16 visualizes the top-5 (proponents) and bottom-5 (opponents) influential training images for selected test points. The strong overlap between exact and approximate results, along with the close influence values, indicates that the approximation preserves semantic relationships in the data.

Table 3. Rank alignment between exact and approximate influence rankings on CIFAR-2. Metrics are reported for both proponents (Top- k) and opponents (Bottom- k). Exact Matches count the number of test points (out of 100) with identical ranked lists; Overlap Ratio is the average set overlap.

Metric	Size (k)					
	1	3	5	10	20	50
<i>Proponents (Top-k Positive Influence)</i>						
Exact Matches (Count)	99	96	89	71	26	1
Overlap Ratio	0.990	0.990	0.992	0.992	0.994	0.996
<i>Opponents (Bottom-k Negative Influence)</i>						
Exact Matches (Count)	99	93	87	71	33	0
Overlap Ratio	0.990	0.983	0.992	0.997	0.995	0.995

C.4.2. MULTI-CLASS CLASSIFICATION ON CIFAR10

Qualitative visualization. Figure 17 visualizes the top-5 and bottom-5 influential training examples for selected test images. Consistent with Table 1, which indicates that the Top-5 proponents and opponents exact match rate can be bigger than 70%, we see that the retrieved examples identified by $\mathcal{I}^{\text{Linear}}$ are quite similar to those identified by $\mathcal{I}^{\text{True}}$, although the influence values are quite different, indicating that Linearization approximation captures ranking properties.

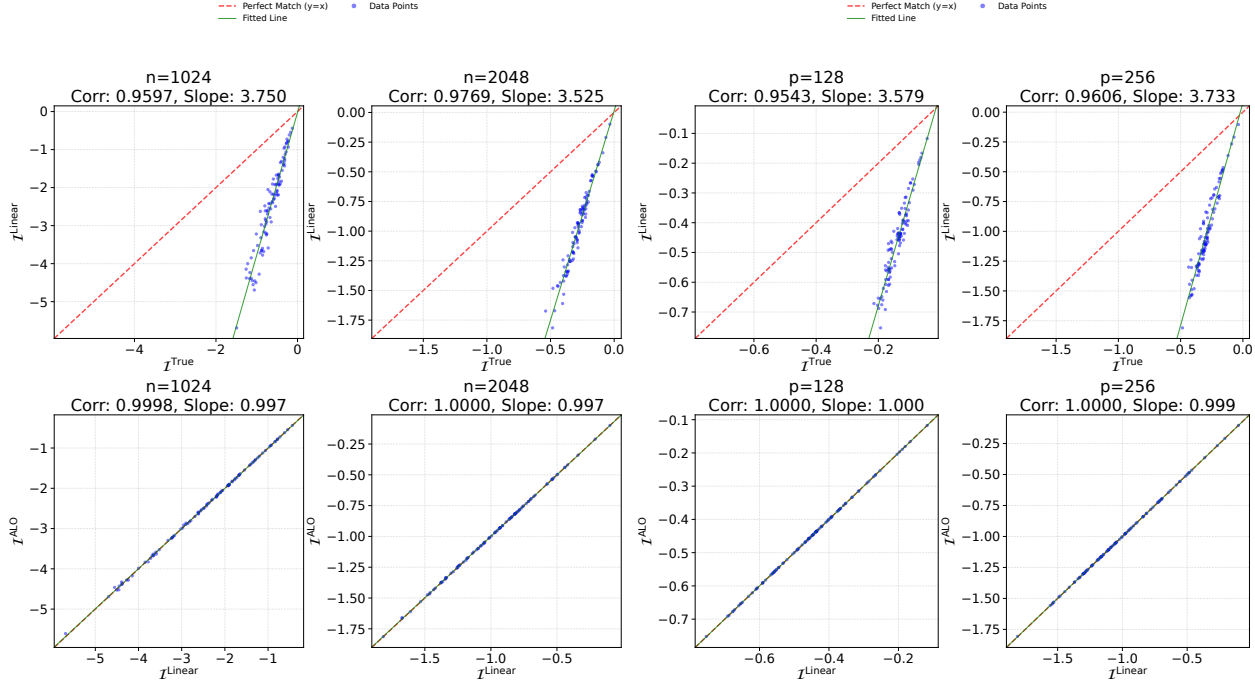


Figure 14. Correlation analysis for 5-class classification where $p = 100$ is fixed. **Left two panels:** results for $p = 100$ fixed; **Right two panels:** results for $N = 5000$ fixed. **Top row:** Linearization step: x-axis is I^{True} and y-axis is I^{Linear} . **Bottom row:** ALO step: x-axis is I^{True} and y-axis is I^{ALO} .

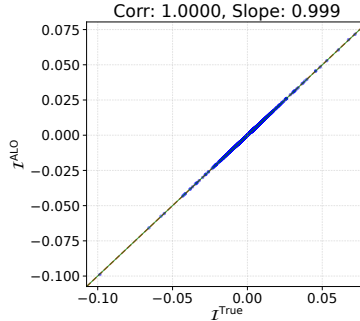


Figure 15. Correlation between I^{True} and I^{ALO} for CIFAR-2. Each plot contains 10,000 points (100 test points \times 100 training points).



Figure 16. Top-5 and bottom-5 influential training examples identified by I^{True} and I^{ALO} for binary CIFAR-2. Labels denote the class; scores indicate the influence value.

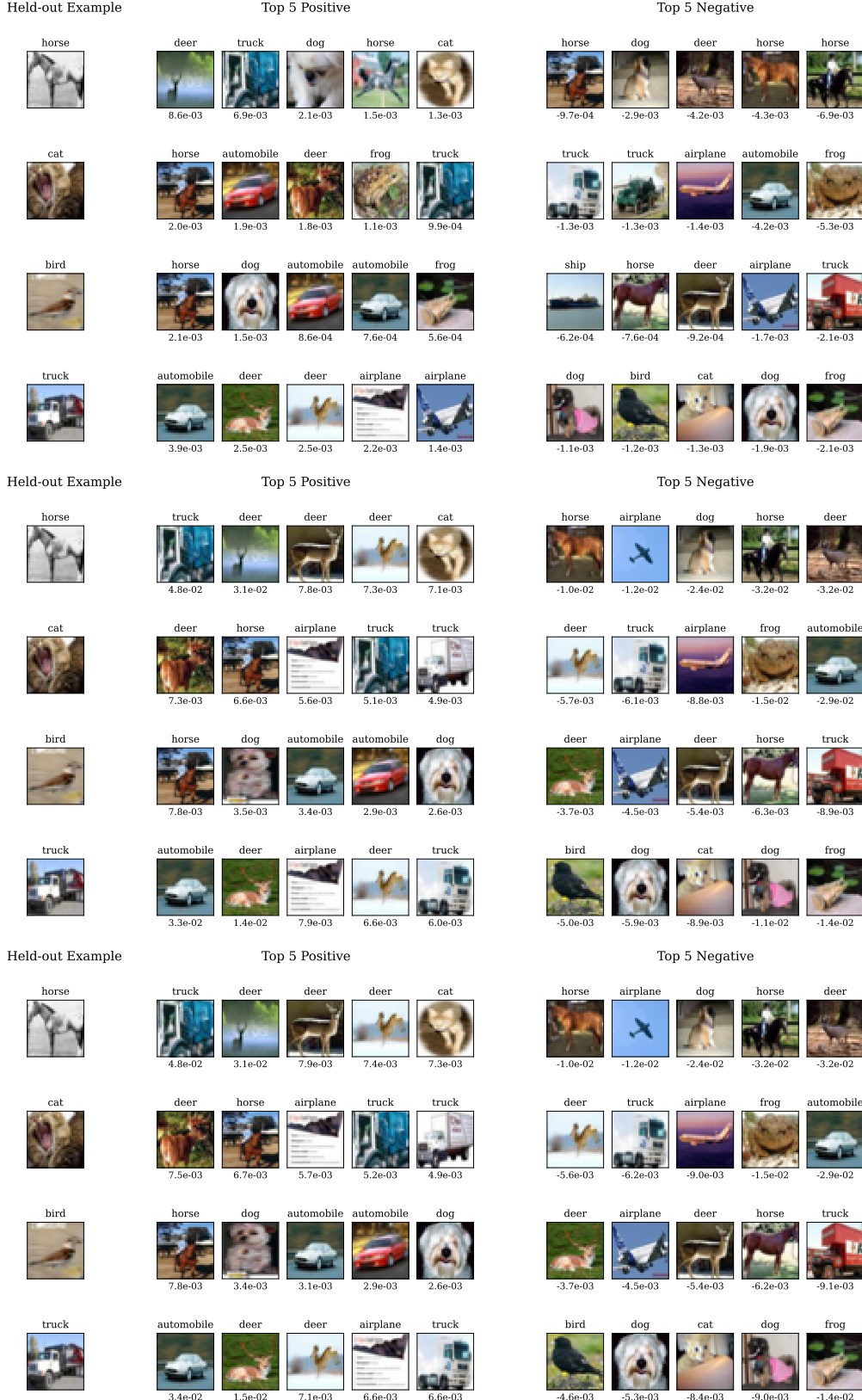


Figure 17. Top-5 and bottom-5 influential training examples identified by $\mathcal{I}^{\text{True}}$, $\mathcal{I}^{\text{Linear}}$ and \mathcal{I}^{ALO} for 10-classification CIFAR10. Labels denote the class, and scores indicate the influence value.